EVALUATION OF CAPACITANCE MOISTURE SENSORS FOR USE IN MUNICIPAL SOLID WASTE

A Thesis Submitted to the College of

Graduate Studies and Research

In Partial Fulfillment of the Requirements

For the Degree of Master of Science

In the Department of Civil and Geological Engineering

University of Saskatchewan

Saskatoon

By

Patrick M. Schmidt

Permission to Use

In presenting this thesis in partial fulfillment of the requirements for a Postgraduate degree from the University of Saskatchewan, I agree that the Libraries of this University may make it freely available for inspection. I further agree that permission for copying of this thesis in any manner, in whole or in part, for scholarly purposes may be granted by the professor or professors who supervised my thesis work or, in their absence, by the Head of the Department or the Dean of the College in which my thesis work was done. It is understood that any copying or publication or use of this thesis or parts thereof for financial gain shall not be allowed without my written permission. It is also understood that due recognition shall be given to me and to the University of Saskatchewan in any scholarly use which may be made of any material in my thesis.

Requests for permission to copy or to make other use of material in this thesis in whole or part should be addressed to:

Head of the Department of Civil and Geological Engineering

University of Saskatchewan

Saskatoon, Saskatchewan

S7N 5A9

ABSTRACT

Current municipal solid waste (MSW) practices have encouraged rapid waste degradation (stabilization) as an alternative to past methods of isolating the waste from the surrounding environment. There are challenges to rapid-stabilization technology, in particular, the management of the in-situ MSW moisture content.

The primary objective of this study was to evaluate the use of capacitance moisture probes for the purpose of measuring the moisture content within MSW. Capacitance moisture probes have not previously been used in MSW, however their use in agriculture is extensive and knowledge of their potential for monitoring MSW is limited.

The specific objectives of this research were to: i) establish a laboratory based correlation between sensor data and volumetric moisture content in MSW, ii) establish a correlation between field-installed capacitance sensors and moisture content derived from continuous-depth in-situ sampling of MSW, and iii) demonstrate the ability of capturing advancing/receding moisture fronts with the field-installed capacitance sensors.

Laboratory trials were conducted using hand-compacted MSW at volumetric moisture contents ranging from 15%-55% and a manual type of capacitance sensor. This series of laboratory trials successfully produced a correlation between sensor output and volumetric moisture content.

To evaluate the sensors in a real-world application, two configurations of capacitance moisture probes were installed in the field: i) an in-place, continuous-time capacitance probe, and ii) a portable, continuous-depth at discrete time, capacitance probe.

Field results indicated that capacitance moisture probes were able to capture the passing of both an artificially and naturally induced moisture front, though quantitative

correlation between the in-situ moisture content of the sampled MSW and the readings of the sensors could not be achieved.

The reasons for this were a combination of three factors:

1. The introduction of void-space during sensor installation significantly reduced sensor output;
2. Poor MSW sampling technique resulted in 57% recovery (causing the exact origin of samples to be unknown); and
3. The sampling technique disturbed the MSW samples, resulting in incorrect volumetric moisture contents in the samples.

ACKNOWLEDGEMENTS

I wish to express my utmost appreciation for the efforts of my academic supervisor, Dr. Ian Fleming, whose enthusiasm, dedication and wealth of knowledge proved invaluable during the course of my research. Indeed, he has become, and will remain a friend beyond the realm of academia.

I also gratefully acknowledge the financial support provided for me by O'Kane Consultants Inc, NSERC, the City of Saskatoon and the Federation of Canadian Municipalities.

Dave Christensen of O'Kane Consultants deserves many thanks for providing me with technical support, and for putting up with my never-ending questions.

The support staff in the Department of Civil and Geological Engineering also deserve acknowledgement. In particular, Mr. Alex Kozlow, Mr. Doug Fisher and Ms. Cynthia Hanke were all selfless in their assistance.

I would like to extend my thanks to my fellow graduate students in the department. Without their support, the task would have been difficult to persevere. Manoj and Chad, your friendship in particular was important in the completion of my research.

Lastly, but certainly not least, I wish to thank my family and friends for their support over the course of this project.

Dedication

This thesis is dedicated to the memory of my grandfather, Herb Dickin, my Great Aunt Doris Llewellyn and Great Uncle Bernard Dickin, all of whom passed away during the course of this research. This thesis is also dedicated to my niece Cassidy Anne Collier, born on February 26th, 2008.

TABLE OF CONTENTS

LIST OF TABLES

LIST OF FIGURES

LIST OF APPENDICIES

CHAPTER 1 INTRODUCTION

1.1 Background

Past design practices for the storage of municipal solid waste (MSW) landfills have attempted to isolate the deposited waste from the surrounding environment. This type of landfill design is referred to as a "dry-tomb" landfill. By preventing the ingress of moisture, the degradation of the waste will be significantly retarded, thereby minimizing the contamination of its surroundings by leachate and methane generation.

However, this model is not ideal, as waste cannot perpetually remain in the same state without some degradation. Additionally, the liner beneath the waste (if present) may not adequately prevent the migration of leachate into the groundwater system, due to leaks, etc.

Current waste management practices have moved towards a rapid-stabilization type approach. Rather than attempting to keep the waste in its original state, these rapid-stabilization (or bioreactor) landfills, attempt to speed the degradation of the waste, and subsequently decrease the length of the "contaminating lifespan". Additionally, if the conditions within the landfill are anaerobic, rapid-stabilization will promote methane production, a major component of landfill gas (LFG), which could be captured and used economically.

The City of Saskatoon has initiated a demonstration project in an attempt to partially retrofit the City's Spadina landfill from a typical dry-tomb landfill into a rapid-stabilization landfill. The term "bioreactor" should not be used, however, to describe the desired outcome of the Spadina landfill. Bioreactors are designed from conception with

the purpose of promoting rapid-stabilization, and it is unlikely that the same degree of efficiency and extent of waste stabilization will be realized for the Spadina landfill.

There are several components that are integral to the operation of a rapid-stabilization landfill:

- a means to add moisture to the waste to ensure proper moisture content;
- wells and a blower to capture the LFG; and
- instrumentation to monitor the moisture content of the waste.

Most modern landfills also have a leachate collection system that intercepts the leachate before it can breach containment. As the Spadina landfill was constructed before widespread implementation of this technology, it employs a groundwater-intercept trench along sections of its perimeter, constructed sometime after its opening.

The operation of a rapid-stabilization landfill requires that the moisture content of the waste be around 35-40% by weight. (Singh and Fleming, 2004). Also, as the LFG has a very high degree of water vapour saturation, its production will remove moisture from the waste, therefore moisture must be added to achieve and maintain optimal conditions. In bioreactor landfills, this is typically achieved by means of vertical addition wells, or horizontal trenches.

The first three LFG wells were installed at the Spadina landfill to a depth of approximately 80', in 2004. During the drilling of the wells, MSW samples were gathered from all depths and analyzed for moisture content. It was determined that the average gravimetric moisture content of the waste, based upon these samples, was approximately 21%. This is significantly lower than the desired value for optimal waste degradation and LFG production.

A more detailed design was drafted following the initial well installation, outlining locations for seven more LFG wells and a blower system, pressure probes, and moisture augmentation trenches. The need to monitor infiltration and water content of the waste was also realized. The ideal technology, however, to achieve this goal is still being actively researched, with many techniques being investigated.

Traditional methods of moisture measurement as used in soils have proven ineffective or impractical for use in MSW. Tensiometry, for example, explored by Korfiatis et al. (1984) and Kazimoglu et al. (2006) produced mixed results. The pore sizes present in MSW creates a water retention curve in which the saturation varies too much over a small span of suction values to attain accurate results. The use of tensiometry in MSW is discussed further in Section 2.2.9.

Gravimetric sampling, though very reliable, is too disruptive and labour intensive to monitor the waste moisture content as frequently as is needed for successful rapid-stabilization operation (SWANA Applied Research Foundation, 2004).

Currently, there has been no documented use of capacitance moisture probes in MSW, though there is extensive research on their operation for agricultural irrigation purposes.

1.2 Research Objectives

The research objectives for this M.Sc. study were as follows:

1) To establish in the laboratory a quantitative relationship between volumetric moisture content in MSW and the response from capacitance moisture sensors to evaluate if the field-scale application of this technology is feasible. To achieve

this relationship, exhumed MSW was compacted at varying moisture contents and surveyed with capacitance sensors.

2) Develop a field correlation between the water content of MSW samples and capacitance sensor readings. Continuous-depth moisture content data was collected by means of continuous-depth core samples taken at the Spadina Landfill. Capacitance sensor surveys over the same interval were then compared to the moisture data collected from the MSW samples.
3) Demonstrate the ability of capacitance moisture sensors to capture the passage of moisture through MSW. Both artificial and natural moisture fronts were relied upon to evaluate the sensors in a field setting.

1.3 Scope

The scope of this project focused primarily on the successful lab investigation and practical techniques of field installation of the capacitance moisture technology. The scope also included evaluation of capacitance technology to generate a correlation between the actual volumetric moisture content and values yielded from the sensors.

CHAPTER 2 LITERATURE REVIEW

2.1 Introduction

This chapter is divided into three sub-sections. Section 2.2 briefly outlines various common and practical methods for moisture sensing in the subsurface irrespective of the type of geomaterial (i.e., soils, rock, waste, etc.). State-of-the-art examples are given to gauge the development and abilities of these technologies.

A more detailed discussion of moisture sensing technologies that have undergone a reasonable level of testing and/or research for use in MSW in section 2.3. Relevant conclusions are outlined regarding the practicality and efficacy of various methods for determination of moisture content in waste.

Finally, section 2.4 discusses in greater detail the background, theory and application of the application of the selected moisture sensing technology.

2.2 Moisture Sensing Technologies

2.2.1 Introduction

An important distinction between moisture measurement and moisture sensing must also be made. Moisture measurement is the act of physically determining the moisture content of the media gravimetrically, either in either the field or lab. Moisture sensing can be considered to be an estimation of moisture content by observing the properties of the media (electromagnetic, nuclear, etc.) and developing a correlation with the actual moisture content (Kelleners et al., 2005).

Repeated sampling for the gravimetric measurement, though more accurate, requires greater continued labour (and therefore cost) and will also disturb the environment that is

to be measured. It is also not preferable to measure real-time moisture changes within the observed media using sampling due to the continual disturbance of the *in-situ* environment. Volumetric moisture analysis is difficult in MSW and less preferable than gravimetric analysis. Volumetric sampling at depth is difficult due to large-sized waste constituents and potential disturbance of original density.

For these reasons, gravimetric sampling was not considered to be a practical method and only moisture sensing methods were researched for application to this project. The following sub-sections will review the general operation of a few moisture-sensing methods.

2.2.2 Nuclear Sensing Methods

Though there are several downhole nuclear logging methods that are used in mineral and oil & gas exploration (i.e. gamma-ray spectroscopy), the neutron log is the method most regularly used for the purpose of sensing moisture content in geomaterials.

Neutron probes can be used on surface or in a downhole application, utilizing vertical access tubes. They were first developed for soil moisture sensing in 1950 (Schmugge et al., 1980). The construction of a neutron probe consists of a nuclear source that sends high-energy neutrons into the media. These neutrons then collide with the surrounding media constituents causing them to slow and be reflected (Yuen et al., 2000).

The probe detects the reflection of these slow, or thermalized, neutrons. Due to its similar atomic weight, hydrogen can slow fast neutrons more effectively than any other atom. Since the vast majority of hydrogen in soils is associated with the porewater, the amount of slow neutrons detected can be used to estimate the moisture content.

Volumetric moisture content (θ_w) of the soil can be estimated using a correlation function that is derived from lab or field-testing (Schmugge et al, 1980).

Hydrogen content of most soils is dominated by water. However, there are other materials that can interfere in the accurate estimation of moisture content. Hydrogen is also the main constituent of hydrocarbons. For example, if soil is contaminated with hydrocarbons, an anomalously high moisture reading will result from the additional thermalized neutrons returned by the hydrocarbons (Akaho et al., 2001, Yuen et al., 2000). Figure 2.1 illustrates this effect.

Another phenomenon that must be taken into account is the neutron-capture effect. Certain materials have an affinity for neutrons and as such will intercept some of the thermalized neutrons resulting in a lower count ratio than would be expected. Elements that are prone to capturing slow neutrons include iron, potassium and chlorine (Imhoff et al., 2007).

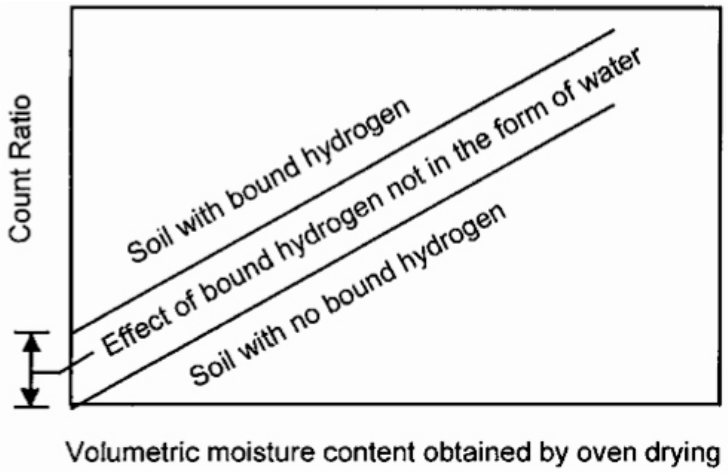

Figure 2.1 – The effect of bound hydrogen on moisture sensing using the neutron probe. Bound hydrogen (in the form of hydrocarbons) will increase the count ratio, resulting in an overestimation of moisture content. (Yuen et al., 2000)

A significant drawback in the application of neutron probes is that they cannot be used remotely and hey cannot be left unattended due to safety hazards and regulations

associated with the radioactive source (SWANA Applied Research Foundation, 2004). As a result, real-time monitoring (i.e. logged data) cannot be performed, making this technique labour intensive (Evett, 2000).

2.2.3 Partitioning Gas Tracer Test

The partitioning gas tracer test (PGTT) is a physical method that has been used to sense moisture content present in the vadose zone. Partitioning gas tracer tests are conducted using two types of gas tracers that move through the void space of the sensed medium. One gas tracer is conservative and the other must be soluble in water. As the tracers move through the void space, the moisture will not absorb the conservative tracer but the soluble tracer will move in and out of the moisture present in the void spaces. This behaviour results in a slower travel time for the partitioned tracer (see Figure 2.2). The time disparity between the conservative and partitioned tracer can then be used to make an estimate of moisture content (Han et al, 2006).

A noble gas, such as helium or argon, may be used as a conservative tracer. Difluoromethane is commonly used as the partitioning tracer due to its resistance to chemical reactions within the waste and high solubility in water (Han et al., 2006, Deeds et al., 1999, Keller et al., 2003).

PGTTs are typically used to determine the amount of non-aqueous phase liquid (NAPL) concentration in the vadose zone though they have also been used to determine the water saturation. (Deeds et al. 1999). In the laboratory Deeds et al. (1999) attempted to estimate the water saturation in the presence of non-aqueous phase liquids (NAPLs) using a PGTT. Though elevated amounts of NAPLs will interfere, Deeds et al. (1999)

concluded that it is possible to accurately determine the moisture content at lower NAPL concentrations.

Additionally, Keller et al. (2003) concluded that at moisture contents nearing saturation, the PGTT would underestimate the actual moisture content due to limited gas flow. In agreement with Keller et al. (2003), both Han et al. (2006) and Imhoff et al. (2003) acknowledge the potential underestimation in moisture content when PGTTs encounter near saturated or saturated zones.

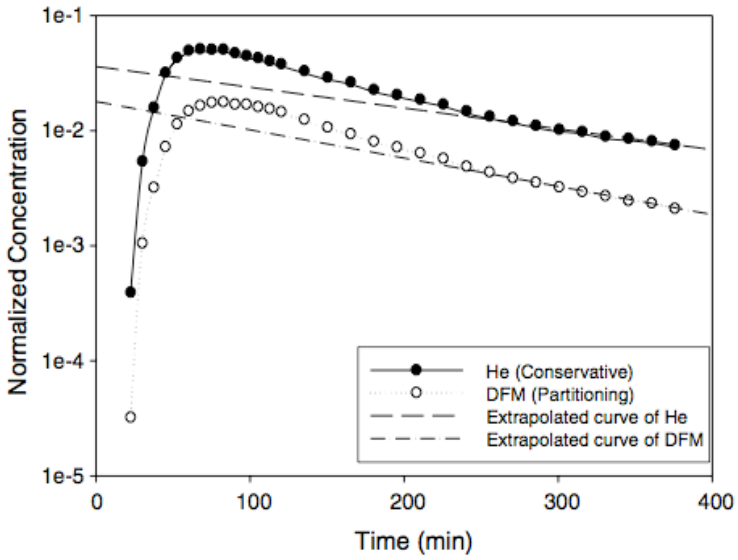

Figure 2.2 - Example of results from a partitioning tracer test. In this case, the difluoromethane (DFM) tracer arrived at nearly the same time as the helium tracer, resulting in near-zero moisture content. Should water have been present the arrival DFM tracer would have been delayed because of its travel through water and air. (Han et al., 2006)

There are distinct advantages of using the PGTT method for moisture estimation. The density and heterogeneity of the media will have much less influence than methods based on sampling. Additionally, this method can utilize existing wells as sites for tracer injection/extraction (SWANA Applied Research Foundation, 2004).

Conversely, the spatial extent of the estimated moisture content is very large and provides only an average value along the flow path of the tracer test. Because the tracer

gasses will tend to flow preferentially among the larger voids, the method may underestimate the moisture contribution arising from the smaller voids (SWANA Applied Research Foundation, 2004).

When considering labour requirements, it has been found that significant human resources are needed for each test. If gas sampling could be automated, it would greatly reduce the labour requirements, and therefore cost (Imhoff et al., 2007).

2.2.4 Time Domain Reflectometry and Time Domain Transmissivity

Time domain reflectometry (TDR) and time domain transmissivity (TDT) are both electromagnetic sensing methods that measure the electrical permittivity of the surrounding medium. An electromagnetic wave of known frequency is sent into the medium and the reflection (in the case of TDR) or transmission (in the case of TDT) of this wave is recorded and the travel time determined from its analysis. The travel time is dependent upon the dielectric properties of the medium (Li et al., 1999, Imhoff et al., 2007).

Electrical permittivity is described as the potential for molecules to become polarized in the presence of an electric field. The molecular polarity and the freedom to align these poles will result in a high or low permittivity. To compare the permittivity of differing materials, a dielectric constant (ε) is given for each material, relative to a vacuum (ε_o). Under this convention, air has a dielectric constant of almost exactly 1, and free water, due to its polar nature, has a dielectric constant of approximately 80. Essentially, when TDR and TDT are used to sense soil moisture, they are measuring the bulk dielectric constant, made up of contributions from air, water and the remaining media constituents (Dean et al., 1994).

Topp et al. (1980) and Topp et al. (1985) established what is now considered to be the foundation for soil water sensing using TDR. Using coaxial transmission lines Topp et al. (1980) measured the dielectric constant of a wide range soil types containing porewaters of varying salinities. Testing soils between volumetric water contents of 0% to 55% they concluded that the permittivity is almost entirely dependent upon water content and virtually ignores density, texture, salt content and temperature dependence.

These results by Topp et al. (1980) are not entirely accurate and have since been refuted by Andrade-Sanchez et al. (2004) in the case of salinity, Gardner et al. (1998) in the case of bulk density and Polyakov et al. (2005) in the case of temperature. However, the authors of these more recent studies conclude that TDR can still provide accurate results provided these factors are taken into account.

For example, Ebrahimi-Birang et al. (2006) attempted to measure both electrical conductivity and volumetric water content in soil. Ebrahimi-Birang et al. (2006) created identical soil columns and varied the electrical conductivity of pore water in a sandy soil at varying water contents. By analyzing the resulting TDR waveforms, Ebrahimi-Birang et al. (2006) were able to sense accurately, with only slight deviation, the actual moisture content at varying porewater conductivities, as shown in Figure 2.3.

TDR, however, has other drawbacks that make it difficult for field scale use. TDR probes require direct contact via two or three electrodes with the sensed media and thus installation and measurement at depth becomes a challenge. Also, the measurements are considered to be "point" scale. This has two implications: the increased effect of media heterogeneity on the sensed properties and the inability to provide large-scale information on moisture content (SWANA Applied Research Foundation, 2004).

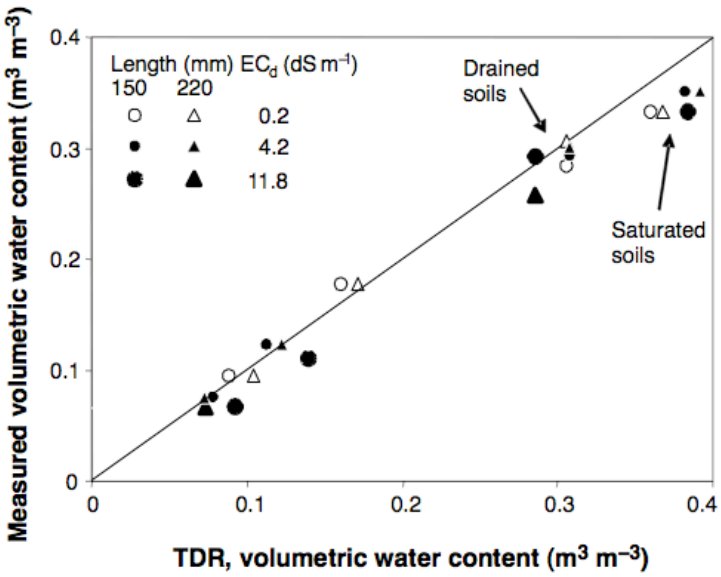

Figure 2.3 - Lab correlation between actual and TDR volumetric moisture contents at specified conductivities. Data point shapes indicate difference in electrode length (Ebrahimi-Birang et al., 2006).

2.2.5 Capacitance Sensors

(Please see Section 2.4.2 for a more detailed description of capacitance sensor theory). Similar to TDR, the operation of a capacitance moisture sensor (Figure 2.4) takes advantage of the relative high dielectric constant (relative permittivity) of water (Kelleners et al., 2004a). The dielectric constant indicates the potential for the molecule in question to polarize itself with an induced electric field. Because water is polar, and generally unbound in geomaterials, it has a strong tendency to align with such a field. Figure 2.5 illustrates the effect of volumetric water content on the relative permittivity of the soil-water system.

When installed in the sensed medium, capacitance sensors oscillate their generated electric field. The presence of permissive material in the media will result in the decrease in the oscillating frequency. The degree to which the resonant frequency will decrease is

dependent upon the amount of such material. Since water has a high relative dielectric constant, the majority of the bulk permittivity can be attributed to the contribution of water content and less to other constituents. Typical soil constituents have a dielectric constant in the range of 4-9, and organics have a constant of about 6-8 (Nadler and Lapid, 1996; Polyakov et al, 2005).

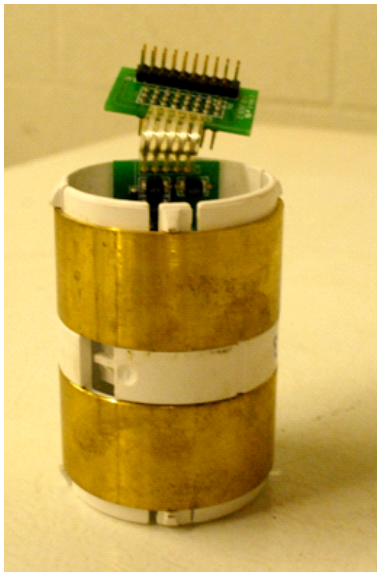

Figure 2.4 - Capacitance moisture sensor, manufactured by Sentek Pty. Ltd. The two brass rings comprise the capacitance electrodes. The brass rings in this photograph are 51mm in diameter.

Capacitance sensors can be configured in several different ways:

- The surface-insertion probe consists of two metal electrodes that are pressed into the ground. It is designed to take moisture content readings at only the near surface (Dean, 1994).
- The manual access-tube version is used in downhole access tubes for reading moisture content at desired depths.
- The automatic installed probe is designed to record continuous moisture data at an installed depth (Dean, 1994).

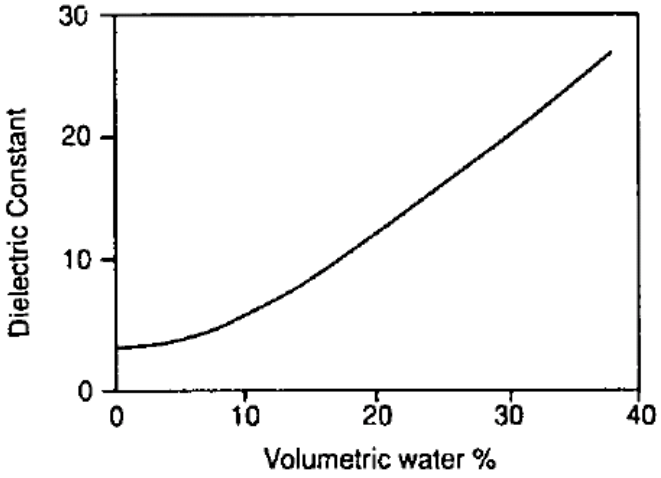

Figure 2.5 - General relationship between the bulk dielectric constant of soil and the volumetric moisture content (Dean et al., 1994).

For all of the above probe configurations, the sensor must be calibrated for the material in which it will be used in order to gain accurate volumetric moisture content readings. Some soil constituents may adversely affect the results attained by methods utilizing the dielectric constant of water. Water may be bound by clay particles and unable to respond to an electric field, reducing the response of water and the apparent moisture content (Polyakov et al., 2005).

2.2.6 Electrical Resistivity Tomography

Electrical resistivity tomography (ERT) is a geophysical method of measuring and interpolating electrical resistance. Artificial electrical currents are introduced into the ground surface by means of electrodes. Generally these electrode arrays are a series of metal stakes at regular spacing (Jolly et al., 2007). Simultaneously, a second series of stakes measures the differences in electric potential in the same region of current flow. From this regularly spaced resistivity data, interpolations can be made as to the properties of the subsurface (see Figure 2.6) (Grellier et al., 2007).

Though moisture content will hold a great influence over the subsurface resistivity, other factors such as ionic concentrations, void connectivity, porosity and temperature will also affect the results (Imhoff et al., 2007). Recent studies utilizing ERT for moisture monitoring (Consenza et al., 2007; Jolly et al., 2007; Guerin et al., 2004) have all concluded that the technology provides good qualitative information of moisture presence but more research needs to be conducted to gain a quantitative correlation between resistivity and moisture content.

Grellier et al. (2007) attempted to gain a resistivity-moisture content correlation using previous studies aimed at correlating temperature and resistivity of pore fluids (Grellier et al., 2005; Grellier et al., 2006). Collecting borehole samples at depth and using ERT imaging to correlate the temperature and resistivity the results were described as promising though the authors acknowledged the need for site-specific measurements for better agreement.

Jolly et al. (2007) make other important conclusions as to the spatial interpretation of the processed ERT images. The depth of reliable imaging is approximately one-half of the electrode spacing. Therefore, if measurements to a depth of 40m are required, then the electrode spacing must be 80m. Jolly et al. (2007) also concluded that the resolution with depth would gradually decrease causing the location and size of areas of moisture change to become less exact. This can cause the overestimation of the spatial extent of moisture change since it will be "smeared" over a greater area by the data processing.

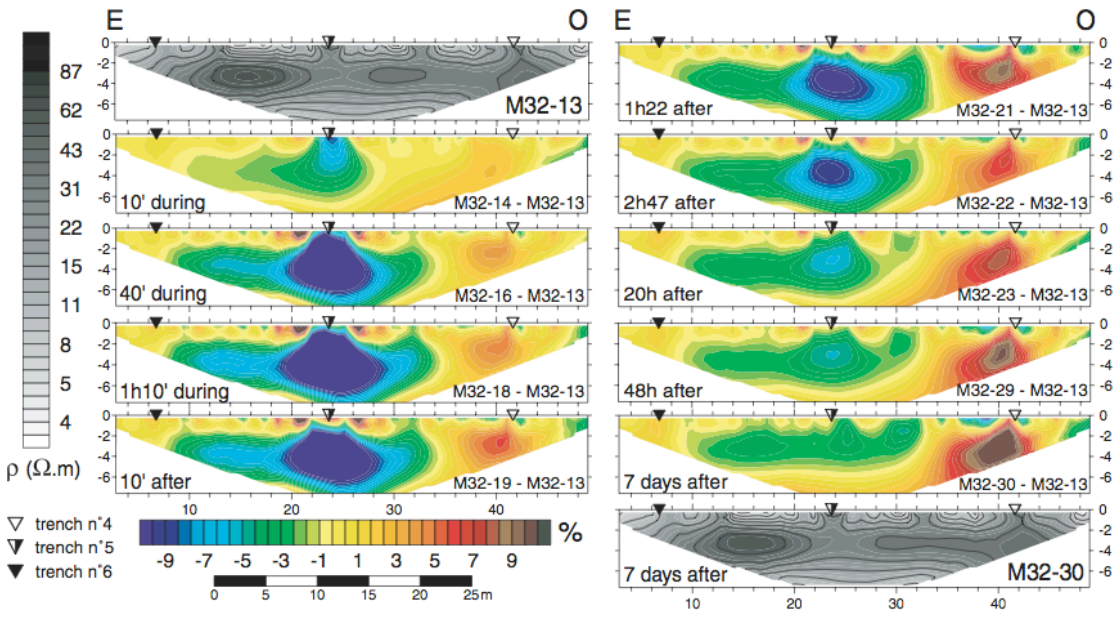

Figure 2.6 - Time-lapse ERT imaging. The top-left and bottom right images the resistivity of the MSW before and seven days after moisture addition, respectively. The images between represent the change in resistivity from the original to the final resistivity profile (Imhoff et al., 2007).

2.2.7 Electrical Resistance Sensors

Electric resistance sensors also take advantage of the conductivity of the pore fluid. These sensors contain a porous medium within the sensor, whose internal moisture content is dependent (by matric potential) on the external moisture content of the surrounding medium. By measuring the resistivity of the porous medium within the senor, a correlation to determine the internal moisture content can be made (Imhoff et al., 2007).

When using this technique, the water retention behaviour of both the soil and the sensor's porous medium must be accurately known. Laboratory calibrations must establish a relationship between internal moisture content of the sensor and the resulting resistivity. General construction of an electrical resistance sensor can be seen in Figure 2.7.

The porous medium used within the sensor will vary depending upon the conditions of the surrounding porewater. In cases where the wetting fluid is sufficiently conductive and the ionic conductivity is known and stable, the porous media within the sensor could be sand or gravel (SWANA Applied Research Foundation, 2004). In situations where conductivity of the wetting medium is low, the two electrodes may be placed within a relatively conductive matrix, such as gypsum (Yuen et al., 2000). When the gypsum becomes wet, its ions will dissolve and create a more conductive pore fluid. This elevated conductivity will also guard against fluctuating ionic concentrations of the pore-water that might make results inaccurate (Imhoff et al., 2007). Other internal porous mediums used are nylon or fiberglass (SWANA Applied Research Foundation, 2004).

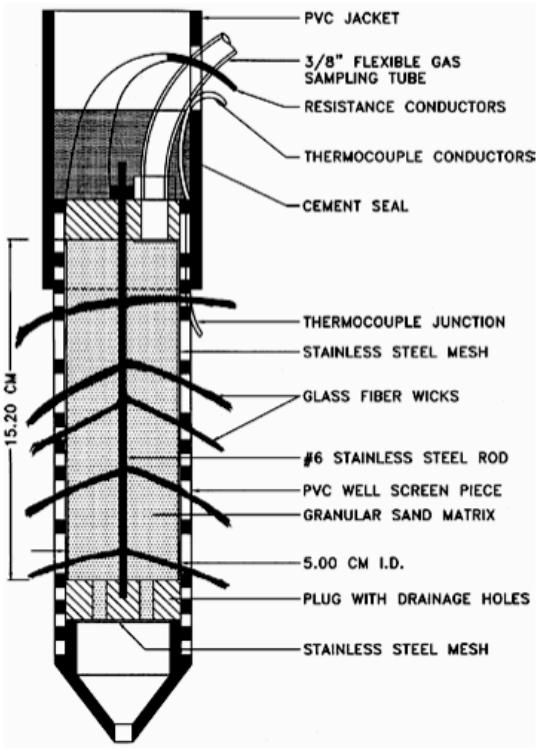

Figure 2.7 - An electrical resistivity sensor as used by Gawande et al. (2003).

There are several issues that must be considered when selecting resistance sensors for moisture monitoring. Because they rely on matric potential, it becomes unreliable for them to be used either above the air-entry pressure or below field capacity, as the ability for the moisture to move in and out of the sensor will be limited (Imhoff et al., 2007). Resistivity sensors also exhibit hysteresis and may have difficulty drying due to isolation of the internal porous media.

2.2.8 Seismic Surveys

Though primarily an oil & gas exploration tool, seismic surveys have also been used to detect moisture content in rock and soil (Bachrach et al., 2005). During the course of seismic resource exploration, it was realized that porewater content in rock would affect the results. For this reason studies have been conducted to quantify this effect of the porewater on seismic surveys.

Seismic surveys rely upon the elastic wave propagation velocity within rock and soil to determine the location of lithological contacts. By firing an energy source in or at the ground, a blank ammunition round for example, seismic waves propagate through the ground. Where differing materials or rock types contact each other, there is a density change. This density change causes the wave to refract and reflect along that contact (Catley et al., 2006).

Reflection type seismic surveys typically have short horizontal distances between the shot source and the geophones that record the reflection, because the direction of wave travel is sub-vertical. In refraction surveys, the horizontal spacing between the shot source and geophones is much larger since the refracted seismic waves travel horizontally

along the material interfaces and refract back to surface some distance from the source (Catley et al., 2006).

Using these techniques, wave velocities can be calculated and the properties of the soil or rock media can be estimated. Many physical characteristics of the medium will affect the wave velocity: porosity, density and water content, among others.

Several studies (Catley et al., 2007; Bachrach et al., 2005) have attempted to detect the change in moisture after simulated or natural moisture addition. While the authors concluded that there is a qualitative correlation, there remains no quantitative relationship between change in wave velocity and change in moisture content. A qualitative correlation may prove difficult to achieve as large distances are traversed by the compression waves and the nature of the technique averages all moisture contents along the wave path, resulting in extremely low-resolution measurement.

2.2.9 Other Moisture Sensing Technologies

In addition to the previously mentioned moisture sensing methods, there are several others that for practical purposes have not been thoroughly investigated. Since these technologies were not investigated further beyond this section, the results of their use in MSW are provided if applicable. Below is a brief summary of these technologies:

- Frequency Domain Reflectometry (FDR)

  The FDR technique bears many similarities to TDR. Where TDR measures the time for the propagation of an electric pulse, FDR measures the frequency of repeated voltage rises transmitted to, and reflected from the medium. As with capacitance and TDR techniques, the resulting

oscillation frequency is dependent upon the bulk permittivity (Irmak and Irmak, 2005).

FDR is used to a lesser extent than TDR in soils though commercially manufactured sensors are available. Irmak and Irmak (2005) tested the accuracy of an FDR sensor in several soils and found that the results were good with the greatest error in soils with a higher clay fraction. This variance in clay-rich soils echoes the overestimation of moisture content sensing using other dielectric techniques, such as TDR or capacitance.

Veldkamp and O'Brien (2000) also reported promising results using FDR sensors in soils of varying compositions. However, they acknowledged that adverse effects of clay and organic-rich soils must be taken into account by establishing a site-specific calibration, as opposed to using a manufacturers calibration.

- Fiber-optics

  Networks of fiber-optic cable have been successfully installed and used to monitor temperature variations along the cable length by means of Raman scattering. This fiber-optic cable is accompanied by heating cables that heat the surrounding medium. By observing the rate and magnitude of these temperature changes, and their locations along the fiber-optic cable, speculation can be made as to the properties of the medium surrounding the optic cable. For example, lower temperature response and quick loss of heat suggests higher moisture content (Imhoff et al., 2007).

Fiber-optic networks show promise, however no quantitative correlations between fiber-optic temperature data and moisture have been developed (Imhoff et al., 2007).

- Tensiometry

  Tensiometry is the method of observing the negative pore pressure (suction) within a particular medium and correlating this suction value over a range of moisture contents in a controlled environment. This correlation, once established, allows for field measurements of suction to be converted to moisture content.

  Though this method is standard for use in soils, Korfiatis et al. (1984) attempted to monitor the moisture content in a solid waste column and concluded that tensiometric equipment was not sensitive enough to detect moisture change between in the moisture content region between field capacity and saturation as the large voids fill.

  Kazimoglu et al. (2006) also attempted to determine the moisture retention function for waste by using the empirical functions of van Genuchten. Though the Kazimoglu et al. (2006) reported good results for low moisture contents, their results agreed with the conclusions of Korfiatis et al. (1984). Specifically, Kazimoglu et al. (2006) concluded that measuring low suction values in large pores produced inaccurate results.

- Ground-penetrating RADAR

  Lunt et al., (2005) attempted to estimate soil-water content using ground-penetrating RADAR (GPR). Using a known reflective soil layer 0.8m-

1.3m deep (characterized by boreholes) and the two-way travel time of GPR reflected by that soil layer, an estimation of the bulk dielectric constant could be made. The bulk dielectric constant could then be converted to volumetric moisture content. To confirm these results, a neutron probe survey was completed and the error was found to be negligible.

Though this method has shown the ability to provide a quantitative correlation for volumetric moisture content, the practicality for use in an MSW landfill is unlikely. It is possible that the landfill base or liner could comprise the reflective layer, however the resulting moisture measurement would be an average of the entire depth of waste. This will be problematic, as the moisture content within the landfill will vary spatially, especially when water addition occurs.

- Downhole resistivity survey

  Similar to seismic surveys, downhole resistivity techniques are typically used for logging oil & gas wells (Luthi, 2001). However, Jackson et al. (2002) attempted to monitor the moisture content in a road embankment using downhole resistivity coupled with borehole sampling for depth correlation. The sensor used was adapted to work in an uncased borehole up to depths of 9m. Reasonable correlation between gravimetric moisture content and downhole resistivity data was found.

  The use of this technique in MSW would likely not be possible. Heterogeneity within MSW would likely prohibit the use of an uncased

borehole for a sensor survey. Further, the monitoring of moisture content for the proposed application requires repeated measurements. An uncased borehole in MSW would likely not remain open over a sufficient period of time to allow these measurements.

- Airborne electromagnetic (EM) survey

  Taking advantage of the conductivity of MSW leachate, Beamish et al. (2003) conducted two airborne EM surveys over a municipal landfill, spaced four years apart. The survey had the ability to sense conductivity up to 15m below the surface. Witnessing a large change in electrical conductivity within the landfill containment between the two surveys, the authors concluded that a conductivity increase during the lapsed time corresponded to an increase of leachate. No quantitative correlation of moisture content and resistivity was made.

  Though it was possible to observe a qualitative change in the waste properties, this technique lacks sufficient resolution and depth of measurement needed to provide proper moisture content estimations for rapid-stabilization operation. In addition, the repeated use of an aircraft for these observations would be prohibitively expensive.

- Nuclear Magnetic Resonance (NMR)

  Nuclear magnetic resonance works by taking advantage of a unique resonant frequency for each atomic nucleus under the influence of an externally applied static magnetic field. By detecting the resonant frequency of hydrogen, the quantity of water within a specific medium can

be determined. This technique has been used extensively in materials testing (i.e. concrete) (Gotz et al., 2002).

Paetzold et al. (1985) used a tractor mounted NMR moisture measurement instrument for sensing moisture up to a depth of 63 mm below the ground surface. Results indicated a good correlation between the NMR signal and the volumetric moisture content of the soil. More recent instances of NMR use for soil moisture sensing could not be found, giving little basis to apply it to MSW.

2.3 Moisture Sensing in MSW

2.3.1 Introduction

The foregoing section was intended to summarize all the various methods that may be used to estimate water content in the subsurface, regardless of the material type. For application in MSW, only a small number of these methods have been documented. This section will discuss results provided by various published studies relating their use for *in-situ* moisture sensing in MSW landfills.

2.3.2 Neutron Probe

Currently, there have been two attempted trials using the neutron probe in MSW. Holmes (1984) attempted to establish a surface water balance by installing aluminum access tubes to a 1 m depth within the waste. Holmes (1984) concluded that although volumetric moisture content could not be quantitatively determined, the moisture content change could be tracked.

Yuen et al. (2000) combined laboratory and field-testing to evaluate the response of the neutron probe to changes in moisture content in MSW. The laboratory apparatus

consisted of an aluminum access tube installed down the centre of a 0.7 m diameter plaster drum. Varying mixtures of sand with either ferrous metal, plastic and wood were compacted within the drum and wetted with water. The sand was also wetted with leachate in separate trials.

The sand and plastic mixture showed the greatest moisture content overestimation (as expected), followed by the wood mixture and the leachate wetted sand. The ferrous mixture returned an underestimation of moisture content as a result of the neutron-capture effect.

For large-scale testing, Yuen et al. (2000) installed seven 12 m-long aluminum access tubes in an experimental MSW cell. The resulting measurements exhibited considerable scatter to an extent where a field calibration for moisture content was not possible. It was also not possible to determine the reason for the scatter, as it could be the combination of several materials affecting the neutron count.

Considering this inability to achieve a field correlation between the neutron reading and moisture content, this technology would not be suitable for the proposed application. Also, as the neutron probe cannot be used remotely for real-time logging, its merits for use in this MSW study are few.

2.3.3 TDR /TDT

TDR has been tested to a greater extent than neutron probes in MSW. Li and Zeiss (2001), Masbruch and Ferre (2003) and Khire and Haydar, (2007) have all evaluated the use of this technology for use in municipal solid waste.

Li and Zeiss (2001) conducted a series of laboratory experiments with two objectives. The first goal was to determine a calibration equation for TDR response and volumetric

moisture content in a range of MSW materials. The second objective was to quantify the effect of leachate electrical conductivity and attempt to compensate for its effect on the TDR calibration.

Extracting samples from the Clover Bar landfill, in Edmonton, AB, Li and Zeiss, (2001) compacted different compositions of waste in a 9.9 cm diameter cell with a TDR sensor embedded within. Each mixture of waste was tested with leachate (conductivity of 2.45 S/m) and water. The moisture content was varied and correlations were made between volumetric moisture content and the bulk dielectric constant for each trial composition.

Based upon their lab results, Li and Zeiss (2001) concluded that the use of TDR in MSW for the purposes of moisture content sensing was promising and empirical correlation curves were generated.

Masbruch and Ferre (2003) conducted similar trials to those of Li and Zeiss (2001), but using TDT instead of TDR. Exhuming in-situ MSW samples from a capped landfill, Masbruch and Ferre (2003) conducted "upward infiltration" tests on these samples in a 0.1 m column, whereby moisture was added at the base. Masbruch and Ferre (2003) conclusions were similar to those of Li and Zeiss (2001); volumetric content measurement in MSW is possible provided material specific calibrations are made.

Despite some promising results, it is the opinion of Imhoff et al. (2007) that TDR/TDT technology does not accurately provide estimates of volumetric moisture content for MSW applications.

2.3.4 Electrical Resistivity Sensors

Electrical resistivity sensors have been field tested in MSW in several projects. Gawande et al. (2003) used a sensor of the design seen in Figure 2.7 to monitor the in-situ moisture content of a MSW landfill. Prior to field installation of the sensors, an attempt was made to calibrate the sensors in the lab using synthetic solid waste, a conductive liquid phase and variable dry densities. It was concluded that using a particle size of 1 mm inside the sensor provided the best mix of speed of response and resolution over expected moisture ranges. The lab trials also indicated that below gravimetric moisture content of 35%, the sensors lost resolution and results became difficult to interpret (Gawande et al., 2003).

The field application attempted by Gawande et al. (2003) was met with mixed results. Immediately after installation the resistance value returned by the sensors indicated results corresponding to a gravimetric moisture content below 35%. This implied that the actual moisture content could not be determined with guaranteed accuracy due to a loss of resolution. Following a precipitation event, however, the moisture content increased to saturation (68%) as reported by the sensors. Subsequent extraction of waste nearby indicated an actual moisture content of 58%. Gawande et al. (2003) suggest that moisture drainage from the samples during extraction may have been to blame for the disparity of results.

2.3.5 Partitioning Gas Tracer Test

Both a laboratory (Imhoff et al., 2003) and a field study (Han et al., 2006) have been recently conducted in an attempt to evaluate the applicability of the PGTT in waste media.

Imhoff et al. (2003) was the first to apply the PGTT technology to MSW. The PGTT test was carried out on four different proportions of waste composition, each at different moisture content over the range of 6% - 39% by volume and each with a variable bulk density. Materials included in the column were yardwaste, foodwaste, paper, plastic and glass.

Using helium and difluoromethane as the conservative and partitioning tracer, respectively, Imhoff et al. (2003) were able to measure the volumetric moisture content of the waste mixes (Figure 2.8). The error, on average, was about 15% with no apparent trend of overestimation or underestimation. The maximum error observed was 48%.

Han et al. (2006) applied this technology in a combined lab and field study. In the laboratory, Han et al. (2006) conducted PGTTs to a well-characterized filter-paper at varying moisture contents to determine the ability of the technique to detect moisture in small pores as a precursor to application in MSW. Additionally, PGTTs were completed on dry refuse to observe the test results when there is no moisture present.

The filter-paper tests yielded accurate results at all moisture contents except for completely dry and humidified paper. The dry paper tests indicated more moisture than a subsequent test with slightly humidified filter-paper. It was concluded that the sorption of difluoromethane onto paper surfaces causes the delay in the arrival of the partitioned tracer, and when the paper is humidified, sorption is decreased (Han et al., 2006).

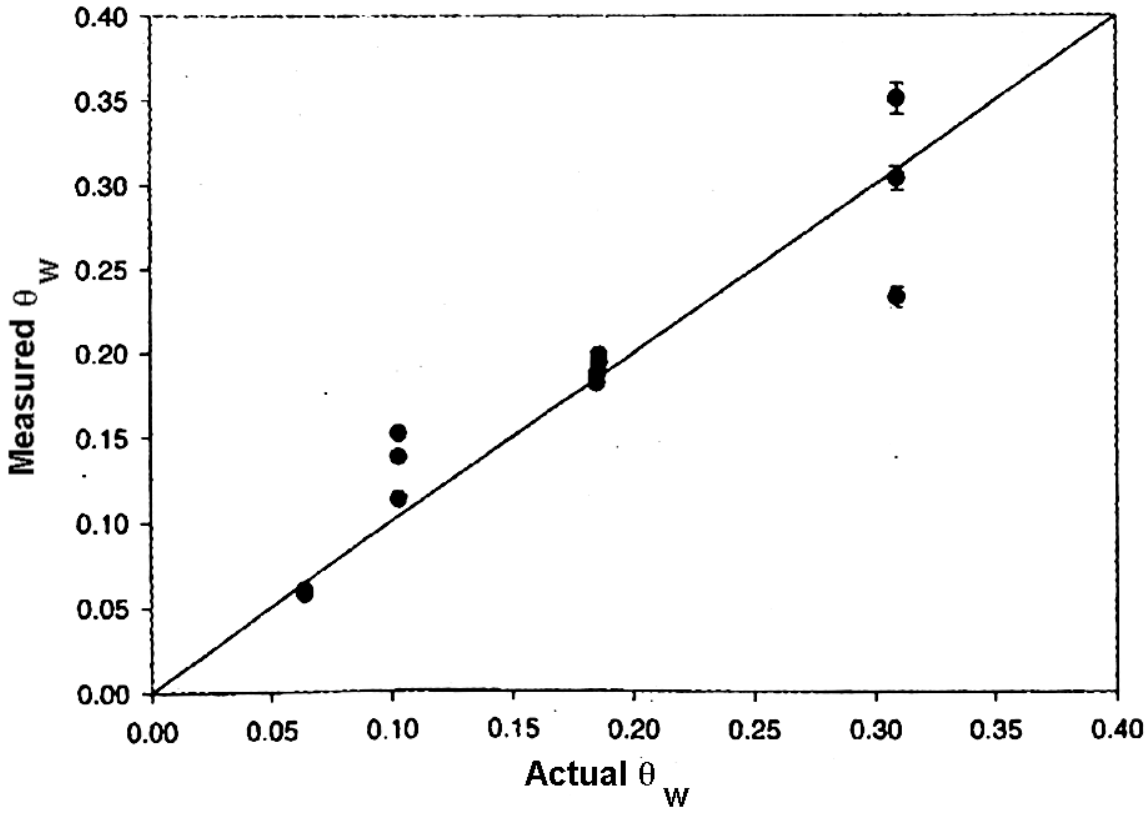

Figure 2.8 - Measurement of volumetric moisture content versus the actual volumetric moisture content in MSW by means of PGTT. θ_w refers to the volumetric moisture content (Imhoff et al., 2003).

Contrary to expectations, tracer tests conducted in dry waste indicated negative moisture content. To achieve this result, it requires that the partitioned tracer arrived ahead of the conservative tracer. It was concluded that the likely reason for this is the greater diffusion coefficient for helium as compared with difluoromethane when very fine pores are in the system (as they are in dry waste) (Han et al., 2006).

Han et al. (2006) conducted seven tests in the field by over a period of 12 months at a municipal solid waste landfill in Delaware. All seven tests were conducted just beneath the landfill cap at the same location. The injector and sampling wells were 1.2 m apart and screened between depths of 1.8 m and 3.5 m, allowing for all of the waste to be exhumed for gravimetric testing following the final test.

The first test indicated that the waste had a gravimetric moisture content of 20.5% though four months later tests #2 and #3 indicated negative or near-zero values for moisture content. Despite some discrepancies with gas sampling data, it was concluded that these results were accurate as there was little precipitation over the elapsed four months.

The final tracer test was compared to the subsequent sampling of the waste in the region of the trials. The tracer test yielded gravimetric moisture content of 24.7% while gravimetric sampling showed a moisture content of 26.5%. Overall, Han et al. (2006) concluded that the PGTT was a very reliable method but recommended further study into the behavior of gas tracers under little or no moisture.

2.3.6 Electrical Resistivity Tomography

Grellier et al. (2003, 2005), Moreau et al. (2003) and Guerin et al (2004) have all investigated the use of this technology at a bioreactor site in France. The surveys generated quick resistivity cross-sections during moisture infiltration and were conducted over short periods of time to minimize the effects of decomposition on the overall change in resistivity. Despite the ability to map resistivity changes within the landfill, estimations of volumetric moisture content could not be made by these studies.

More recently, Grellier et al. (2007) attempted to make a direct correlation between electrical resistivity and the moisture content of MSW. At three locations borehole sampling was conducted to determine the moisture content of the waste. ERT surveys were also conducted at these locations to correlate the ERT data with the moisture content of the sampled waste. Using Archie's law and the moisture content from borehole samples, the resistivity at downhole locations was calculated and then compared

to the resistivity generated by the ERT surveys. Additionally, the ERT resistivity data was used to calculate the moisture content and was then compared to moisture contents derived from borehole sampling. (Figure 2.9)

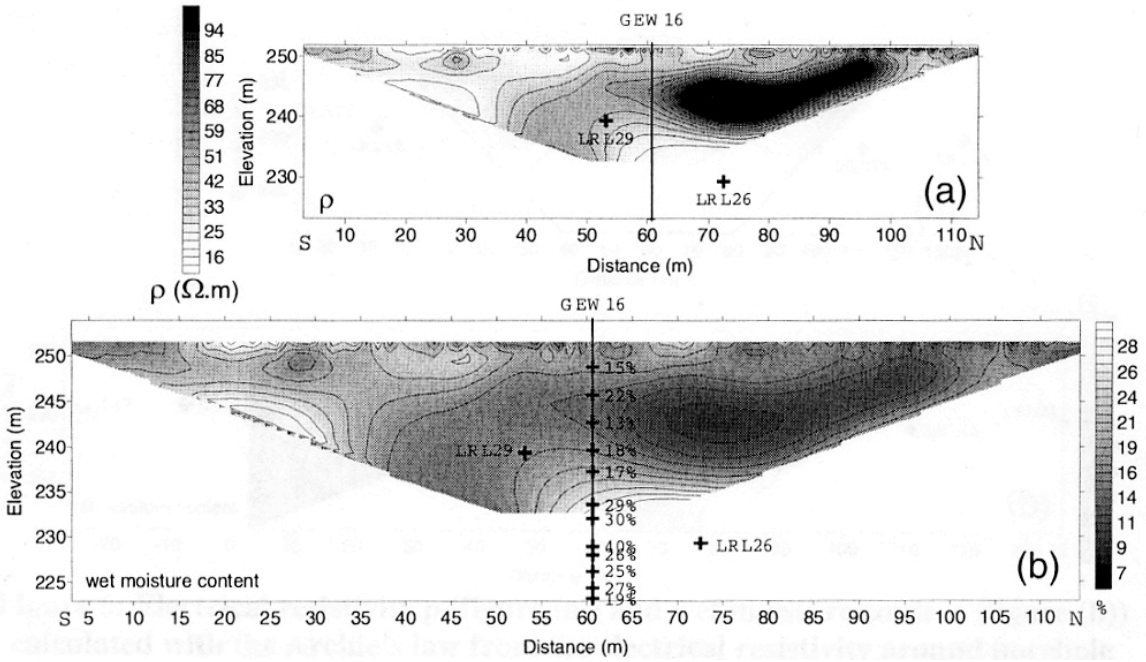

Figure 2.9 - Electrical resistivity (a) and the gradient wet moisture content (b) calculated using Archie's law from the electrical resistivity using the ERT survey around the borehole GEW-16. The wet moisture contents from the borehole sampling are shown (Grellier et al., 2007).

Grellier et al. (2007) concluded that the method worked well but acknowledged the difficulty in applying it routinely. Since the properties of the waste are spatially variable and changing continuously, the empirical parameters for the correlation must also be altered.

Jolly et al. (2007) monitored a planned infiltration event using continuous ERT surveys but did not attempt to correlate resistivity data with moisture content. Jolly et al. (2007) were able, however, to observe regions of wetting due to the moisture addition event.

2.3.7 Evaluation of moisture sensing technologies for MSW

The technologies discussed in Section 2.3 have been tested to varying degrees to determine appropriateness of use in MSW. Each technology has drawbacks and advantages. Table 2.1 outlines these characteristics for each technology.

There are constraints to the selection of a moisture sensing technology for this project that the method of choice must not violate. The selected moisture sensing technology must:

- have the potential to provide a quantitative estimation of moisture content
- provide accurate moisture estimation over all ranges of moisture content;
- be able to monitor the moisture conditions remotely and continuously with no personnel present;
- not be influenced by the composition of MSW to the extent of rendering the results unusable; and
- not be prohibitively expensive or require excessive amounts of human resources to operate.

Considering these constraints the following technologies could not be considered for use in this project for the respective reasons:

- Neutron probe - cannot be used remotely
- ERT - does not provide quantitative moisture content data.
- Electrical resistivity sensors - do not provide accurate moisture data below 35% moisture.
- PGTT - need excessive time requirements for each test and not currently setup for automated measurement.

Table 2.1 - Advantages and disadvantages of some existing technologies for moisture sensing in MSW. Adapted from Imhoff et al. (2007).

Sensing Technology	Advantages	Disadvantages
Neutron Probe	-Moisture content can be measured regardless of its physical state in soils or waste -Offers large radius of influence (150mm – 700mm in wet or dry soil, respectively)	-Measurement of absolute moisture content is difficult -Presence of non-water bound hydrogen interferes with the measurement -Some elements other than hydrogen have a propensity to absorb high-energy neutrons -Changes in density affect the results -The radioactive source of neutron probe is a highly regulated material -Automation is not possible
Electrical Resistance Sensors	-Sensors are relatively inexpensive - Sensor installation is easy - Automated measurement is possible - Can be produced inexpensively - Density does not affect readings - Fast response to leachate front arrival	- Sensors suffer from hysteresis at low moisture contents - Results affected by changes in electrical conductivity and temperature - Once wet the sensors do not drain quickly - Sensor must be calibrated using extracted waste
Time domain reflectometry / time domain transmissivity and capacitance	- Sensors are relatively inexpensive - Results are reproducible - Automated measurement is possible - Fast response to leachate front arrival	- Results affected by changes in electrical conductivity - Local heterogeneity of material properties affects the results - Sensor must be calibrated using extracted waste
Electrical resistivity tomography	- Non-intrusive technique - A two-dimensional evolution of a leachate injection plume can be obtained - Fast response to leachate front arrival	- Requires the knowledge of leachate electrical conductivity - Needs measurement of in situ temperatures from additional temperature sensors - Expensive instrumentation costs - Technique not evaluated for moisture content measurement
Partitioning Gas Tracer Test	- Provides reasonably accurate assessment of moisture content - Measurement accuracy is unaffected by the measurement volume - Relatively inexpensive field setup is required - Tracer gases can be injected through existing injection wells of a landfill	- Gas sample collection and laboratory analysis pose difficulty for automation - Needs measurement of in situ temperatures from additional temperature sensors - On larger scale provides assessment of average conditions and may not identify relatively wet spots

2.4 Capacitance Moisture Sensors

2.4.1 Introduction

As discussed, the constraints of cost and required human resources were important factors and excluded promising methods such as ERT and PGTT. The neutron probe and electrical resistance sensors were also shown to be not ideal for use in this project.

Considering the relative effectiveness of TDR technology for use in MSW, it stands to reason that capacitance sensors could provide similar results as both technologies measure the same medium property (electrical permittivity) to estimate moisture content.

Capacitance probes also have several advantages over TDR/TDT that made them more suitable for this application. TDR probes require that the electrodes remain in intimate contact with the waste, and cannot generate a continuous profile over depth without the installation of a continuous array of sensors. Since capacitance sensors are used in preinstalled access tube, they can be used to obtain a continuous "swipe" of data with one sensor as deep as required (provided successful access tube installation). Ultimately, this decreases cost and ease of installation because fewer sensors are required. Like TDR sensors, capacitance sensors can also be used in-place.

The application of capacitance sensors in this project will provide important insight as to their suitability in MSW, and could prove to be a practical and inexpensive tool.

This section outlines in greater detail the theory of operation and the effects of the *in-situ* MSW conditions may have on the capacitance sensors. Since there have been no published investigations of suitability of capacitance moisture probes in MSW, the majority of the relevant literature relates the use of these probes in soils. The following

sub-sections will address factors that may affect the sensor's operation, based upon these studies in soil.

2.4.2 Fundamental Theory of Operation

The operation of the capacitance sensor relies upon the high permittivity of water. Permittivity is also represented as a unitless dielectric constant that is relative to the permittivity of a vacuum. Water has a greater dielectric constant than other naturally occurring soil constituents, with a value of ~80. The dielectric constants of other materials can be seen in Table 2.2. Permittivity represents the degree to which a material will align its poles to an induced electric field. Greater permittivity thus results in greater capacitance, or, the ability for the medium to store energy from the induced field as represented by the following relationship:

$$C = g\varepsilon_r\varepsilon_o \qquad [1.1]$$

where C is capacitance, g is a geometric factor resulting from the electric field penetrating the medium, ε_r is the dielectric constant of the medium and ε_o is the permittivity of a vacuum (Kelleners, et al., 2004a)

The material(s) within the electric field storing this energy is called the dielectric. It is recognized, then, that in the soil-water dielectric system, the presence of water will greatly change the capacitance of the system relative to the influence of the soil constituents.

Table 2.2 – Dielectric constants of various materials. Compiled from Nadler et al (1996), Polyakov et al (2005), and Stacheder (2005).

vacuum	0
air	≈1
soil constituents	4-9
organics	6-8
water	≈80
ice	≈3

To measure the in-situ capacitance of the soil-water system, the soil and water must comprise the dielectric of a capacitor. To achieve this the capacitor plates are placed one above the other in the shape of circular rings, as seen in Figure 2.4, causing the electric field to arc beyond the sensor housing, into the soil-water system. The capacitor plates cannot directly be in contact with moisture so the sensor must be encased in a plastic tube. As a result, the plastic tube also becomes part of the dielectric, however, its contribution is constant over all soil-moisture conditions. To measure the capacitance of the system, the electric field must oscillate. The capacitance of the soil, water and plastic tube will influence the resonant frequency, as represented by the following equation:

$$F = \frac{1}{2\pi\sqrt{LC_t}} \qquad [1.2]$$

where F is the resonant frequency, L is the circuit inductance and C_t is the total capacitance of the system. It is this resonant frequency that the sensor measures. From Equation 1.2, it is apparent that with an increase in capacitance the resonant frequency will be lessened. Therefore the more water present in the system, the lower the resonant frequency.

Kelleners et al. (2004a) described an equivalent circuit of a capacitance moisture sensor shown in Figure 2.10. For this circuit the total capacitance, C_t, would equal:

$$C_t = C_s + \frac{C_p C}{C_p + C} \qquad [1.3]$$

where Cs is the stray capacitance of the circuit, Cp is the capacitance of the plastic tube and C is the capacitance of the dielectric soil-water system. Equation 1.2 then becomes:

$$F = \frac{1}{2\pi\sqrt{L(C_s + \frac{C_p C}{C_p + C})}} \qquad [1.4]$$

Equation 1.3 is only valid if the dielectric is non-lossy (i.e. there is no current leakage across the dielectric, nor loss from dipole relaxation of the dielectric). Because water is conductive this affect on capacitance must be accounted for. The nature of lossy dielectrics can be described through permittivity, which is a complex function:

$$\varepsilon_r^* = \varepsilon_r^{'} - j\varepsilon_r^{''} \qquad [1.5]$$

where ε^*_r is the complex dielectric constant of the soil-water medium, $\varepsilon^{'}_r$ is the real portion of the dielectric constant (representing energy storage) and $\varepsilon^{''}_r$ is the imaginary portion of the dielectric constant (representing energy losses), and j^2 is -1. The imaginary portion of the dielectric constant can be further described by:

$$\varepsilon_r^{''} = \frac{\sigma}{\omega\varepsilon_o} + \varepsilon_{r,rel}^{''} \qquad [1.6]$$

where σ is conductivity, ω is angular frequency (=2πF) and $\varepsilon^{''}_{r,rel}$ is the loss factor due to relaxation (-). As a result of the losses across the dielectric, the capacitance of the medium, C, becomes a complex capacitance: C*:

$$C^* = C' - j(\frac{g_m\sigma}{\omega} + g_m\varepsilon_{r,rel}^{''}\varepsilon_o) \qquad [1.7]$$

where C' is the real capacitance of the medium. The dielectric loss, G from Figure 2.10, can be described as:

$$G = g_m \sigma + g_m \omega \varepsilon''_{r,rel} \varepsilon_o \qquad [1.8]$$

where g_m is the geometric factor of the medium and G is expressed in Siemens.

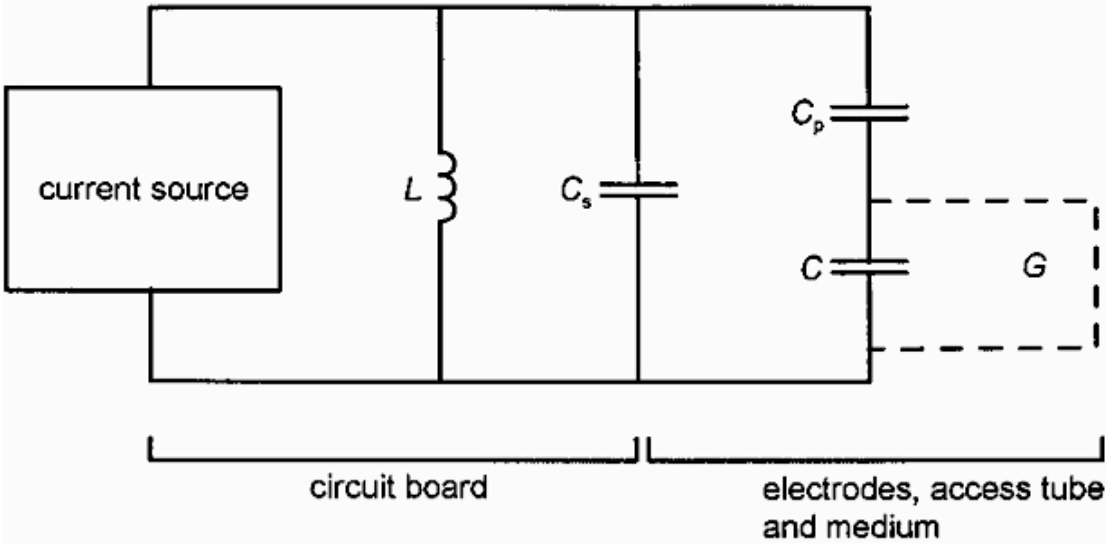

Figure 2.10 – Equivalent circuit of a Sentek EnviroSCAN capacitance sensor. *L* denotes the inductance of the circuit, C_s is the stray capacitance of the circuit, C_p is the capacitance of the plastic access tube, *C* is the capacitance of the sensed medium and *G* is the loss due to conductivity or relaxation of the sensed medium (Kelleners et al, 2004a).

By using the capacitance sensor to measure resonant frequencies in conditions of known moisture contents in a controlled environment, the sensor can thereby be calibrated to report in-situ moisture contents.

2.4.3 Effect of Ionic Strength

As the electrical conductivity of the system increases the losses, the resistivity decreases resulting in an increase in effective capacitance (Dean, 1994). As outlined mathematically in Equation 1.4, an increase in capacitance will cause a decrease in the resonant frequency and thus overestimate the amount of water in the soil-water system (Kelleners et al, 2005; Li and Zeiss, 1999). When applying capacitance sensors in MSW this effect must be taken into account, as MSW leachate is generally saline and therefore conductive.

Kelleners et al. (2004) tested the sensitivity of the capacitance sensor to conductivity in a variety of liquids, each varying in conductivity and dielectric constant. Results were compared to calculated values based on upon analyzing the sensor's circuitry. **Figure 2.11** shows that for the dielectric constant of water (~80), increased conductivity will depress the resonant frequency.

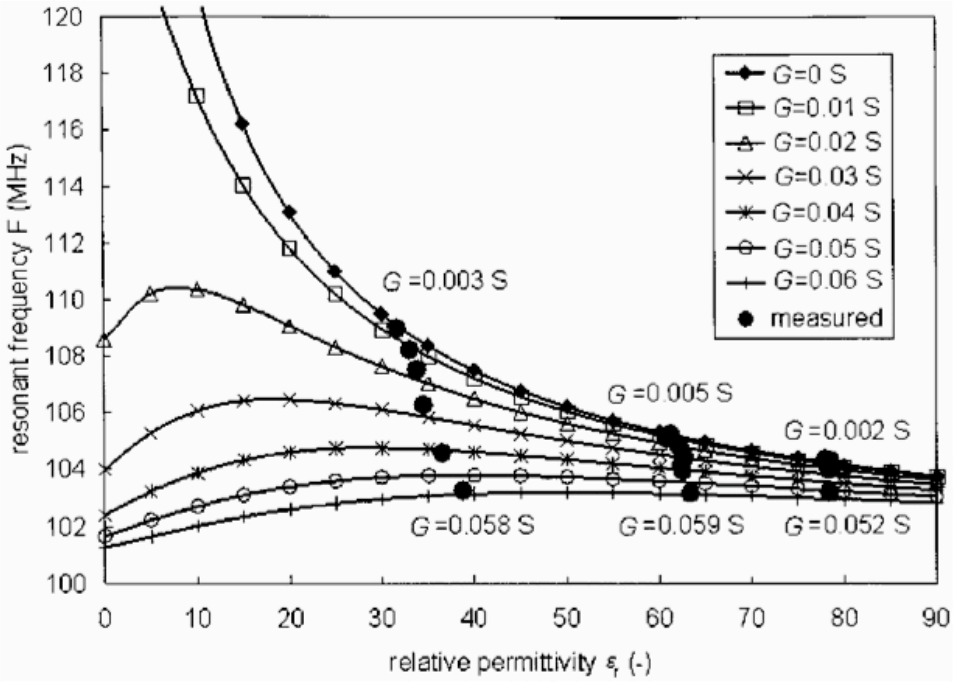

Figure 2.11 – Results of measurements (solid circles) and calculations (trendlines) relating the relative permittivity and losses due to conductivity and relaxation (G) to the resultant resonant frequency. The resonant frequency has been depressed at dielectric constants around that of water (~80) due to dielectric losses (Kelleners et al., 2004a).

Overestimation of volumetric moisture content from dielectric losses from porewater conductivity may be extreme, especially at high moisture contents. Kelleners et al. (2004b) reported errors of +0.35 m3/m3 using the manufacturer's calibration curve in soils with actual volumetric moisture content of 0.40 m3/m3 at conductivities of ~90 dS/m. By calibrating the correlation between resonant frequency and volumetric moisture content, the errors could be corrected for.

2.4.4 Clay Content

As mentioned previously, the ability for the capacitance method to sense moisture relies upon water's freedom to align its poles with the induced field. However, in the presence of clay, some water will become bound to clay surfaces and respond differently to the field. Wang and Schmugge (1980) and Wang (1980) conducted experiments relating the behaviour of water in clay-bound states, and concluded that the dielectric constant of water becomes approximately 4.

Polyakov et al (2005) conducted field and laboratory calibration trials using a sandy soil and a silty clay loam using Sentek capacitance sensors. It was concluded that the default (manufacturer) sensor calibration underestimated the moisture content in the silty clay loam, presumably, due to bound water. (Manufacturer calibrations between sensor response and moisture content are typically derived without the consideration of complex effects such as ionic conductivity or clay content.)

However, laboratory studies using bentonite (Kelleners et al, 2005) have indicated that large amounts of clay may contribute to the permittivity of the soil due to additional polarization of clay minerals and cause an overestimation of moisture content.

Clay content is expected to be less of a concern in MSW, though its extent throughout the waste mass cannot be known exactly as there will be intervals of intermediate and daily cover within the waste mass.

2.4.5 Organic Content

Though the clay fraction in MSW is expected to be minimal, organics typically provide the bulk of the waste mass in municipal landfills, thereby contributing the most important response (Tatarniuk, 2007). Few studies have been conducted to specifically

investigate the effect of organics on capacitance moisture probes, but observations have been made in related tests.

For example, Gardner et al. (1998) tested various soil horizons, each containing different amount of organic matter, represented by organic carbon contents ranging from 5.4% to 0.5%. These soils were tested at moisture contents ranging from oven-dry to saturation. By analyzing the different soil compositions Gardner et al. (1998) were able to determine that the organic matter content did not alter the bulk permittivity of the soil to a significant extent.

Nadler et al (1996) suggested that although organic content may be relatively large, its contribution to the overall relative permittivity of the soil would not be significant due to its low dielectric constant ($\varepsilon_{om} \approx 6\text{-}8$). It should be noted that despite elevated organic content, the dielectric constant of organics is not that dissimilar from mineral soils ($\varepsilon_s \approx 4\text{-}9$) (Nadler et al., 1996).

A longer-term effect of the high organic content of MSW will be the resulting degradation of organics and density increase change over time. Since the sensors relate volumetric moisture content, this process will alter pore structure, thereby altering the established correlation between capacitance sensor data and moisture content.

2.4.6 Operational Frequency

To call the relative permittivity a "dielectric constant" is a misnomer. In fact, the dielectric "constant" actually varies with the frequency of oscillation. Early investigations into capacitance sensors attempted moisture measurement at frequencies in the kHz range. Below ~27 MHz, water is a relaxed dielectric and capacitance sensors cannot be relied upon to give meaningful results (see Figure 2.12). Thomas (1966) first

conducted trials with a capacitance sensor operating at 30 MHz and was able to sense moisture contents within 0.5% (by volume) of actual.

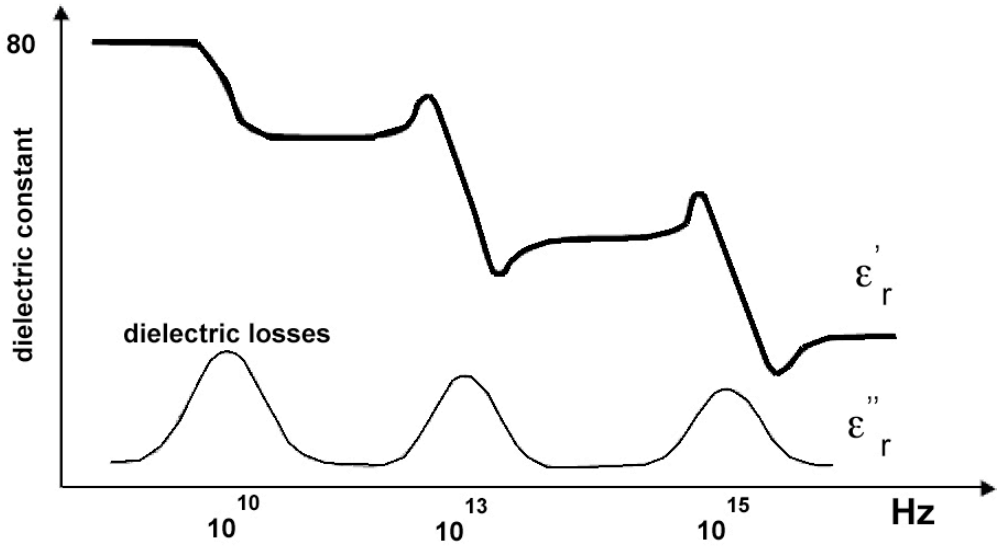

Figure 2.12 - Relationship between the real and imaginary portions of the dielectric constant of water and the frequency of oscillation. The far left plateau of ε'_r corresponds to the dielectric constant for dipole polarization. Subsequent plateaus are for atomic and electrical alignment, respectively. The imaginary portion of the dielectric constant is plotted beneath. Redrawn from DoITPoMS (2010).

Currently, most commercial capacitance sensors operate in the 100 MHz (10^8 Hz) range, at which the dielectric constant of pure water is relatively constant at ~80. This frequency is high enough to avoid extreme dipole relaxation of water and lessen the losses due to system conductivity, though this phenomenon is not entirely eliminated (Kelleners et al., 2004b). Recently, Kelleners et al (2005) investigated further the effect of sensor frequency on the sensing of water in sand and clay environments. It was concluded that above 500 MHz, losses due to conductivity and clay ion interference are minimized.

2.4.7 Temperature

With capacitance sensors used in many different climactic zones and field conditions, the effect of temperature on the circuitry and the electrical properties of the sensed medium must be considered.

In one of the pioneering investigations of capacitance sensors, Dean et al (1987) tested the effects on moisture sensing accuracy across a temperature range of 0°C - 30°C. Over that range, the volumetric moisture content was found to be incorrect by an amount equivalent of +10%. It was not revealed however, at what actual moisture content those readings were taken.

In a more recent study, Paltineanu et al (1997) concluded that temperature changes in the range of 10°C - 30°C would have a negligible effect on the sensed volumetric moisture content, though a 1% change in θ_w was realized at a temperature of 50°C. Paltineanu et al (1997) neglected to comment on the cause of the observed error, though Dean et al (1987) suggested the error was attributed to effects on the sensor circuitry.

In other studies, the variance of sensed moisture content with temperature differences has been associated with clay content. Wraith et al (1999) experimentally demonstrated that the bulk permittivity is increased with temperature in the presence of clay-rich soils, resulting from the release of bound-water. Polyakov et al (2005) also noted a positive error when clay-rich soils were sensed under elevated temperatures. When sensed at 45°C, there was a +15% error in the actual volumetric moisture content (Polyakov et al., 2005).

Conversely, it appears there is little or no temperature dependent behaviour when sensing mineral soils. Yu et al. (1999), using theoretical methods, established that the permittivity of mineral soils do not vary significantly with temperature.

When considering temperature effects on capacitance sensors in MSW, the temperatures that occur may be beyond the range of previous studies. Internal temperatures of MSW landfills can be extremely variable. Temperatures of 50°C would not be uncommon, and temperature will likely increase with depth (McBean et al., 1995). The top portion of waste (0m-15m depth) could be influenced by ambient climactic conditions, though the remainder of the waste is likely not (McBean et al., 1995). It can then be inferred that the temperatures near surface could range from below freezing to as high as the summer-time ambient temperatures, or higher given the flux of heat from the waste mass below (McBean et al, 1995).

It should also be noted that ice does not have the same dielectric constant as liquid water, since it can be considered "bound" by its crystal lattice. Stacheder (2005) reports a dielectric constant of approximately 3 for ice, similar to typical soil constituents.

2.4.8 Bulk Density

Since permittivity is defined as the electric dipole moment per unit volume, all correlations between the dielectric constant and moisture content must be conducted volumetrically (MSW moisture content as percent by volume). This presents challenges for *in-situ* applications as sampling must be conducted carefully, so as not to disturb the original density. Additionally, and especially in the case of MSW, density can change over time from degradation of organics and long-term settling, affecting the volumetric moisture content (SWANA Applied Research Foundation, 2004).

Though the response from the non-water soil components is relatively small, as inferred by the small relative dielectric constant (4-9), the effect must still be considered. Huang et al (2004) attempted to calibrate several types of dielectric sensors for specific soil types both in the laboratory and in the field. Soil bulk densities ranged from 1200 – 1600 kg/m^3 in the laboratory and 1160 – 1510 kg/m^3 in the field.

Huang et al. (2004) concluded that with increasing soil bulk density, the sensors further overestimated the volumetric moisture content at a factor of roughly 0.05 m^3/m^3 per 20 kg/m^3 increase in soil bulk density. These results are in agreement with Jacobson et al (1993) who concluded similarly that increasing bulk density overestimates the volumetric moisture content for constant calibrated parameters.

In MSW, the *in-situ* bulk density is typically less than found in soils (except in zones of daily cover). According to McBean et al. (1995) the average density of compacted waste, before long-term settlement, is ~ 700 kg/m^3. Due to extremely heterogeneous composition, this can be expected to vary spatially within the waste mass.

Of further concern is the variability of the bulk density as a function of time. As the waste mass degrades and settles the density will increase and the accuracy of the sensed moisture content based on previous conditions may diverge from the actual moisture content.

2.4.9 Void Space and Installation Considerations

Air-gaps surrounding the downhole access tubes for capacitance sensors were indentified immediately as a cause of error for downhole capacitance sensors (Bell et al., 1987). Several studies have been conducted, attempting to determine the vertical and horizontal extent of the probe's sensitivity.

Dean et al (1987) were the first to develop a downhole, PVC bound capacitance sensor. They reported that 90% of the vertical sensitivity reading was from ± 8.5 cm from the centre of the sensor and that the horizontal radial sensitivity was 7.5 cm.

Using Sentek EnviroSCAN capacitance sensors (the type used in this study), Polyakov et al (2005) have reported that 99% of the sensor's response is within a 10 cm radius from the sensor's axis and Paltineanu et al (1997) reported that 99% of the sensor's response is within 10 cm of the PVC wall and the axial sensitivity is ±5 cm.

These qualities have important implications for field use. Because of the very small volume of soil/MSW affecting the sensor reading and as air has a dielectric constant of 1; the presence of void space will significantly influence the sensor's response (Bell et al., 1987). Installation procedures must be conducted carefully to minimize the amount of void space and ensure a tight fit between the PVC sensor housing and the surrounding waste matrix.

2.4.10 Accuracy and Expectations of Capacitance Sensor Technology

Included with capacitance moisture sensor technology, is the manufacturers calibration for correlation between sensor response and volumetric moisture content. This calibration is intended to provide a basic correlation in "average" soils (i.e. mineral soils without conductive pore-fluid or other complex constituents) (Sentek). In ideal situations the manufacturer's correlation may yield results of $\theta=\pm 0.01$ m^3m^{-3}.from the actual volumetric moisture content (Baumhardt et al., 2005).

In soils with conductive pore-fluids or elevated clay content, site-specific calibrations must be made to achieve accurate results. Gardner et al. (1998) utilized a relative permittivity-mixing model whereby they estimated the relative permittivity of a given

soil by assigning each soil, water and free-space fraction and a dielectric constant (with the sum of these fractions equaling 1). Using this technique with an empirical correlation between resonant frequency and relative permittivity, the water fraction could be calculated. In clayey soils Gardner et al. (1998) experienced errors in measurement of up to $\theta=\pm 0.24\ m^3m^{-3}$, however moisture measurement in silica soils saw a maximum error of $\theta=\pm 0.04\ m^3m^{-3}$.

Permittivity mixing models were not considered for use in MSW due to the large number of constituents, each possessing unique relative permittivities and spatially variable composition fractions.

CHAPTER 3 MATERIALS AND METHODS

3.1 Introduction

Chapter 3 outlines the materials and methods used by this study to evaluate the effectiveness of capacitance sensors in MSW. Experimental trials were first conducted in the laboratory setting to establish a basis for field application. Following the laboratory trials, two distinct, co-current, field studies were carried out. The first was the evaluation of a continuous-time at discrete-depth probe configuration (utilizing the EnviroSCAN probes). The second was the evaluation of a continuous-depth at discrete-time probe configuration (utilizing the Deep Diviner probe).

3.2 Laboratory Testing: Materials and Procedure

3.2.1 Introduction

Since the capacitance moisture sensors have never been used in waste, laboratory testing was an important initial step. By attempting to correlate capacitance sensor readings in waste across a range of moisture contents, a basis for field installation could be achieved.

3.2.2 Laboratory Probe and Apparatus

The sensor used in laboratory trials was the Diviner 2000 (Figure 3.1) manufactured by Sentek (Sentek Pty Ltd.) of Australia. The Diviner 2000 is a manual capacitance probe, accompanied by a handheld control and logging unit. It is capable of sensing and recording soil moisture data up to a depth of 1.6 m below the top of the access tube. The capacitance sensor oscillates at frequencies above 100MHz, though the exact frequency depends upon the bulk permittivity of the sensed medium (Sentek Diviner 2000 Manual).

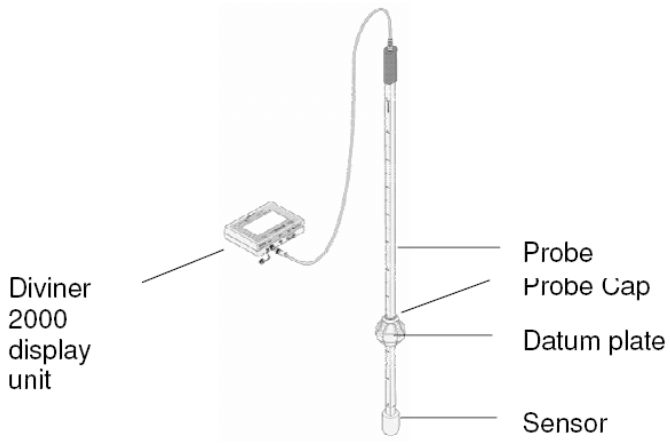

Figure 3.1 - Sentek Diviner 2000 capacitance probe (Sentek Diviner2000 Manual).

The vessel for waste compaction, and moisture addition, seen in Figure 3.2, was a 0.3 m inner-diameter HDPE pipe, 0.75 m in height, connected by means of tie-rods to a PVC base. The pipe and base interface were sealed with silicon to prevent loss of moisture.

Running longitudinally down the centre of the pipe was a specially manufactured PVC access tube with an inner diameter of 51 mm. Within the access tube was a plug, 0.1 m in length, at the bottom of the tube to prevent moisture from entering the access tube from the base. The access tube is also sealed by silicon to the PVC base to ensure stability and to prevent the ingress of moisture.

Three piezometers were installed along the side of the vessel at 0.15 m, 0.3 m and 0.45 m from the base. Their purpose was to ensure there were no perched water tables and that saturation was complete at the end of each lab trial.

Figure 3.2 - Lab apparatus for compaction and testing of moisture content in MSW, pictured here in a saturated condition at the end of a trial. The vessel in this photograph is 0.75m tall.

3.2.3 Waste Properties

The waste that was used in the laboratory trials were samples that had been taken from a depth of approximately 7.6 m from within the Spadina Landfill. Table 3.1 outlines the general waste composition and characteristics of the MSW samples used in laboratory testing. The waste components recognized at the Spadina landfill by Tatarniuk (2007) were divided into four categories:

- wet putrescible: readily degradable organics (grass, leaves, etc.);
- dry combustible: dry organics (paper, wood, etc.);
- inert: non-degradable components (metal, glass, etc.), and
- plastic.

Table 3.1 - Waste composition and characteristics from previous studies at the Spadina landfill.

Waste component	(From Tatarniuk, 2007)	
wet putrescibe	45	%
dry combustible	39	%
inert	7	%
plastic	9	%

Waste characteristic	(From Singh and Fleming, 2004)	
volatile solids	53.5	%
age	~30	yrs
redox potential	+200 to -120	mV
pH	7.8	
in-situ m/c	21	% grav.

The waste composition provided by Tatarniuk (2007) does not include the presence of daily or intermediate cover soil, which was present in the laboratory samples used in this study. The amount of cover soil in these laboratory samples was assumed to be representative of the overall landfill composition, though its exact amount was not known due to mixing.

Singh and Fleming (2004) studied other waste characteristics important to potential methane production. Volatile solids are determined by loss-on-ignition testing. The amount of volatile solids is considered to be an indicator of the amount of available organic material present in the waste that can be converted to methane upon degradation.

Redox potential indicates the tendency of the solution to either gain or lose electrons within the waste. In an MSW environment a low (negative) redox potential indicates anaerobic conditions ideal for methanogenesis, whereas a high redox potential indicates less than ideal conditions (i.e. aerobic). The pH of the waste before drying was found to be 7.8 and the *in-situ* moisture content was, on-average, 21% by weight.

3.2.4 Laboratory Procedure

The laboratory procedure was as follows:

1) Determine the desired bulk density of waste for the laboratory trial;
2) Determine how much dried waste was needed for compaction in vessel. From the desired bulk density, knowing the entire volume of the vessel that will be filled and assuming a moisture content of 30% by weight, the weight of the dried waste was calculated;
3) The dried waste was compacted in the vessel while adding a known amount of moisture in 0.1 m lifts;
4) With the vessel filled and compacted with waste of known density and moisture content, initial measurements were taken with the Diviner 2000;
5) 5% moisture by volume was added to the top of the waste column and let stand for 12 hours for the system to equilibrate;
6) Readings were taken after the elapsed 12 hours, then a further 5% moisture by vol. was added;
7) Steps 5 & 6 were repeated until ponding occurred on the surface of the waste and the piezometers confirmed that all zones were saturated.

3.3 Field Studies: Site Characterization and Preliminary Field Work

3.3.1 Site Description

The City of Saskatoon's Spadina landfill was the location of this project's fieldwork. The Spadina landfill has been in operation since 1955 and contains approximately four million tonnes of municipal solid waste. With a footprint of 30.9 hectares, it is located in southwest Saskatoon, with close proximity to the South Saskatchewan River and the

Queen Elizabeth Power Plant. The landfill is approximately 35 m deep from the crest, as of 2004, and no further landfilling occurred at this location throughout the duration of these field trials (Singh and Fleming, 2004).

The Spadina Landfill was constructed initially as a "non-engineered" landfill. As a result, it has no engineered base barrier system or leachate collection system. The landfill sits atop glacial till and terrace sands and any leachate that flows from the base of the landfill will enter these units and flow laterally. To minimize the spread of leachate-contaminated groundwater, trench drains have been constructed as groundwater intercepts. This collected water is diverted to the municipal wastewater treatment plant (Singh and Fleming, 2004).

The fieldwork for this project was conducted on the northern crest area of the landfill as shown in Figure 3.3. This section had been capped with a clay cover of variable thickness. At the time of fieldwork, landfilling was still in operation on the southern portion of the crest.

3.3.2 In-Situ Waste Properties

Saskatoon is located in a semi-arid environment and has an annual rainfall of ~350 mm/year (National Climate Archive – Environment Canada). Singh and Fleming (2004) indicated that the average gravimetric *in-situ* moisture content of the Spadina Landfill in 2004 was approximately 21%. This was based on initial borehole sampling to an approximate depth of 24.4 m.

The bulk *in-situ* waste properties were assumed to be identical to those measured by Singh and Fleming (2004) and Tatarniuk (2007), as in Table 3.1. However, it was

expected that there would be significant spatial variation of these properties, most notably in composition and moisture content.

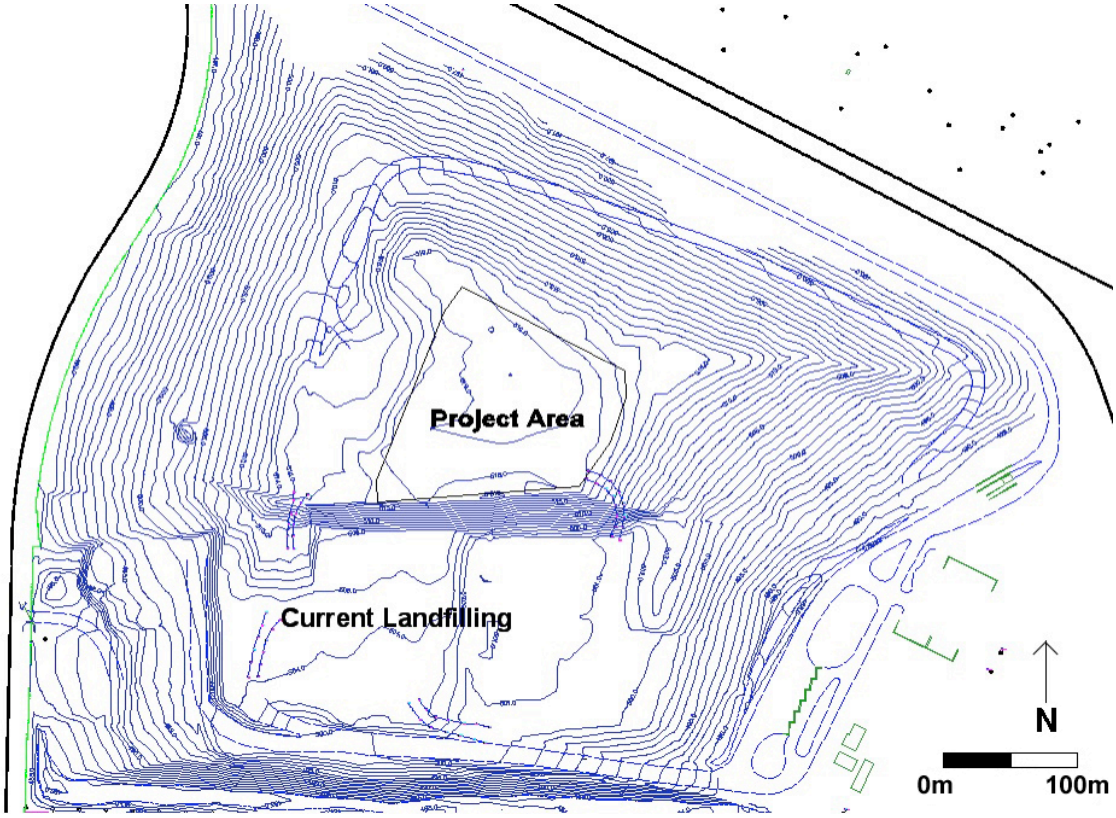

Figure 3.3 - Topographical map of the Spadina Landfill in 2005, showing project area. Topographic intervals are 1.0m intervals with the crest having an elevation of 519m above sea level (Courtesy of City of Saskatoon).

3.3.3 Installation of Access Tubes

Two types of access tubes were installed in the landfill for the purposes of moisture sensing. The EnviroSCAN (ES) probe assembly is designed to be installed in specially made 51 mm PVC access tube (ID=51 mm, OD=56 mm). This results in a friction fit between the sensor electrodes and the tube wall. The Deep Diviner can operate within the more readily available 2" schedule 40 PVC tubing (ID=60 mm, OD=53 mm). The EnviroSCAN access tubes connect by means of threadless external sleeves and the 2"

PVC uses threaded connections. All tube splices used PVC cement or a two-part epoxy to ensure their seal.

As discussed previously, the presence of an air-gap between the access tube and the sensed medium will significantly affect the sensor response (Bell et al., 1987). For this reason, continuous-flight augers were avoided for access tube installation, as they have the tendency to "wobble" laterally during drilling thus widening the hole.

For the best possible downhole conditions, a cone-penetrometer test rig (CPT) (Figure 3.4) was used for installation. The advantage of the CPT technique is that the hole can be continuously cored, providing baseline moisture data, and also, it is a percussive technique that does not widen the hole severely.

In total, four EnviroSCAN probe access holes and 13 Deep Diviner access holes were installed at the landfill (see Figure 3.5; and see Table 3.2 for locations).

The installation procedure of the access tubes using the CPT rig was as follows:

1) For the installation of the Deep Diviner access tubes, the waste was sampled from surface using a 42 mm sampling bit. Samples were taken at 1.5 m intervals. After each sample, all the rods were pulled from the hole to retrieve the sample. In cases where the sampling bit could not penetrate through a particular zone, a 51 mm solid steel cone was sent down the hole and any blockage was broken or pushed aside. Sampling was conducted only for the installation of the Deep Diviner access holes and was not carried out during the installation ES access holes.
2) Sampling was conducted until the interval was complete or the bit became blocked.

Figure 3.4 - Installation of ES and Deep Diviner access tubes using the CPT rig. In this photo, the larger 83 mm casing is being installed following sample coring.

3) With sampling completed, a hollow 83 mm OD casing with a disposable steel cone drive-tip was installed to the bottom of the sampling interval, or as deep as possible.

4) With the hollow casing in the ground, the PVC access tube was placed within the casing, dislodging the disposable drive-tip.

5) The casing was then pulled from the hole, leaving the access tube in the ground with an approximate 20 mm annular gap between the waste and the tube.

Since waste is not removed but only displaced and compressed during the installation of the 83 mm casing, the waste was expected to gradually reclaim the space it occupied and eventually eliminate the air-gap.

Table 3.2 - Location, depth and date of installation of ES and Deep Divner access holes.

Hole ID*	UTM N	UTM E	Final Depth below surface (m)	Date Installed
ES-01	382775.1	5773557.6	5.0	15-Feb-07
ES-02	382779.6	5773559.1	4.3	15-Feb-07
ES-03	382785.1	5773560.9	5.0	15-Feb-07
ES-04**	382790.1	5773562.7	9.5	31-Jul-07
DH-01	382775.8	5773552.7	8.18	30-Jul-07
DH-02	382767.9	5773553.3	7.29	30-Jul-07
DH-03	382757.3	5773554.0	10.09	30-Jul-07
DH-04	382745.9	5773556.9	8.32	30-Jul-07
DH-05	382678.0	5773551.0	8.28	31-Jul-07
DH-06	382720.6	5773613.3	5.03	31-Jul-07
DH-08	382789.6	5773577.0	10.20	1-Nov-07
DH-09	382769.5	5773577.4	10.75	1-Nov-07
DH-10	382758.2	5773591.1	10.49	1-Nov-07
DH-11	382756.2	5773599.0	9.68	2-Nov-07
DH-12	382703.7	5773576.2	5.89	2-Nov-07
DH-13	382716.6	5773550.3	8.93	2-Nov-07

*ES - EnviroSCAN hole, DH - Deep Diviner Hole

**ES-04 was used as DH-07, until ES instrumentation was installed on Dec 12 , 2007.

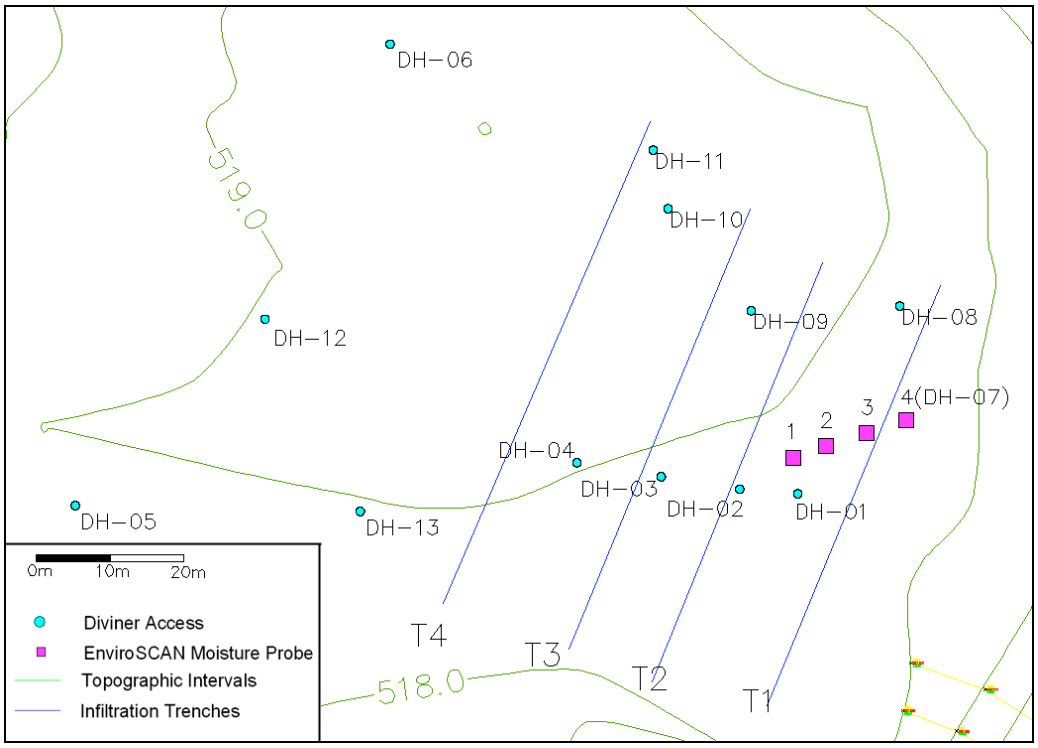

Figure 3.5 - Plan map of Deep Diviner and ES hole locations on the landfill's northern crest.

3.4 Continuous-Time / Discrete Depth Field Testing

3.4.1 EnviroSCAN Probe

Sentek also manufactures the ES capacitance probe system, used in this study. Though it uses a sensor similar to the Diviner 2000, the design differs in several ways. The ES probes are an in-place system and log continuously and automatically at discrete depths of the operator's choice. The primary components of the ES system are:

- ES capacitance sensors (Figure 2.4)
- SDI-12 circuit board (one per probe);
- data-logger system (see Figure 3.6) consisting of:
    - Campbell Scientific CR200 data-logger;
    - 12V Ni-Cad battery;
    - solar panel; and
    - all-weather fiberglass enclosure;
- PVC sensor rail, 20-way ribbon cable and connection ports at 0.1m spacing;
- top handle and access tube cap; and
- 51 mm PVC access tubes in 1 m or 2.5 m lengths with connection sleeves and end-caps.

Each probe will have one uniquely addressed SDI-12 circuit board with the capability to sample from up to 16 ES sensors. As often as is desired (defined by the user in the data-logging program), the logger will communicate to each SDI-12 circuit board which will in turn sample the raw data from each sensor and communicate it back to the logger. Time between sensor samples can be no more frequent than once per second (Campbell Scientific Online Resource).

Figure 3.6 - Logging station (foreground) and ES probe (background).

Figure 3.7 - SDI-12 circuit board, ES top handle and sensor rail.

In the case of ES probes, the data returned moisture data returned as a "scaled frequency". All sensors will not return the same resonant frequency in identical conditions due to inherent differences, so comparison of results between sensors require that each sensor be normalized to return the scaled frequency (*SF*):

$$SF = \frac{(F_a - F_m)}{(F_a - F_w)}$$

where F_a and F_w are the normalization resonant frequencies measured in 100% air and 100% water (or leachate, in this case) for each sensor and F_m is the resonant frequency reading in the sensed medium. In this format, a SF=1 response equals the conditions of 100% water and a SF=0 corresponds to 100% air.

Since conductivity has been shown to affect the accuracy of capacitance sensors (Dean, 1994), the conductivity of the leachate was determined by centrifuging leachate from the samples taken during installation of access tubes. In the laboratory, a batch of

synthetic leachate was then made to match the measured conductivity of 150 S/m in order that the sensors could be normalized with a liquid of similar electrical conductivity.

The data returned and stored in the data-logger has the capability to be converted to volumetric moisture content by using the scaled frequency and inputting empirically established correlation constants to each SDI-12 board, though this feature was not used.

3.4.2 Initial Field Response Testing

After successful installation of the first three ES probes, a field trial was conducted to test the response of the sensors. Since the waste was relatively dry, it was not expected that the natural *in-situ* moisture content would change rapidly and therefore not change the response of the sensors.

To test the initial sensor response, water was percolated into the waste in the vicinity of the installed ES sensors. Figure 3.8 illustrates the configuration of the ES probes. To quicken the sensors' response the water was added to waste directly, bypassing the clay cap of the landfill surface. Two 0.15 m diameter auger holes were drilled, adjacent to the installed ES probes for this purpose. Figure 3.8 illustrates the test configuration. The holes were drilled through the clay cap, to a depth of 2.6 m, so that the moisture would percolate directly into the waste and ensure a quick sensor response. The holes were maintained full of water for periods of approximately 4 and 6 hours over ~26 hrs

3.4.3 . Ambient Moisture Monitoring

Apart from the initial planned moisture addition, the remainder of the ES probe study monitored the natural moisture dynamics throughout the season. Precipitation data was also recorded from the nearby Saskatoon Water Treatment Plant weather station, when

available, or from the Saskatoon Airport (YXE) weather station. These data are discussed in Chapter 4.

Table 3.3 - Times and volumes of water added during the initial infiltration test.

Time	Elapsed Time (hh:mm)	Hole 1 volume (L)	Hole 2 volume (L)
5/14/2007 14:48	0:00	56	115
5/14/2007 15:30	0:42	56	43
5/15/2007 15:47	0:59	41	41
5/15/2007 16:15	1:27	36	26
5/15/2007 16:40	1:52	26	23
5/15/2007 16:55	2:07	14	8
5/15/2007 17:10	2:22	10	15
5/15/2007 17:49	3:01	31	26
5/15/2007 18:30	3:42	20	26
5/15/2007 18:35	3:47	5	8
5/15/2007 18:50	4:02	18	23
5/15/2007 19:15	4:27	19	19
5/16/2007 11:00	20:12	31	26
5/16/2007 11:40	20:52	26	20
5/16/2007 11:58	21:20	18	8
5/16/2007 12:30	21:42	15	13
5/16/2007 12:45	21:57	8	8
5/16/2007 13:33	22:45	28	26
5/16/2007 14:46	23:58	10	8
5/16/2007 15:10	24:22	13	15
5/16/2007 15:45	24:57	28	15
5/16/2007 16:15	25:27	20	20
5/16/2007 16:50	26:02	13	15
5/16/2007 17:05	26:17	15	18
5/16/2007 17:30	26:42	15	15
TOTAL		572	578

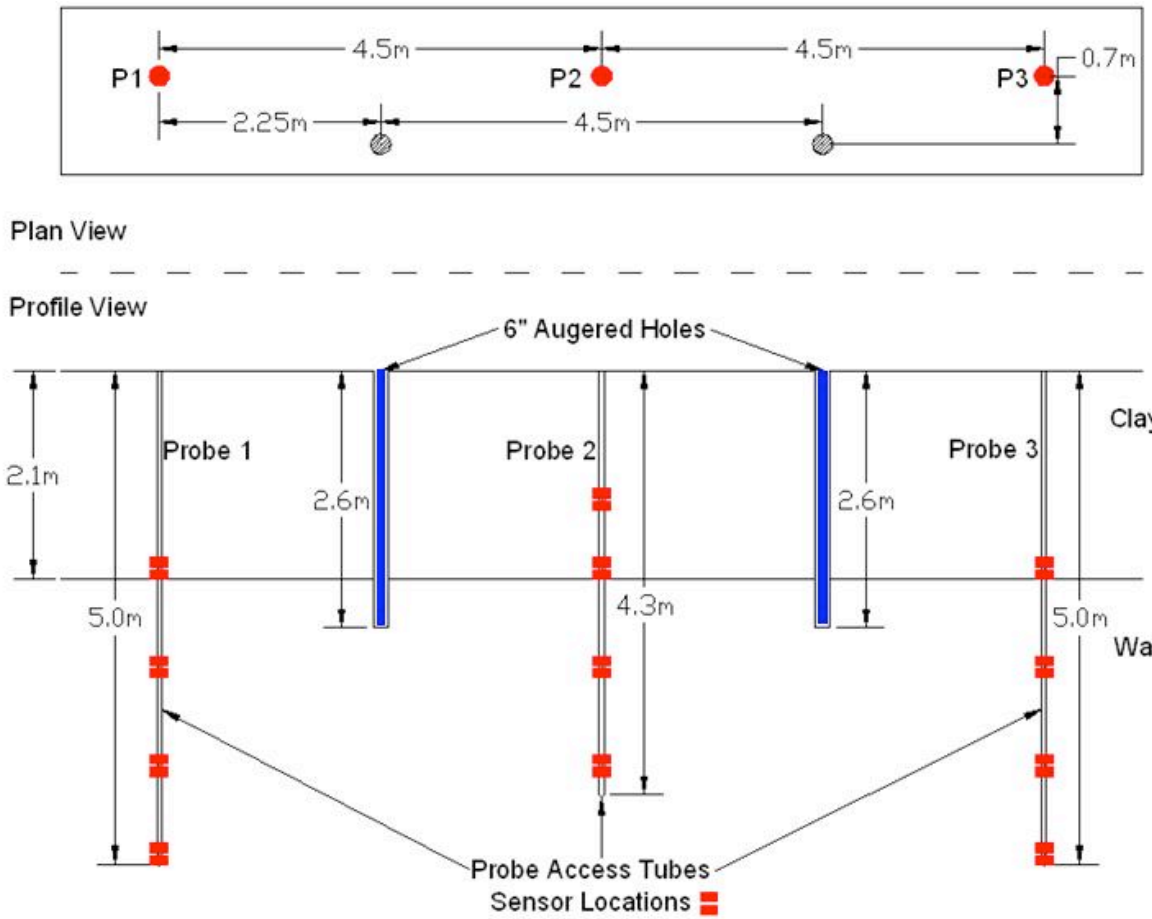

Sensor Depths in m

	Probe #		
Sensor #	1	2	3
1	2	1.3	2
2	3	2	3
3	4	3	4
4	4.9	4	4.9

Figure 3.8 - Schematic of initial ES probe configuration during infiltration test including initial sensor configuration. Hole #1 (left) and Hole #2 (right) were kept full to encourage quick infiltration of water into the surrounding waste.

3.5 Continuous-Depth / Discrete-Time Field Testing

3.5.1 Deep Diviner Probe

The Deep Diviner sensor (Figure 3.9) is a prototype design based upon the Sentek Diviner 2000 that was constructed by O'Kane Consultants Inc of Saskatoon. It uses the same sensor as the Diviner2000, but has been retrofit for depth readings of up to 19 m at 0.1m intervals. It is capable of logging up to 15 holes before data must be uploaded.

The Deep Diviner consists of the following components:

- Sentek Diviner 2000 capacitance sensor;
- tripod assembly: depth control sensor attached to pulley on tripod head;
- motor and cable spool;
- handheld control and logging unit;
- power control for sensor and logger; and
- 12V DC power supply.

The Deep Diviner returns data in a different format than the Diviner 2000 and the EnviroSCAN system. The resonant frequency from the oscillator circuit is scaled in such a way as to read approximately 1235 in a saturated medium, and 1670 in air. To compare the results from the Deep Diviner to data from the Diviner2000 and EnviroSCAN sensors, the scaled frequency was calculated using these minimum and maximum values:

$$SF = \frac{(1670 - F_m)}{(1670 - 1235)}$$

Figure 3.9 - Deep Diviner moisture probe.

3.5.2 Moisture Content Determination and Correlation

The purpose of the waste sampling was to gather *in-situ* baseline moisture data and correlate it to the initial Deep Diviner readings. From this relationship, it was hoped that changes from the initial volumetric moisture content, resulting from both natural and artificial moisture addition, could be estimated and that the moisture content could be tracked over time. Immediately following the installation of the Deep Diviner access holes, the Deep Diviner was used to survey the hole for correlation with the MSW sampling conducted during hole installation.

Though the samples were taken at 1.5 m intervals, they were sometimes split up into more discrete intervals since the Deep Diviner has a 0.1 m reading interval. The samples were split up on the basis of visual inspection of moisture content, or in some cases, composition. Noticeably wetter intervals were separated from drier intervals and sealed

until lab analysis could be carried out. Because of the size of the waste constituents, breaking the samples into 10 cm intervals would not represent the moisture condition accurately.

For DH-01 to 07, each sample per 1.5m interval was not split, or split only once, whereas the samples from the installation of DH-08 to 13 were split up into finer depth intervals for greater moisture content resolution with depth. Refer to Appendix B for detailed outline of sample intervals and moisture/density measurements and calculations.

Each core sample was measured, photographed and described qualitatively for composition and moisture. Following this, each sample was removed from its plastic casing, and divided into smaller samples based on moisture. The samples were then weighed to determine their wet weight, and placed in an oven at 60ºC for several days, until the sample weight did not change any further.

Though this method gives the gravimetric moisture content, it is the volumetric moisture content that was needed for correlation purposes. Volumetric moisture content was calculated by using the volume that the sample filled in the plastic casing and dividing the volume of water lost from drying by this sample volume. It is unavoidable that some sample disturbance would occur, altering the actual *in-situ* θ_w, though it could not be known to what extent this would occur. It was assumed that following the initial Deep Diviner survey, all the necessary data for a field moisture correlation would be collected.

CHAPTER 4 PRESENTATION AND DISCUSSION OF RESULTS

4.1 Introduction

This chapter presents the results of the laboratory and field trials to achieve a correlation between capacitance data and θ_w. Section 4.2 introduces and discusses the laboratory results and implications for interpretation of the field results. Section 4.3 presents the field results from the in-place, continuous-time monitoring, using the ES sensors. The response of the ES probes to infiltration fronts will be highlighted. The results of the MSW sampling and the observations using the Deep Diviner probe (continuous-depth, discrete-time) will be discussed in section 4.4.

4.2 Lab Results using Diviner2000

As previously discussed in section 3.2, the first step was to determine if it was possible to track the moisture change in MSW using a capacitance moisture sensor. Laboratory trials were conducted to generate a quantified correlation between capacitance sensor readings and bulk volumetric moisture content. Table 4.1 outlines the specifications of the lab trials.

Table 4.1 - Summary of laboratory test parameters. Initial bulk density includes the initial mass of dry waste and water.

Date	Trial	Mass of dry waste (kg)	Initial volume of water (L)	Total volume occupied (L)	Initial bulk Density (kN/m^3)	Initial Water Content (% vol)	Final Water Content (% vol)
June 26/06	Trial 1	39.8	8.0	32.3	14.5	25	46
July 10/06	Trial 2	40.7	6.0	40.4	11.3	15	55
Aug 25/06	Trial 3	40.7	7.5	37.3	13.7	20	40
July 12/07	Trial 4*	41.9	8.2	39.1	12.0	16	46

*Trial 4 used the Deep Diviner rather than the Diviner 2000

Figure 2.1 shows the results of lab trial 1. The waste was packed without giving preference to particular waste components while adding water intermittently to ensure it would be packed to the desired density. This method of water addition is apparent when observing the initial sensed profile of the waste column as some lifts needed more moisture than others to be compacted (bulk θ_w =15%). The zone around the depth of 0.3 m did not hold much initial moisture whereas at 0.2 m depth, there appeared to be a greater retention of water.

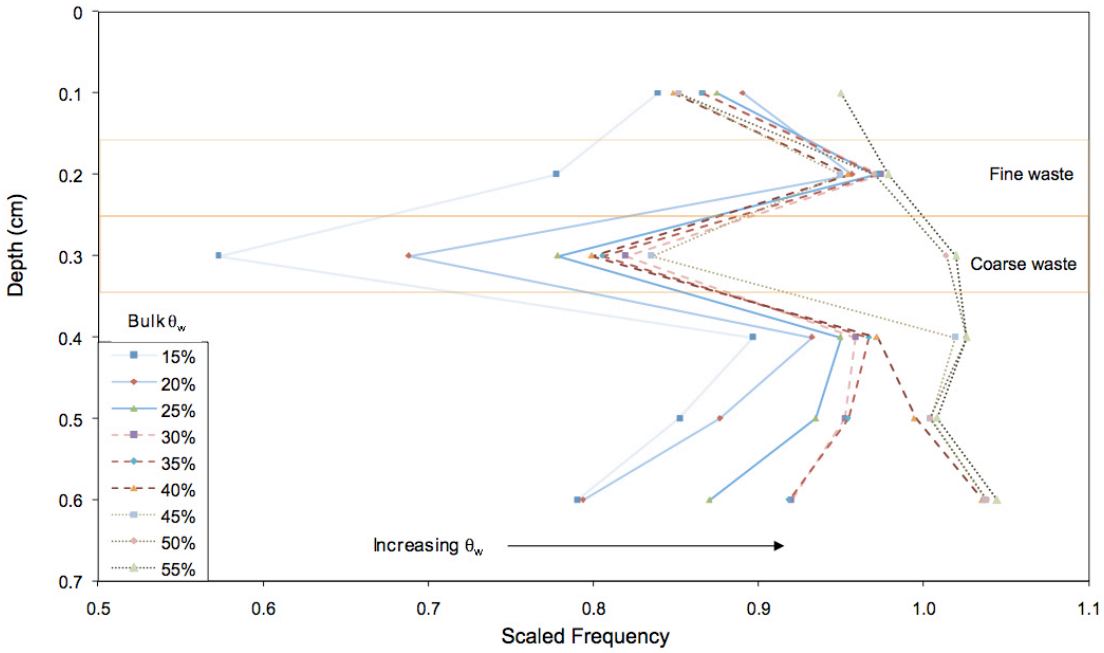

Figure 4.1 - Results of lab trial #2 testing capacitance sensor response (scaled frequency) over varying bulk moisture contents in a 0.75m deep vessel.

The response by the sensor is apparent as water addition progresses, with the scaled frequency increasing gradually as the bulk moisture content is increased. The sensor response at all depths is not uniform, however, indicating that the water added does not spread evenly within the waste after each addition.

The zone at a depth of 0.2 m nearly reaches saturation after the first water addition whereas the zone at a depth of 0.3 m only becomes saturated near the end of the trial.

Upon dissection of the column, after saturation, it was observed that the waste at 0.2 m depth was primarily fine (cover soil, yard waste, paper) and the zone at 0.3 m was coarser waste such as plastics and coarse canvas. This behaviour is consistent with the expected moisture retention properties of the varying components of the waste, in which the large pores will not be filled with water until a low suction value is present. The smaller pores on the other hand, having a higher suction (i.e. a higher air-entry or lower water-entry-value), will become wetted sooner. During the later stages of moisture addition, air bubbles could be observed at the top surface of the column as infiltrating water displaced air.

Observing the progression of moisture addition in Figure 4.1 it is possible to see the saturation of the waste moving gradually upward. The zones at 0.6 m, 0.4 m, 0.3 m and 0.1 m become effectively saturated when θ_w reaches 40%, 45%, 50% and 55% respectively, as the wetting trend of the SF values reach their maximum for their respective depths.

The final SF profile upon saturation of the column has a non-vertical shape, with the bottom of the column generating a higher SF value (>1) and the top generating a SF value below 1. SF values greater than 1 are not expected, however, they may be a result of pore-water conductivity, which was not accounted for in these lab trials. The addition of water to dried waste may have returned salts to solution resulting in a conductive water phase. As the water was added, it may have washed the salts to the base resulting in greater conductivity of pore-water in the base and less-conductive pore-water in the top portion.

Using these lab results, an attempt was made at developing a quantitative correlation between scaled frequency and θ_w. Since the water in the column is not distributed evenly (as evidenced by the variable SF readings with depth) it is not possible to know θ_w at each point during the trial. However, by averaging the SF over the depth at each bulk θ_w for the system, a total system correlation can be made.

This averaging technique has its flaws, most notably the extreme variability of θ_w at certain depths. To improve the averaging technique, SF values that obviously showed saturation (most notably the values from the 0.2 m interval) were not included for the weighted SF values for lower bulk θ_w values. The result of this calculation can be seen for laboratory trial 2 in Figure 4.2.

As discussed in Section 2.4.8, greater bulk density will cause the volumetric moisture content to be over-estimated. In hindsight, trial 2 had a bulk density closest to the MSW samples (these sampling results will be discussed in sub-section 4.4.2) so it was decided to analyze that trial. Additionally, trial 2 had the greatest moisture range of all the trials, making it more applicable for comparison to field values.

The trendline from trial 2 defined as $SF=0.156\ln(\theta_w)+0.368$ reveals a good correlation with the plotted data points; $R^2=0.985$. The results of the laboratory trials are compared with the Sentek default correlation in Figure 4.2. The correlation produced by laboratory trials shows less sensitivity to SF than the manufacturer's default correlation over the same volumetric moisture contents, with values intersecting at a SF and volumetric moisture content values of 0.98 and 50%, respectively. It is possible that salts in the dried waste returned to solution upon water addition, resulting in the upward-shifted graph.

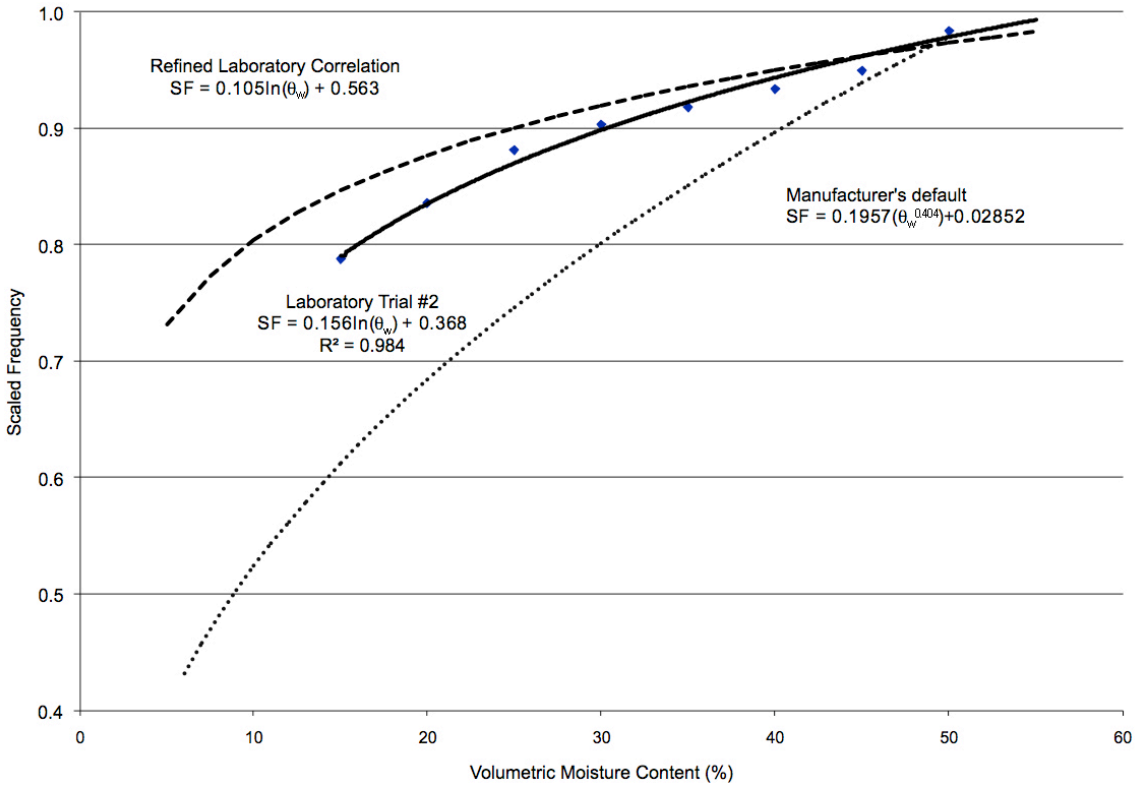

Figure 4.2 - Correlation between the averaged scaled frequency over depth vs. bulk θw for trial 2 (solid line) and the refined laboratory correlation (dashed line). The Sentek manufacturer's default calibration curve is plotted for comparison.

The laboratory data was also refined in an effort to account for the overall water balance within the laboratory vessel. Taking the first laboratory correlation trend (as plotted in figure 4.2) moisture contents were calculated for each depth interval using the original SF values reported from the Diviner 2000. These volumetric amounts were then altered by equal amounts necessary to bring the overall moisture volume to equal the known bulk volumetric moisture content. These revised moisture contents were plotted versus the original SF values and a best-fit logarithmic trend was derived.

The uneven distribution of moisture within the vessel may lead to errors due to segregation of water in the outer edges. As mentioned in Section 2.4.9, Polyakov et al (2005) reported the sensor's lateral sensitivity was 0.1 m from the axis of the sensor. Should that be the case, there would be a 0.05 m fringe along the outer extent of the

vessel that would not contribute to the sensor's response. However, horizontal isotropy was an assumed property of the compacted waste for these trials, implying that the moisture content at any depth should not vary horizontally.

It is also important to realize the waste properties during the laboratory trial are ideal. The waste has been packed in a consistent manner to eliminate large voids and create a uniform density. In the field, these conditions will be highly variable. The *in-situ* waste density will vary spatially as a function of the compaction efforts and equipment and with the age of the waste.

Typical unit weight upon deposition to the landfill is approximately 6.87 kN/m^3 (McBean et al., 1995). This will evolve as waste is added above and as it decomposes. Void spaces may also be encountered in the waste mass as large incompressible waste components may prevent complete compaction.

4.3 EnviroSCAN Field Results

4.3.1 Introduction

Section 4.3 will present the results from the continuous-time at discrete-depth moisture monitoring using the EnviroSCAN probes. Results from the initial infiltration testing will be introduced, as well as the probe response to a natural precipitation event. Further results from ambient moisture monitoring will also be presented.

4.3.2 Initial Infiltration Testing

As outlined in Section 3.4.2, an initial infiltration test was conducted to determine the quality of response of the ES sensors in MSW. In total, over 1100 litres of water was added to the waste through two holes in the vicinity of the sensors over the course of ~26 hours. Figure 4.3 shows the resulting sensor response from ES Probe 1.

The responses from each sensor of Probe 1 vary. The two uppermost sensors show no response from the water addition. Almost certainly, the sensor at 2 m (P1S2m) did not show a response because it is too high to sense the passing moisture front. The water was added at an approximate depth of 2.6 m, and 2.3 m away from the location of Probe 1.

This may also be the case for P1S3m. In contrast however, P1S3m also shows a very low initial SF reading of just under 0.2. This can mean one of two things: either the waste is very dry around the sensor (below the moisture contents realized in laboratory conditions), or there is significant void space within the sensor's resolution. Should the low SF be caused by large voids, it is likely that the response would be poor or not present near a moisture front, as the water would preferentially follow smaller voids away from the sensor under unsaturated conditions.

Sensor responses from P1S4m and P1S4.9m show a strong response from the moisture addition. Each sensor shows two obvious rises corresponding to the two intervals of water addition. Comparing the SF values to laboratory correlation values, the initial sensor values fall below the range in the laboratory trials, with initial values for P1S4m and P1S4.9m reading approximately 0.49 and 0.32, respectively. During the water infiltration, the values peak at 0.64 and 0.82, respectively. Again, if these are compared to the laboratory calibration values and assumed to be accurate, P1S4.9m reached approximately 15% moisture content by volume.

Observing the sensor responses after the peak values are reached, P1S4m gradually tails, settling at a value not much less than its peak, and P1S4.9m tails to a much greater extent, generating a "noisy" response following its peak, to settle at a value still higher than its initial reading.

Interpreting these results, it seems likely that the voids around P1S4.9m are larger than the voids around P1S4m. Though the peak SF value for P1S4.9m reached a higher value, it did not retain this moisture and fell quickly. This greater drainage (or less retention) compared to P1S4m, suggests larger voids are present. It is also possible, however, that the lack of tailing behaviour in P1S4m was a result of perched water. The lower initial SF value for P1S4.9m than for P1S4m could also indicate larger voids, and hence less moisture in the sensed volume.

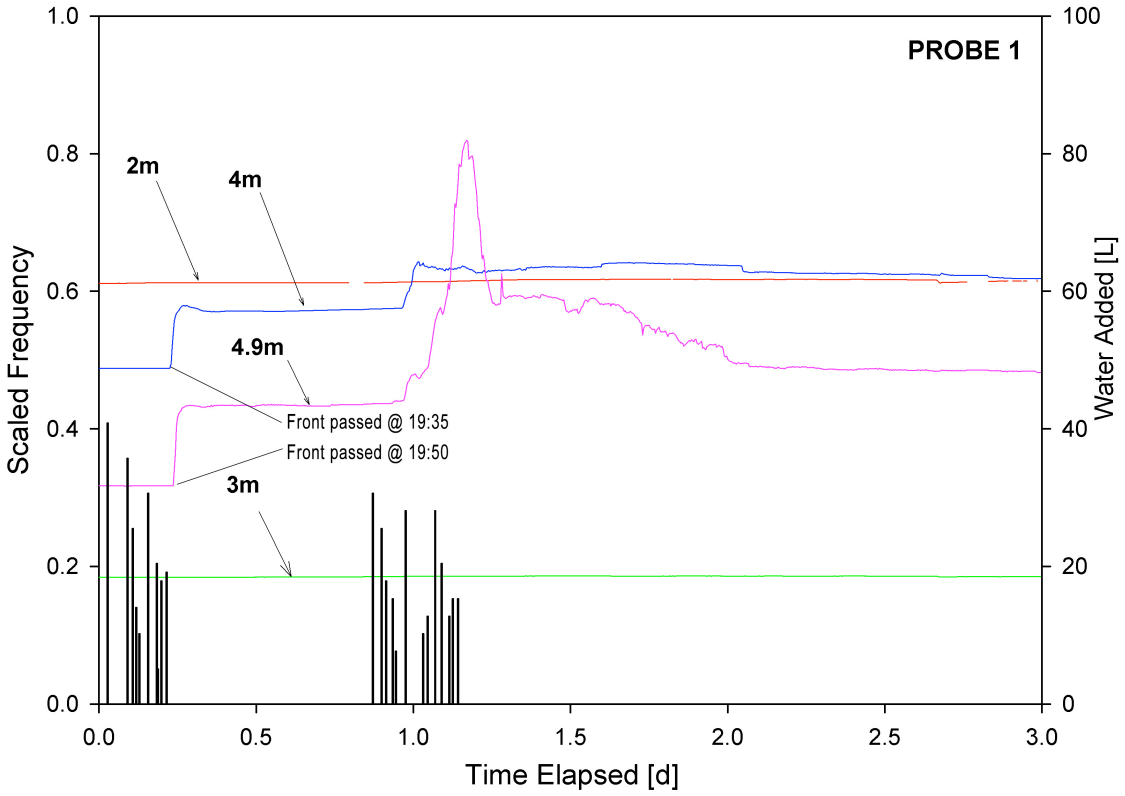

Figure 4.3 - Results from the initial infiltration testing at the Spadina Landfill from ES Probe 1. The "Water Added" bar graph indicates water added in Hole 1 and amounted to a total of 572L.

More water was added during the first bout of infiltration than the second in hole 1 (332L vs. 240L). When comparing the responses of the sensors, P1S4m had a greater response after the first addition (SF=+0.08 or +16%), and a smaller response after the

second addition (SF=+0.05 or +8.8%). The response for the second water addition is disproportionately smaller compared to the first, however, SF becomes less sensitive to changes in volumetric water content as defined by both the MSW laboratory correlation and manufacturer's default correlation. Using the manufacturer's default correlation (because the MSW laboratory established correlation does cover these SF values) the increase in moisture content becomes +4.0 m^3/m^3 and +3.1 m^3/m^3 for the first and second moisture additions, respectively, which are more proportional.

Conversely, P1S4.9m had a stronger response from the second moisture event. This suggests that during the first addition the waste at 4 m absorbed and stored more water (evidenced by the plateau after the first addition) and transmitted more moisture after the second addition, due to a decrease in storage space. The lack of complete draindown following the artificial moisture infiltration for both sensors implies that the moisture content of the waste was below field capacity before moisture addition.

From the 15 minutes elapsed during the passing of the moisture front at P1S4m and P2S4.9m the velocity of the front was calculated to be 2.1×10^{-3} m/s, assuming a vertical flow. Assuming a porosity of 0.48, (the average maximum volumetric moisture content experienced in laboratory trials) and a gradient of 1, this front velocity results in a hydraulic conductivity of 4.7×10^{-4} m/s. The sensors, however, were sampling at a 5 minute interval so the time elapsed between detection could have been just over 10 minutes, or almost 20 minutes depending upon the exact time. Therefore, the range of possible hydraulic conductivities is from 7.1×10^{-4} m/s to 3.5×10^{-4} m/s.

For these calculations unit flow under saturated conditions were assumed. The SF values within Probe 1 were below those realized in laboratory calibration, and were

therefore unreliable with which to estimate moisture content. Saturation and unit gradient were used for simplicity and sake of generating a rough estimate.

The response from Probe 2 can be seen in Figure 4.4. Probe 2 showed weaker responses from the water addition despite being in-between both water addition holes. Similarly to Probe 1, P2S2m showed no response; however, P2S1.3m depth did show a weak response.

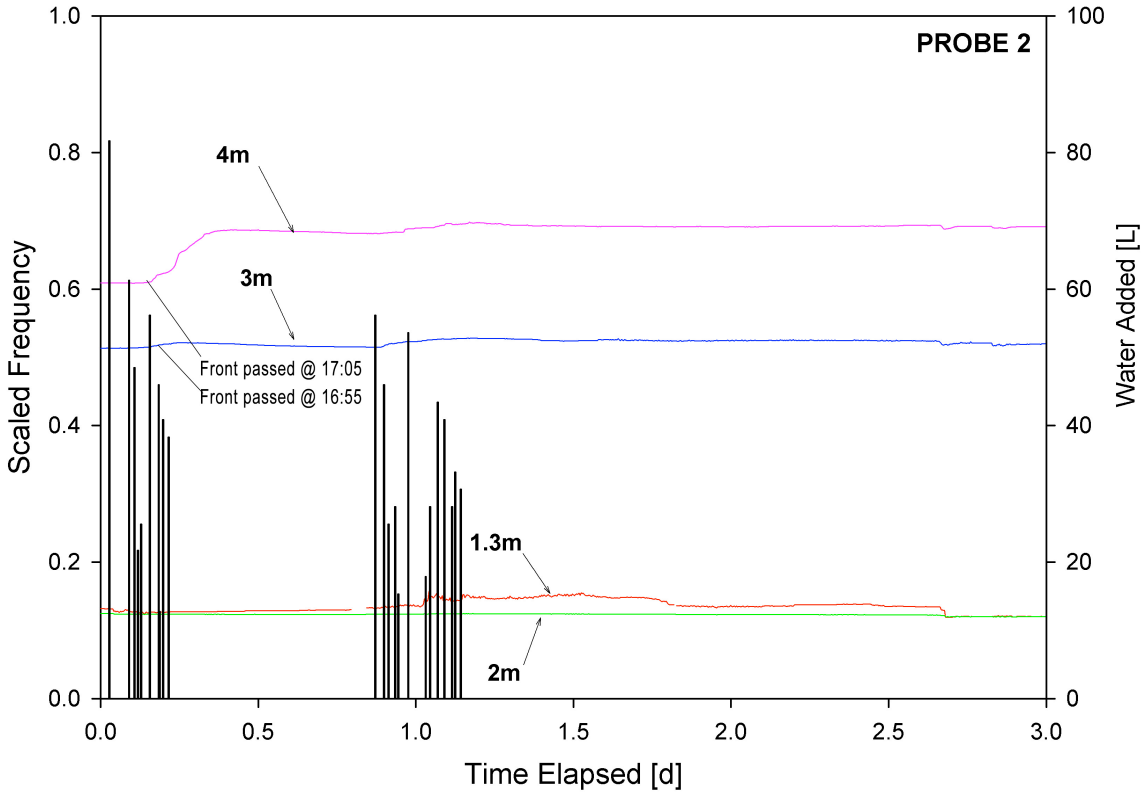

Figure 4.4 - Results from the initial infiltration testing at the Spadina Landfill from ES Probe 2. The cumulative water addition from Holes 1 & 2 is plotted, as Probe 2 was located between the holes.

P2S1.3m is shallow enough that it is located in the clay cover, above the upper extents of the waste. It is possible that water was added at such an amount that it became saturated near the waste/soil interface and migrated laterally to the probe location and

upwards to the sensor. This, however, seems unlikely considering the lack of response from P2S2m.

P2S3m and P2S4m also show a distinct though muted response compared to Probe 1. The pre-infiltration SF values of Probe 2 were 0.51 and 0.61 for P2S3m and P2S4m, respectively. These initial values are fairly good in comparison to those of Probe 1 so it would have been suspected, based upon the Probe 1 infiltration response, that Probe 2 would have a similar or greater response considering the greater water addition in the vicinity. P2S3m and P2S4m peaked at SF values of 0.53 and 0.70, respectively. With the heterogeneity of MSW is it possible that preferential flow paths within the waste limited the amount of water near the sensors. Preferential flow paths will develop in the presence of large pores and high suction values, resulting in flow through finer pore-spaces. At greater fluxes, these maco-pores may fill to transmit moisture (Uguccioni and Zeiss, 1997)

From the time elapsed during the passing of the moisture front at sensors P2S3m and P2S4m, the velocity of the moisture front was calculated to be between $1.1x10^{-3}$ m/s and $3.3x10^{-3}$ m/s. Applying the previously used assumptions (n=0.48, gradient=1) the hydraulic conductivity ranges between $1.6x10^{-3}$ and $5.2x10^{-4}$ m/s

The sensors of Probe 3 (Figure 4.5) generated no response from the water addition trial. The initial values of P3S2m, P3S3m, P3S4m and P3S4.9m were 0.36, 0.35, 0.31 and 0.18, respectively. These initial values are low, though the initial SF value of P1S4.9m was 0.32 and generated a very strong response. S2m and S3m could be too high to capture the spreading water front, though a comparison of Probe 1 results would suggest that P3S4m should respond well if the wetting front has reached the sensor. As

with the results of Probe 2, preferential flow may have prevented the water from reaching these sensors. Additionally, P3S4.9m has a very low initial reading and it is possible that excessive void space contributed to the absence of response.

Overall, the results of the infiltration testing were positive and indicated it was possible to detect a moisture front, provided there was good contact with the surrounding waste. It was concluded, based upon these data, that if a high initial SF value is achieved, the response to subsequent moisture events will likely be strong. Therefore, the initial SF value should be used as a guide to determine if the placement of each sensor is suitable.

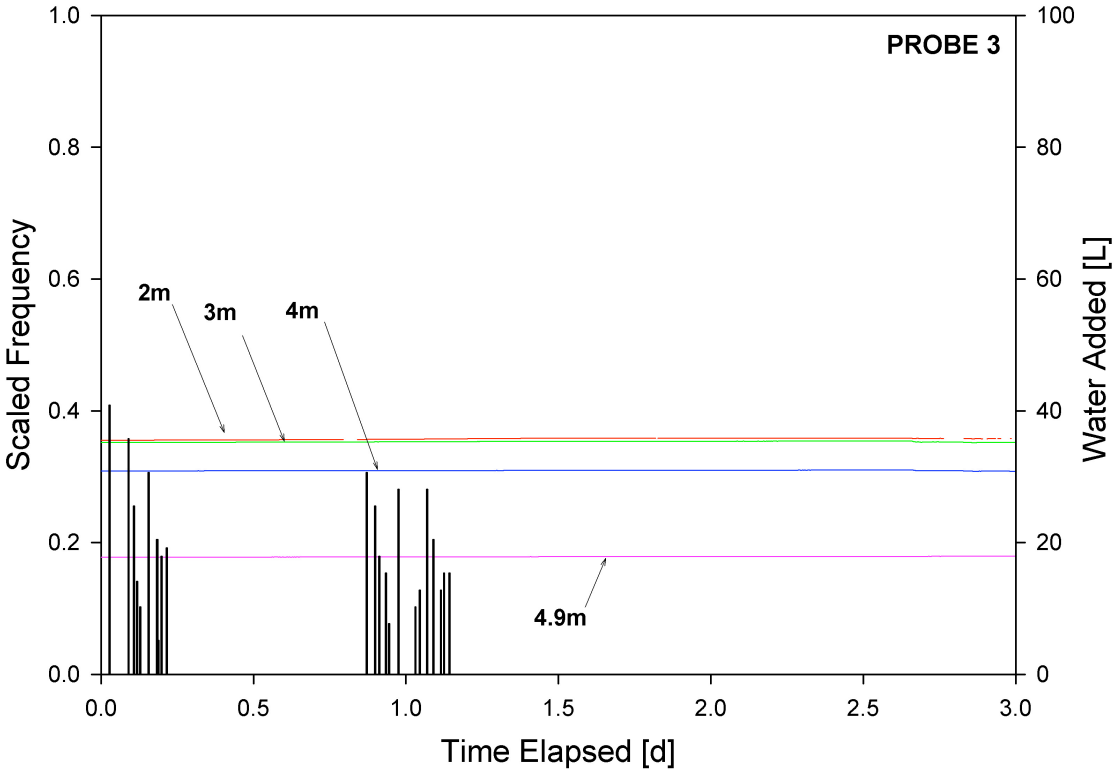

Figure 4.5 - Results from the initial infiltration testing at the Spadina Landfill from ES Probe 3. Water added in this plot is from Hole 2.

In comparison to laboratory data, the likelihood of void space surrounding sensors of low response is supported. For example, there were no SF values below 0.5 at any zone

in the laboratory column even when the bulk moisture content of the compacted MSW was ~15%.

4.3.3 ES Response to Precipitation Events

Following initial testing, the probes were left to monitor the natural moisture variations in the waste. On June 17 and 18, 2007, after approximately 33 days of monitoring, a significant precipitation event occurred in the area of Saskatoon, amounting to approximately 102 mm of rainfall (Environment Canada – Online Climate Data). The actual duration of the precipitation event is not known, and since it occurred during the night, it is spread between two full days of recorded climate data

Observing the results of the rainfall on Probe 1 (Figure 4.6) it is clear that all sensors show a response. Sensors P1S4.9m, P1S4m and P1S2m show the greatest response, having initial SF values of 0.57, 0.62 and 0.66, and P1S3m shows a muted response, with an initial SF value of 0.21.

As expected the first response is observed in P1S2m, then in P1S3m, and finally a nearly simultaneous response from P1S4m and P1S4.9m. Following the precipitation event, all sensors stabilized at a higher SF value than was observed prior.

Based upon the initial infiltration testing the responses of the sensors were mostly as expected. P1S3m showed a very small response, consistent with the low initial SF value. P1S2m and P1S4m both had a quick spike, followed by a gradual rise and decline. P1S4.9m exhibited slightly different bahviour, showing a sharp rise, but no tailing, and settled at an SF value of 0.94. This could be the result of a perched water table. Subsequently, the plateau that P1S4.9m reached did not decline for several months afterward.

Considering the value (SF=0.94) that P1S4.9m remained at, and the steadiness of the SF value for a long period of time, it seems likely that the waste surrounding the sensor was at or close to saturation. A SF value of 1.0 indicates conditions identical to the sensor access tube being surrounded by 100% liquid phase. A value, therefore, of 0.98 would seem likely in the case of saturation since the remaining waste matrix would contribute less to the SF value, because of its lower dielectric constant. However, it should be recognized that media with higher porosity would have a higher SF value at saturation than media with low porosity, as the volumetric moisture content will be higher in a more porous medium.

To validate the sensors' response, an estimate of volumetric moisture change was calculated using the data collected during the rainfall. Relating the unrefined laboratory calibration to the response from the sensors, it appears only sensors P1S4.9m and P1S2m showed appreciable increases in moisture. (All comparisons and volumetric calculations will be made using the unrefined laboratory calibration). P1S4.9m increased from 0.57 to 0.94. The laboratory calibration does not include SF values below 0.8 (15% by volume), however we can assume that the moisture content is ~10% by volume, for purposes of estimation. An SF value of 0.94 is equal to 39% moisture by volume. P1S2m increased from 0.64 to 0.8, values corresponding to ~10% and 15% moisture by volume, respectively.

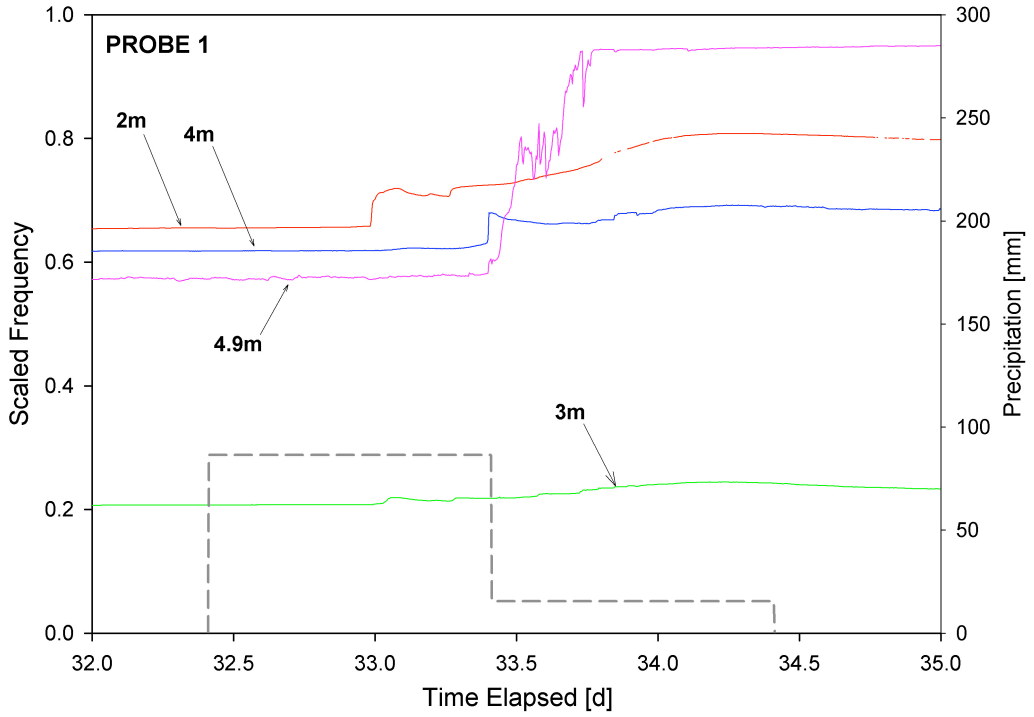

Figure 4.6 –Response of Probe 1 from rainfall event. The dashed bar-plot represents precipitation data from the Saskatoon Airport. The precipitation event happened over midnight, spreading the data between two days.

To calculate a water volume increase, porosity and a sensed volume must be assumed. The average maximum volumetric moisture content achieved in the laboratory studies is 48%, thus the porosity for this calculation is assumed to be 0.48. The vertical interval that the probes measure is assumed to be 0.3 m (the vertical sensitivity plus the equivalent above and below the sensor resolution). The resulting increase in volume of moisture for P1S4.9m and P1S2m (assuming a $1m^2$ area) is 0.087 m^3, and 0.015 m^3. This corresponds to a precipitation amount of approximately 100 mm, as compared with an actual value of 102 mm.

It is very unlikely that the entire volume of moisture due to precipitation would gather around these sensors, however this calculation shows the ability to track moisture quantitatively may be possible.

Probe 2 (Figure 4.7) responded similarly to Probe 1 from the precipitation event. In Probe 2, however, the upper two sensors appeared to react simultaneously to the precipitation, suggesting that water may have short circuited down the side of the access tube. The responses from sensors at 4m and 4.9m are slightly delayed, indicating the moisture front traveled through MSW and did not short circuit along the access tube.

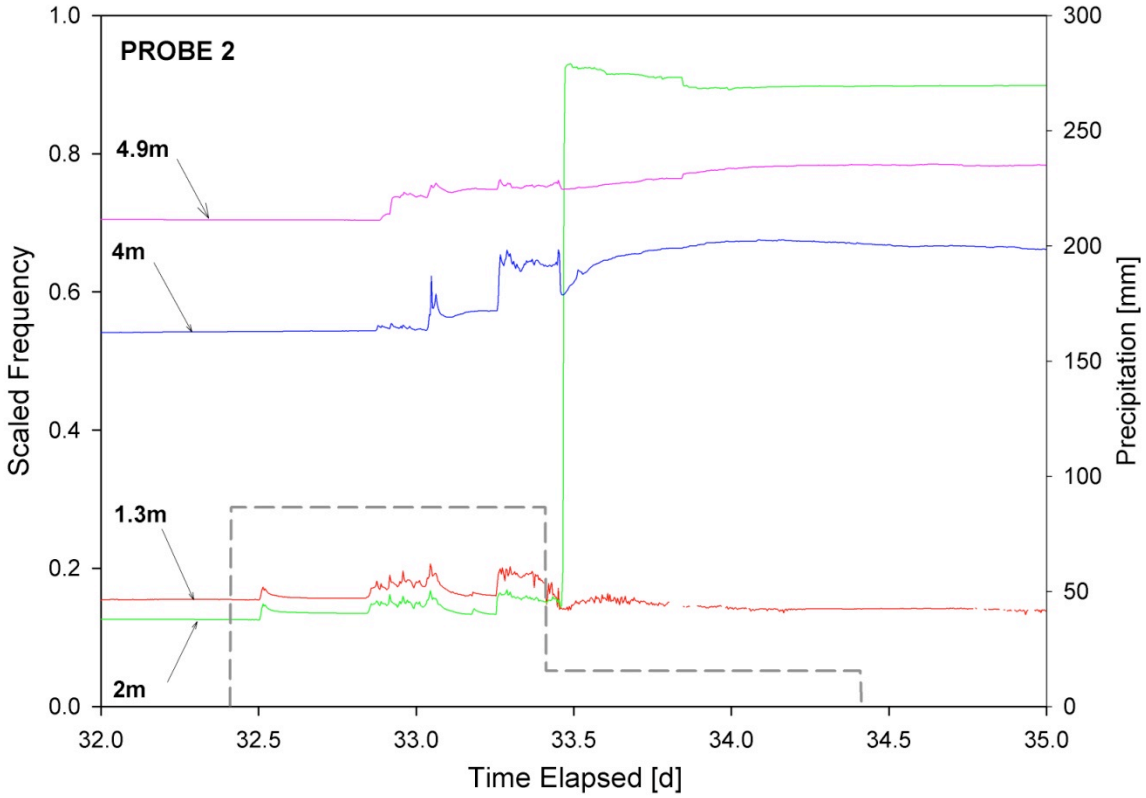

Figure 4.7 - Response of Probe 2 from rainfall event.

Following most of the precipitation (based upon the response of all sensors) P2S2m spikes very quickly to a SF value of 0.92 before settling at 0.90. Similar to P1S4.9m of Probe 1, these data suggest that conditions near saturation occurred. The possible reason for the large increase of P2S2m from ~0.16 to ~0.90 could be the washing of fines from the landfill cover, down the side of the access hole, accumulating near P2S2m. It would seem more likely that if the waste were very dry (resulting in a SF value of 0.19) it would

increase more gradually as it wetted. Another explanation of this sudden spike could be the collapse of waste surrounding the access tube at the sensor's elevation. The very low initial SF value of 0.16 could be caused by a large annular air gap, collapsing after the infiltrating water had wet the waste.

P2S4m and P2S4.9 exhibited results consistent with the initial infiltration testing, showing obvious responses the wetting front with the SF values settling above the values prior to the precipitation. Additionally, there was a slight delay from the onset of the precipitation (presumed to be approximately when the upper two sensors first responded) similar to that of the initial infiltration testing.

The most dramatic response from the precipitation event was from the sensors located in Probe 3 (Figure 4.8). Having shown no response from initial infiltration testing, all sensors responded strongly to the precipitation. The difference could be the breadth of moisture addition from the rainfall, versus the point location of moisture addition in the initial testing.

The responses from P3S2m, P3S3m and P3S4m were all proportional to their initial value. P3S2m, showing the greatest SF value before precipitation, had the highest steady SF value after the rainfall event. P3S3m and P3S4m generated smaller respective responses proportional to their initial value. These trends in SF values seem to be consistent with the expected water retention as a function of void space. P3S2m retained more moisture following the precipitation, after showing a higher initial SF value. P3S3m and P3S4m having a lower initial SF value, were able to retain less moisture, suggesting a greater amount of void space within the sensors' resolution.

The response from P3S4.9m is also consistent with the presence of much (and probably large) void space. During distinct peaks of precipitation (as theorized by the responses of the other sensors) P3S4.9m spikes as the voids fill with water and drain quickly when the precipitation abates. P3S4.9m drains significantly after the precipitation and exhibits tailing behavior much like the other sensors, settling at a SF value slightly above the pre-rainfall value. The responses from all sensors are near instantaneous, possible indicating short-circuiting of moisture along the access tube.

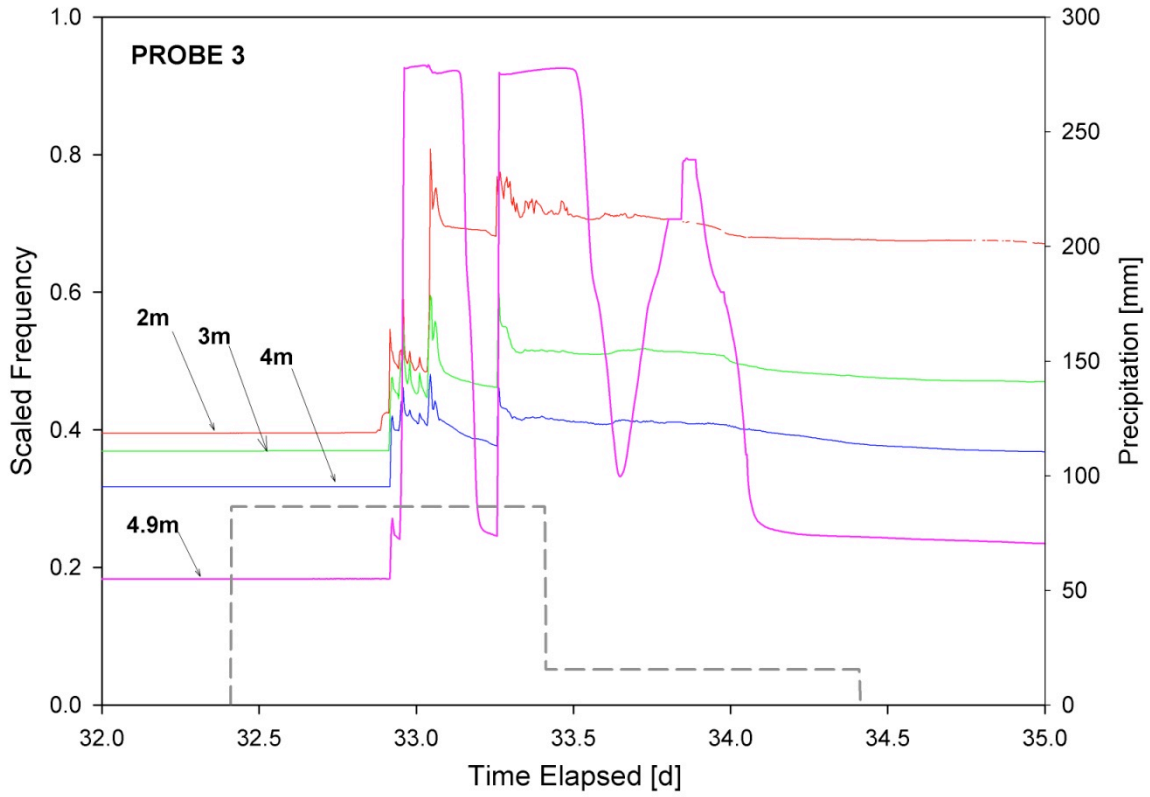

Figure 4.8 - Response of Probe 3 to precipitation event, amounting to 102 mm.

4.3.4 ES Sensor Relocation

On July 6, 2007, following the initial water infiltration trial, the depths of several ES sensors was shifted to find a zone of greater response. A summary of the changes can be seen in Table 4.2. The sensor relocations resulted in higher SF values in two of the five

sensor shifts. Though P2S2m showed a very high SF value, it was moved to keep equal space gaps between sensors.

Table 4.2 - Summary of ES sensor relocation.

	Sensor	Initial Depth [m]	Final Depth [m]	SF value before shift	SF value after shift
Probe 1	2	3.0	3.5	0.24	0.29
Probe 2	1	1.3	1.6	0.13	0.05
	2	2.0	2.2	0.90	0.61
Probe 3	3	4.0	3.5	0.34	0.19
	4	4.9	4.5	0.20	0.71

4.3.5 ES Response During Winter

Apart from responses to natural or artificial precipitation events, the ES sensors did show a noticeable trend during the winter months. Figure 4.9 shows the response by the sensors on Probe 1 during the winter season.

P1S2m and P1S4.9m both show distinct tailing behaviour during the winter. In the case of S4.9m, it is likely that the lack of moisture addition from precipitation is the cause for the apparent drop is moisture content. With neither P1S3.5m nor P1S4m showing a decline, it is unlikely that the response of the deepest sensor is due to freezing. Freezing of water is a possible explanation for the downward trend of moisture at near-surface sensors, however, it can be seen that the decline of P1S2m started before the average daily temperature fell below 0C. The slope of the decline of P1S2m closely resembles the decline of P1S4.9m, suggesting the draining of moisture from P1S2m may be also due to moisture drainage.

Further, during the installation of a gas-well in the 2007/08 winter season, approximately 12.2 m of continuous-flight auger was lost around 2.43 m below ground level. It was necessary to use an excavator to recover the auger, and during excavation it

was discovered that the ground was not frozen below the clay cap, possibly indicating that conditions around P1S2m were not freezing.

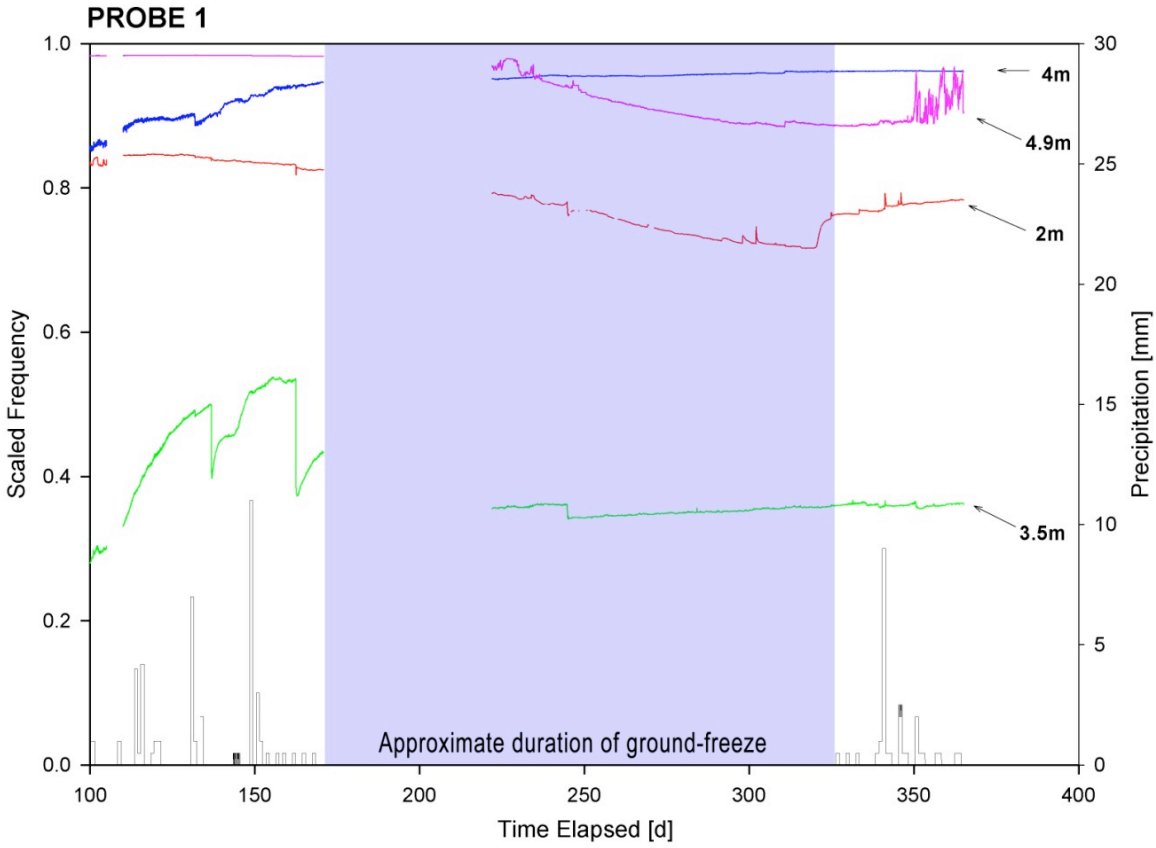

Figure 4.9 - ES sensor response during the winter season. The shaded area represents the duration where the average daily temperature was below zero. The precipitation due to snowfall was not plotted, as it did not infiltrate the cover during this time.

Sensors P1S3.5m and P1S4m did not exhibit the same behaviour as P1S2m and P1S4.9m. P1S4m seemed to level off, completing a lengthy wetting trend that began in the summer and autumn seasons. However, caution should be exercised when predicting the causes of this trend. Early Deep Diviner data (discussed in section 4.4.4) exhibited a gradual increase in apparent moisture in the time following installation. It is possible that the gradual increase seen from P1S4m is the result from the waste gradually squeezing in towards the access tube following installation.

Precipitation in the form of snow was not plotted against the ES data, as it would not have infiltrated the soil cover during the winter. It is also important to note that there was little snow-on-ground at the landfill because of the crest's exposure to high winds and lack of sheltered areas. For this reason, the amount of infiltration after snowmelt was likely less than surrounding areas.

4.3.6 ES Sensor Response and Implications for Hydraulic Conductivity of MSW

Based upon the sensors' spatial configuration, values can be drawn from the ES sensor data to estimate the hydraulic conductivity. In this field setting data from both short-term (precipitation fronts) and long-term (prolonged drainage) hydraulic activity can be processed to yield hydraulic conductivities in differing conditions.

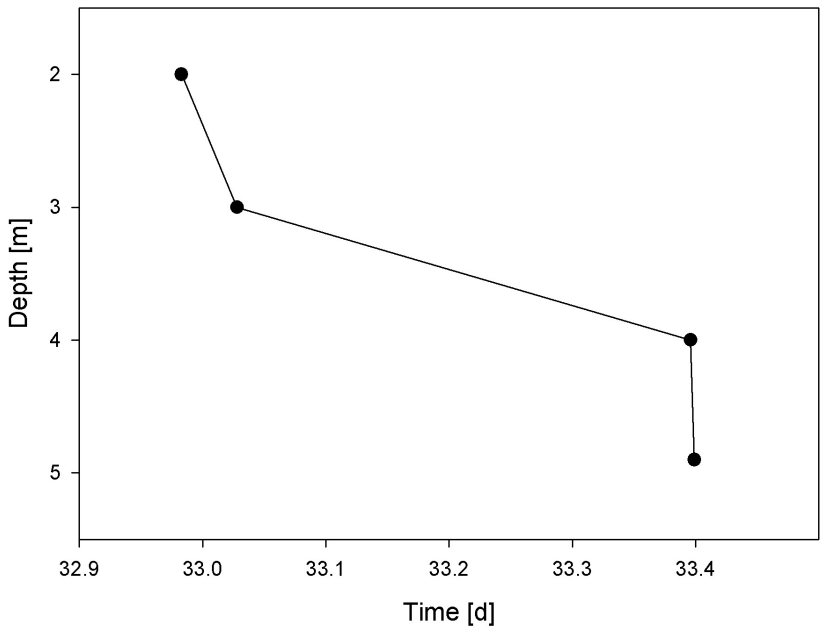

Figure 4.10 – Time of arrival of moisture front plotted versus position as sensed by Probe 1.

The June 17th precipitation event caused a pronounced moisture front in all probes. The moisture front as sensed by Probe 1 (Figure 4.6) is plotted in Figure 4.10 showing the times of arrival at each sensor location. By picking the times at which the front

passed the respective sensors an estimate of hydraulic conductivity. These results can be seen in (Table 4.3).

Table 4.3 – Times of arrival and calculated front velocity between sensors for passing of moisture front as sensed by Probe 1. Seepage velocity is obtained by dividing the elapsed travel time of the wetting front by the distance between sensors.

	Depth	time of arrival (days)	elapsed time (sec)	seepage velocity (m/s)	hydraulic conductivity (m/s)
Sensor 1	2	32.983			
Sensor 2	3	33.028	3888	2.57E-04	1.23E-04
Sensor 3	4	33.396	31795	3.15E-05	1.51E-05
Sensor 4	4.9	33.399	259	3.47E-03	1.67E-03
Over entire interval (2.49 m):			35942	8.07E-05	3.87E-05

To calculate the hydraulic conductivity the volume of water to pass between sensors for a 1 m^2 column was calculated and divided by the time elapsed time between arrival of the front as the respective sensors. Flow under unit gradient was assumed. As suggested earlier, the moisture front appears to short-circuit between sensors 1-2 and 3-4 relative to the front velocity between sensors 2 and 3.

These shortened times result in a relatively high apparent hydraulic conductivity. The moisture front between sensors 2 and 3, however, progresses at a slower rate suggesting it is moving through a zone of lower permeability. It could be suggested that the two faster times result from lower conductivity material, however considering the disturbed nature of the surrounding MSW, the hydraulic conductivity between sensors 2 and 3 is assumed to be closer to the original in-situ conductivity. This results in a hydraulic conductivity of 1.51×10^{-5} m/s. If the entire interval between 2m and 4.9m is considered, the hydraulic conductivity is 3.87×10^{-5} m/s. Probes 2 and 3 exhibited excessive short cutting between sensors and could not produce reliable hydraulic conductivities.

These data also allow hydraulic conductivity to be calculated based upon water volume changes at the same location before and after the precipitation event (using the time elapsed from the arrival of the front to stabilization of SF value after the front has passed). The governing equation is Q/A = K., where A is assumed to be 1 m^2. Because only sensors P1S4.9m and P1S2m had high enough SF values to generate a reliable volumetric water content change, hydraulic conductivities could only be calculated for these two positions. See Table 4.4 for the results of these calculations.

Table 4.4 – Calculation of hydraulic conductivity from volumetric moisture changes at sensor locations.

	Time of arrival of front (d)	Time of stabilization (d)	Change in q_w*	Time elapsed (d)	Hydraulic conductivity (m/s)
Sensor 1	32.983	33.774	5	0.791	7.3E-07
Sensor 4	33.399	34.278	29	0.879	6.6E-07

* See section 4.3.3 for derivation of these values

The difference of the values in Table 4.4 from Table 4.3, could be due to the assumptions made when deriving the volumetric moisture change from the respective SF values. Some SF values were below the laboratory calibration values, rendering low SF values difficult to correlate.

The ES sensor data collected during the winter presents an opportunity to observe the natural moisture migration within the waste while the frozen landfill cap prevents further influx of moisture. If it is assumed that there is no lateral migration at the sensed intervals, the decrease of moisture sensed during the winter is likely a result of vertically downward drainage. Probe 2 sensed this trend during the winter months.

If we further assume a porosity of 0.48 (based upon the average maximum volumetric moisture contents experienced in laboratory trials) and determine the degree of saturation

from each sensor, the volume of water lost to downward migration can be calculated, thereby yielding an unsaturated hydraulic conductivity.

The degree of saturation is not immediately apparent from the ES data. For those sensors that appear to have achieved saturation (P1S4.9m for example) it can be assumed the degree of saturation is 1 where the highest past scaled frequency occurred. For the sensors that have not obviously achieved saturation, it was assumed that S=1 when SF=1. Plotted below in Figure 4.11 is the resulting degree of saturation for Probe 2 over the winter.

Using instantaneous profiling, an estimate of hydraulic conductivity can be made. Using a 1 m^2 column and the above field of saturation in Figure 4.11, the volume of water present at each time was calculated. The moisture loss between t=152.2 days and t=301.8 days was determined to be 0.115 m^3 resulting in a hydraulic conductivity of 8.91×10^{-9} m/s. Because this water loss took place over winter it was assumed that there was no water input through the frozen landfill cap, and there was no lateral migration of fluids in the column.

It must be considered that not all sensors will yield a scaled frequency of 1 when saturation occurs in its surroundings. If sensor has excessive void space, effective saturation may occur in the surrounding water but the value returned could be less than 1. To determine the range of error in the above calculation, the degree of saturation was recalculated assuming that all sensors had reached saturation at their respective past maximum reading. The degree of saturation was then scaled to match this assumption (i.e. if a sensor's past maximum reading is 0.68, S will be equal to 1 at this value and

scaled to 0 when SF=0). This analysis was conducted to determine the maximum possible hydraulic conductivity.

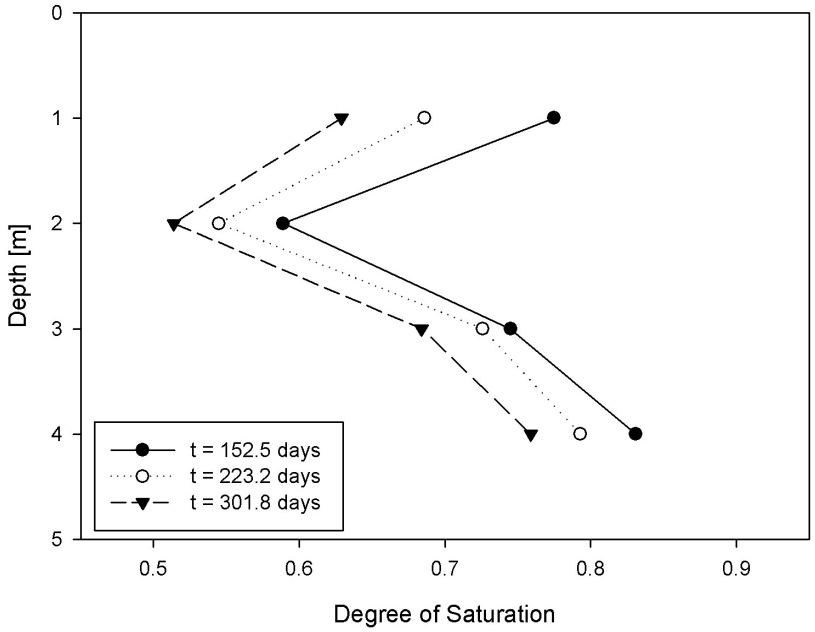

Figure 4.11 – Degree of saturation resulting from a proportional scaled frequency versus depth at various times for Probe 2. There is a clear drainage pattern as S lessens with time.

This scaling means more moisture is in the system and drains over the same amount of time, resulting in a greater hydraulic conductivity of 1.16×10^{-8} m/s for the same scenario as above.

4.4 Results of Manual Moisture Content Monitoring using the Deep Diviner Probe

4.4.1 Introduction

This section presents the results from the manual moisture monitoring campaign. Specifically, the moisture analysis results from in-situ MSW sampling will be outlined, followed by the initial observations from the Deep Diviner surveys. Following this, results from the attempted correlation between MSW moisture data and the Diviner survey data will be presented and discussed, with further patterns in Diviner data presented afterward.

4.4.2 Diviner Access Hole MSW Sampling Results

Sampling of the waste during access tube installation proved to be difficult. Overall, the sample recovery was 57%, with two 1.5 m intervals yielding no sample at all. The cause of the poor recovery was likely the small size (42 mm diameter) of the sampling bit. Because of the large variability of the waste element sizes, the bit would frequently become blocked, preventing the recovery of sample over the rest of the interval. In several instances (as discussed in section 3.3.3 regarding the sampling procedure) the sampling bit could not penetrate certain zones and a steel drive-cone was inserted in the hole to break or push aside the blockage, resulting in zones with no sample.

As mentioned in the sampling procedure, each MSW sample extracted was described qualitatively in terms of composition and moisture content. These detailed logs can be found in Appendix A.

The average moisture content of the waste samples was 24.1% by weight, slightly greater than previous investigation by Singh and Fleming (2004) who found an average of ~21%, sampling to a depth of ~24 m. The small discrepancy could be explained by the greater than average precipitation in Saskatoon over the past three years. Analysis of precipitation data from 2002 through to the end of 2007 showed that precipitation for the years 2002-2004 were below the annual average while precipitation for the years 2005-2007 were above the annual average.

The moisture content showed extreme variability over short intervals. For example, in DH-08 over a 1.06m sample, the gravimetric moisture content varied between 8% and 42%. In waste, however, the representative elemental volume is much larger than in soil, and moisture content should be expected to change to a greater extent spatially, based

upon the waste constituents and porosity. Zekkos et al. (2006) suggest a sample diameter of at least 760 mm for reliable estimations of MSW unit weight. This suggests that the representative elemental volume is of similar size.

Initially, because of the extreme scatter of the moisture content, there did not appear to be any correlation between depth and moisture content. However, by taking moisture content averages over greater intervals, it became apparent that moisture did increase with depth. Table 4.5 shows the average moisture content above and below 6.1m for each hole. In only one of the holes (DH-04) is the moisture content greater in the upper portion of the hole. For detailed moisture analysis data, refer to Appendix B.

Observing the moisture trends in holes DH-08 and DH-13 (**Figure 4.12**; considered to be average values) despite the greater average moisture content at depth, the moisture profiles do not show an obvious wetting trend. Relatively unchanging moisture content with depth suggests that the moisture content of the waste is near its residual value.

Table 4.5 - Average gravimetric moisture content, above and below 6.1m in depth for each hole.

	Gravimetric MC [%]	
Hole	<6.1m	>6.1m
DH-01	16.6	31.9
DH-02	14.9	16.2
DH-03	17.7	26.1
DH-04	22.5	16.3
DH-05	16.2	24.5
DH-06	22.1	N/A
DH(ES)-07	20.6	23.4
DH-08	23.4	27.9
DH-09	18.5	22.4
DH-10	21.6	30.9
DH-11	26.5	27.1
DH-12	18.0	22.7
DH-13	18.8	21.2
Average	**19.8**	**24.2**

It is difficult to know how the current moisture content of the waste differs from the original moisture content at time of placement. Placement moisture content is dependent on type of waste (organics vs. non-organics) and environmental conditions such as rainfall. As a result it is difficult to comment on the cause for the greater average moisture content at depth.

An increase in waste density would require a proportional increase in moisture to result in equivalent gravimetric moisture content. However, the same increase in moisture content will increase the volumetric moisture content despite an increased density.

It should also be addressed that there is no way to be certain, for samples with less than 100% recovery, where in the 1.46 m interval the sample was derived. It was therefore assumed that whatever sample length was recovered that it constituted the topmost section of the sample interval, leaving the bottom portion unsampled.

The bulk density of the waste sampled varied from 2166 kg/m^3 to 403 kg/m^3, with an average value of 890 kg/m^3. This average density falls in the range of expected values. Disturbance of the sample is certainly a possibility for this type of sampling technique, and the density (and the volumetric moisture content) could be skewed from such disturbance, however, as discussed later, there was no correlation between moisture content and sensor response for any range of density or recovery.

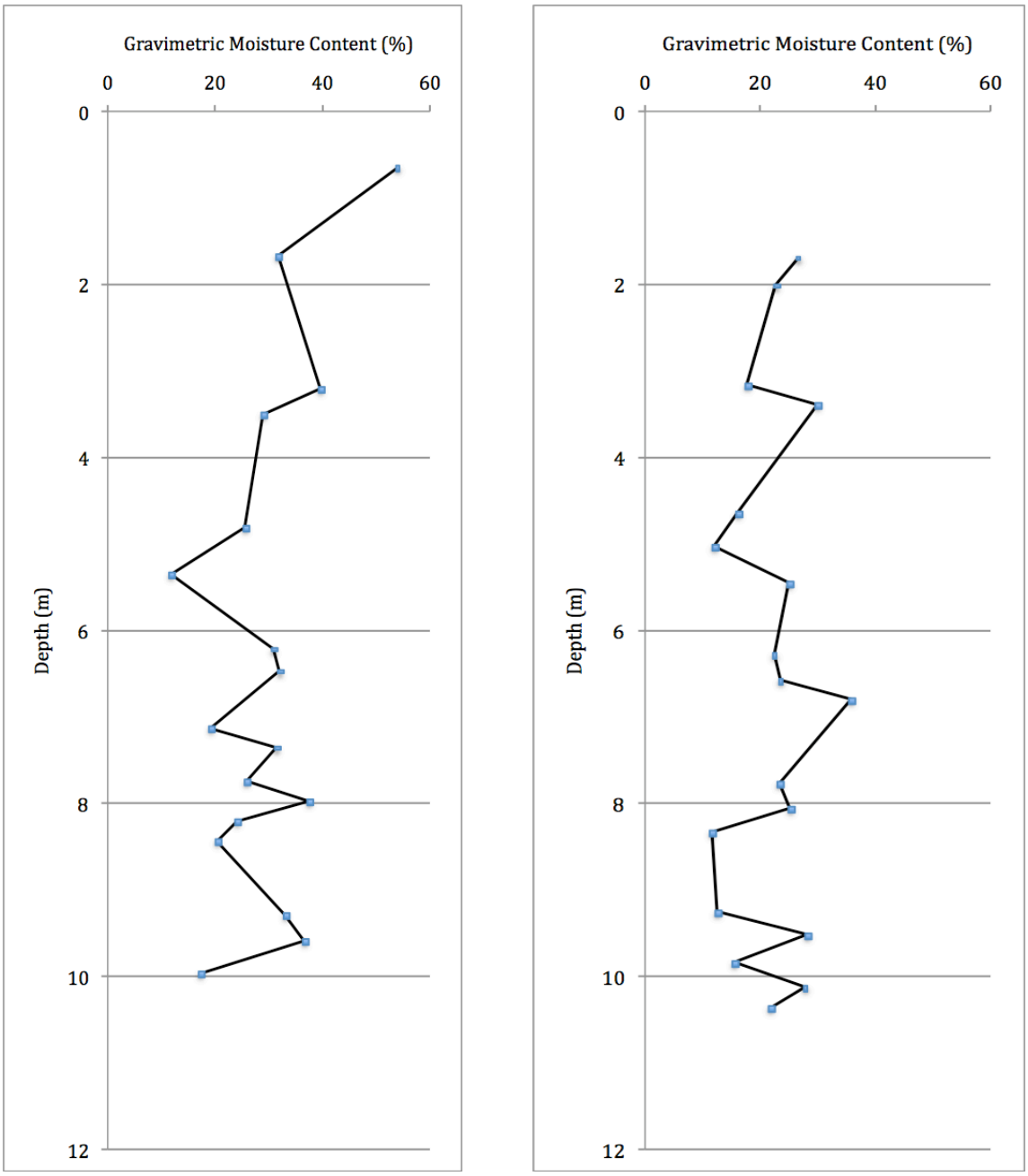

Figure 4.12 – Gravimetric moisture content versus depth for holes DH-08 (left) and DH-13 (right).

4.4.3 Depth Scaling of Diviner Data

One particular phenomenon that had to be addressed was the varying apparent depth to which the Deep Diviner would survey. In below-freezing weather, the Deep Diviner surveys would consistently report a deeper final depth than surveys in warm weather. It

was determined that the PVC cable sheath to which the sensor was attached, would shrink in cold weather and be less prone to complete straightening while off the spool, resulting in a longer apparent depth.

This problem was largely overcome by surveying each hole from the top of the access tube with a metal survey chain and bob. All Deep Diviner measurements were then scaled to be exactly the same length as the surveyed hole-depth. Some depth errors are still noticeable in diviner data when comparing Deep Diviner surveys from different dates. For example, noticeable patterns in Deep Diviner data may be offset by up to 0.2 m. Listed in Table 3.2 are the actual depths for each Diviner access hole from surface.

4.4.4 Initial Diviner Readings and Evolution of Hole Conditions

Following successful sampling and installation, an initial Diviner survey was conducted for purposes of correlation with the moisture data derived from the samples. It was initially assumed that the first survey would provide the best correlation with the moisture content from MSW samples, recording the conditions of the waste surrounding the access tube at the time of waste sampling (before any possible changes in moisture could occur from precipitation, leachate migration or waste degradation).

Regular Diviner surveys were conducted in the following months, revealing what initially appeared to be gradual moisture increases at various locations in each Diviner hole, though usually in deeper portions of the hole. Approximately three months after installation and the first profile reading, these changes stopped and the data obtained from subsequent surveys had stabilized at near-constant values. Figure 4.13 illustrates this effect as seen in holes DH-03 and DH-04.

The greatest change in SF response should theoretically be due to changes in water content in the sensor's zone of sensitivity. However, due to the method of installation, there was an annular air gap present at the time of the access tube insertion as the waste surrounding the access tube was displaced and slightly compressed. Over time it was expected for the waste to reclaim the space due to the pressure from the overlying mass. The fact that the greatest change in SF typically occurred between the initial survey (taken on the day of installation) and the very next reading seems to support this theory of waste squeezing. This behavior can be seen plainly in hole DH-03 in Figure 4.13, particularly from 8.3 m to 9.2 m. The SF values realized in the field surveys were lower than expected, based upon the laboratory calibration and the actual moisture content resulting from downhole sampling. This implies that the laboratory calibration cannot be readily applied to Deep Diviner surveys under these conditions.

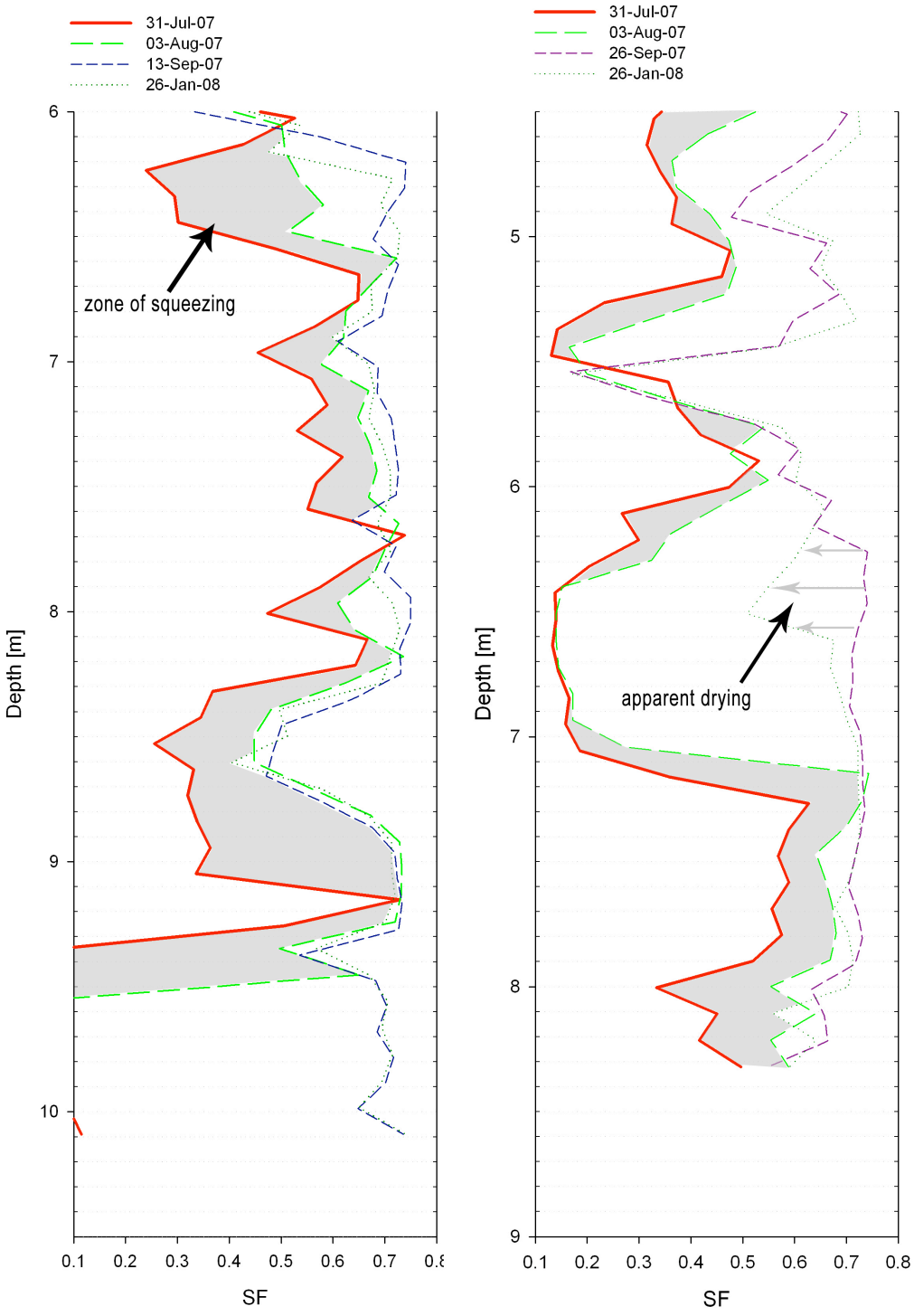

Figure 4.13 - Evolution of SF values over selected ranges in holes DH-03 (left) and DH-04 (right).

Additionally, after the surveys in September 2007, there is very little or no change as evidenced by the surveys on January 26, 2008. This suggests that the hole conditions have stabilized. It should be noted that there was little precipitation from August through to the onset of winter, meaning that the SF changes between the end of July and September were not likely the result of water addition and more likely to be a result of changing hole conditions. It is emphasized that the in-situ MSW moisture contents were generally low, (i.e. 24 %, by weight, on average) suggesting that the leachate was not likely free to migrate. As mentioned previously, the moisture profiles could suggest that the moisture content of the waste is at the residual value, resulting in non-connective pores and limited pathways for moisture migration.

Accordingly, a correlation between the measured volumetric moisture content data and the downhole Deep Diviner readings was attempted using the downhole surveys conducted in September, after the hole conditions stabilized, rather than the initial survey data collected in July immediately after installation.

For Diviner holes 08 – 13, installed in November 2007, the surveys of February 7, 2008 were used, assuming the same type of hole-condition evolution occurred.

4.4.5 Correlation of Diviner Data with Sampled Moisture Data

To correlate the moisture data, the derived θ_w data from downhole sampling was plotted versus the average scaled frequency value over the presumed source location of the sample. Figure 4.14 shows the downhole results of θ_w and Diviner SF values over depth for holes DH-03 and DH-10. These two holes are examples of visually good correlations between θ_w and the Diviner survey.

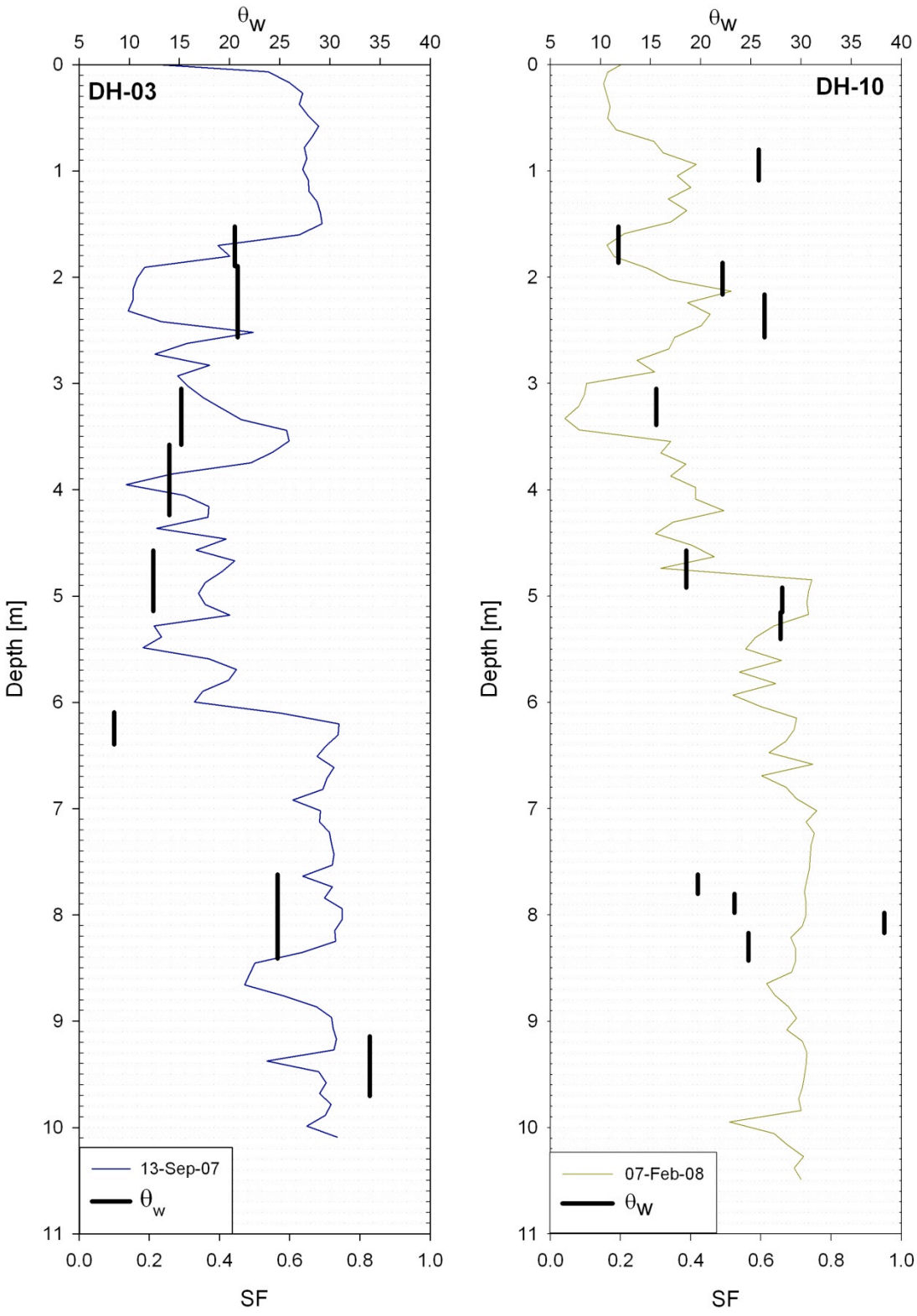

Figure 4.14 – Deep Diviner surveys compared with volumetric moisture data derived from samples over depth for holes DH-03 and DH-10.

Visually comparing the moisture and Diviner data for DH-03, it appears there is a correlation between θ_w and the Diviner survey. In particular, the interval 2 m-6 m shows a limited Diviner response, and an improved response for the 6m-10 m interval. This corresponds with lower θ_w values near over 2 m-6 m and greater values over 6 m-10 m.

Similarly, observing the Diviner and θ_w values for DH-10 from 1 m-5.5 m, the zones of increased moisture content seem to correspond to zones of increased Diviner response, and vice-versa. However, farther down the hole, θ_w does not correspond well with the Diviner data due to the extreme local variations of θ_w.

Figure 4.15 shows similar data from DH-04 and DH-13. The quality of correlation seen between θ_w and the Diviner count data for these holes is more representative of the bulk of the data. Though it may be possible to see some qualitative trends (i.e. the low θ_w value and corresponding trough in the Diviner SF values at 5.5 m depth in DH-04) the quantitative relationship between the two sets of data is not significant.

Shown in Figure 4.16 is the scatter-plot of θ_w vs. average Diviner scaled frequency values for all holes and samples. It also shows the bulk moisture content of the laboratory trials versus the scaled frequency response from separate depths within the column. It is plain to see from this plot that no reliable quantitative relationship can be established between θ_w and Diviner data. Ideally the trend should match the manufacturer's default calibration or laboratory data (plotted) seen in Figure 4.2. Gravimetric moisture content correlation with Diviner data did not provide a better correlation, however this was expected, based upon the theory behind the sensor's operation.

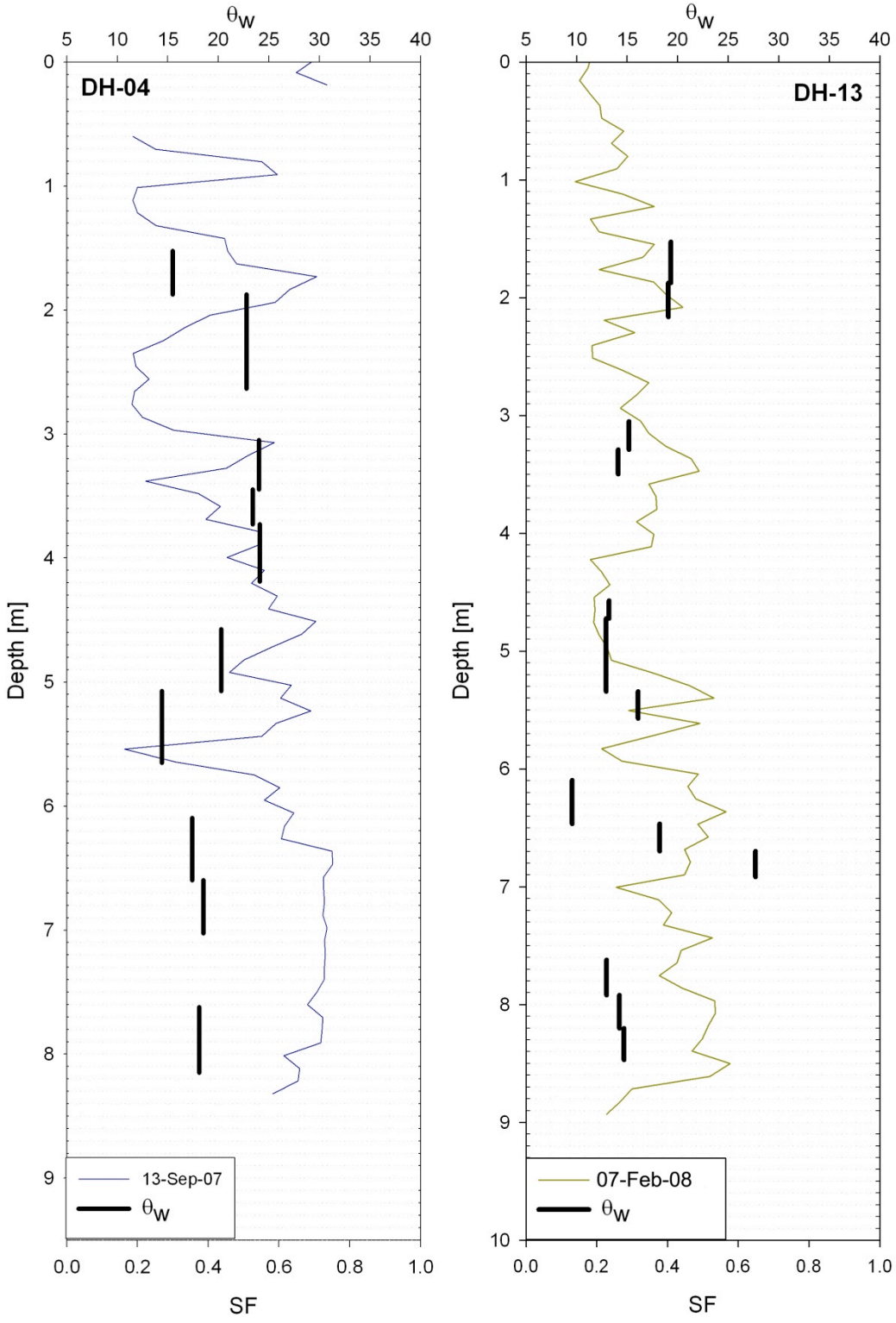

Figure 4.15 - Deep Diviner surveys compared with volumetric moisture data derived from samples over depth for holes DH-04 and DH-13.

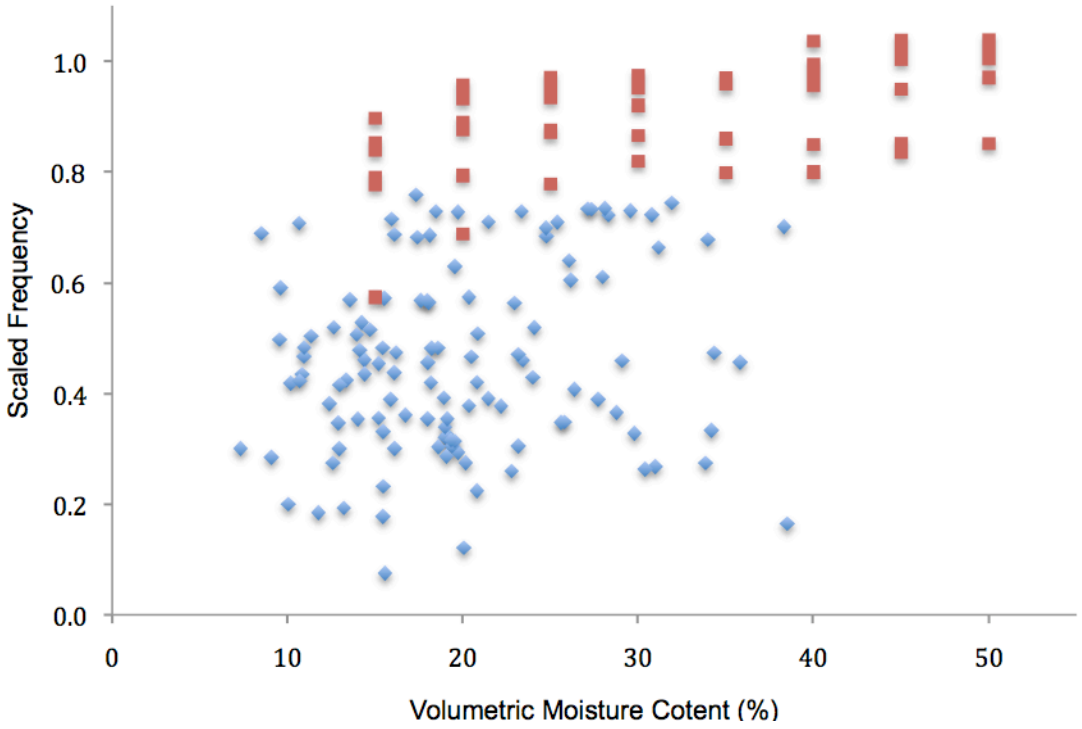

Figure 4.16 - Volumetric moisture content from downhole samples (diamonds) plotted against the average calculated Diviner scaled frequency over the corresponding sample interval. Bulk volumetric moisture contents from laboratory trials (squares) versus the scaled frequency from all depths within the column.

"Filtering" of the Deep Diviner data was also attempted by removing extreme values over the sample interval or shifting the Deep Diviner data up or down by 0.1m. This improved the correlation only marginally and its results are not shown here.

As mentioned, the moisture content of the samples sometimes varied widely over short intervals due to the splitting of large samples. For this reason, grouping the split samples and again comparing it to Diviner data evaluated the moisture content for each complete 1.5 m sample interval. This quality of this relationship, however, was not noticeably better, though it did prevent some extreme volumetric moisture values from occurring.

The possible correlation between density and recovery of the MSW samples versus the scaled frequency response was also plotted (not shown). θ_w versus SF were plotted

for a range of densities (<700 kg/m^3, 700-100 kg/m^3 and >1000 kg/m^3), however there was no relation between sample density and quality of fit. θ_w and SF were also plotted for a range of sample recoveries (<50%, 50%-75%, and 75%-100%) though, there was also no clear relationship with recovery.

It is probable that the influence of void space interfered with the sensing of *in-situ* moisture with Deep Diviner surveys, as also concluded with the ES data. SF values in the field were consistently lower than those realized in the laboratory setting, despite some zones of high θ_w in the Deep Diviner holes as observed in the MSW samples.

4.4.6 Trends in Deep Diviner Data

Apart from the attempted correlation with moisture data, there are several trends in Deep Diviner data that can be described to better understand the limitations of the technique and the behaviour of MSW in this application.

Though no quantitative correlation between Deep Diviner data and moisture content could be established, Diviner SF values collected at greater depths are frequently higher than those from a shallower depth. The cause for higher SF values at depth is not entirely clear. Gravimetric moisture analysis from boreholes revealed greater average moisture content below 6.1m depths, than above.

An example of a wetting trend can be seen in hole DH-10 (Figure 4.14), where the moisture content varies from 21.6% to 30.9% above and below 6.1 m, respectively. In the Diviner profile of DH-10, there is an obvious shift in Diviner trend beginning around 5 m, showing higher apparent moisture content lower in the hole. DH-03 also exhibits this behaviour (Figure 4.14), with the moisture content varying from 17.7% to 26.1% above and below 6.1 m, respectively. The reason for increased moisture content at depth

is not certain, though original waste placement moisture content and historic precipitation may have an influence.

This higher apparent moisture content with depth cannot likely be attributed entirely to moisture content, however. The deeper the hole becomes, the more likely that the waste will squeeze in closer to the access tube due to the increasing pressure from the waste above, causing more material to push within the sensor's resolution. This may be the case with DH-04 (Figure 4.15), with the Diviner data again showing an increase in moisture at depth, but MSW sampling data showing that the hole has less moisture below 6.1 m, than above (16.3% and 22.5%, respectively).

Regardless of moisture content correlation, the zones of higher sensed SF values in the deeper portion of the Diviner access hole will likely generate a strong response to future moisture augmentation as observed in the ES probe responses.

4.5 Chapter Summary

The lab trials successfully indicated that is was possible to track moisture changes in MSW over the range of 15%-55% volumetric moisture content with capacitance moisture sensors. As a result, the trials yielded a correlation between capacitance sensor output and volumetric moisture content in MSW under ideal conditions.

In the field, the ES sensors were able to capture both simulated and natural moisture fronts. Results, however, from each individual sensor varied, based generally on the initial reading before the moisture front was encountered. Typically, sensors with higher initial SF readings would respond with a lower peak in SF value, but retain the moisture post-peak better than ES sensors with a low initial SF reading. It is likely that the sensors exhibiting the low SF readings are located in a high porosity zones with large pore sizes.

These pore conditions could be the combined result of large, coarse waste constituents in the sensor's resolution and the annular air-gap created during installation of the access tubes.

Hydraulic conductivity calculations using ES data generated by moisture fronts yielded values between 1.6×10^{-3} and 5.2×10^{-4} m/s. Analysis of ES data resulting from long-term drainage yielded a hydraulic conductivity of 8.91×10^{-9} m/s.

MSW sampling during the installation of the Deep Diviner holes revealed average moisture content of 24% by weight in the upper 9 m and an average density of 890 kg/m^3, based upon 57% sample recovery. The moisture content profile of the waste exhibits a slight wetting trend with depth, with 11 of 12 holes having greater moisture content below 6.1 m, than above. These moisture contents are greater than those measured in 2004, likely as a result of increased precipitation from 2005 – 2007.

Following several months of Deep Diviner surveys, it was not possible to create a reliable correlation between the Diviner data and the volumetric or gravimetric moisture content of the MSW samples. The largest factors are the uncertainty of sample location within the sampled interval, probable disruption of MSW samples (resulting in inaccurate estimates of θ_w) and variability of the waste condition surrounding the access tube.

There were, however, noticeable trends in Diviner data. Most holes returned Diviner data that indicated greater apparent moisture content in the deeper portions of the hole. This agrees with the moisture analysis from the MSW sampling. The increased pressure at depth, however, will also cause a greater amount of movement into the void space surrounding the access tube, resulting in a greater response.

CHAPTER 5 SUMMARY AND CONCLUSIONS

5.1 Study Objectives

The study objectives were presented in Section 1.2. The research was conducted to evaluate the ability of capacitance moisture sensing technology to measure and track moisture changes in MSW. The application of capacitance probes used in this study is to assist in the operation of a demonstration project to retrofit a capped MSW landfill with rapid-stabilization technology. The study had three distinct objectives:

- Laboratory investigation to establish proof-of-concept and preliminary correlation between capacitance sensor results and MSW moisture content; and
- Installation of capacitance sensor technology to generate a field correlation between actual volumetric moisture content and sensor data; and
- To evaluate the potential for monitoring the passage of moisture through MSW in the field using the capacitance moisture sensors.

Chapter 2 provided a brief summary of the current state-of-the-art moisture sensing technologies used in geomaterials and in MSW, with emphasis on electrical/geophysical techniques. Chapter 2 also discussed the theory of capacitance moisture sensors and the different medium properties that may affect their operation in MSW. All results and relevant observations for both the laboratory and field trials are described in Chapter 4.

5.2 Conclusions

5.2.1 Laboratory Studies

The laboratory trials of the Diviner2000 capacitance moisture probe in compacted municipal solid waste were able to establish a relationship between volumetric moisture

content and sensor data. The laboratory correlation did not match with correlation curves for typical soil, however the results were sufficient to warrant the implementation of a field-scale study.

5.2.2 EnviroSCAN Sensors

The results of the initial field tests showed that the ES probes have the ability to respond in a qualitative manner to artificially and naturally induced moisture fronts. The performance of each ES sensor varied depending upon the conditions of the waste within the resolved area of sensing. Sensors that exhibited low initial readings of apparent moisture, tended to exhibit a muted response to infiltration events. Conversely, sensors with a high initial reading upon installation had a greater response to infiltration events.

Though the reason for poor ES sensor response cannot be known with complete certainty, by evaluating the sensor data and with comparison to laboratory data, it was concluded that the likely reason was the presence of void space within the resolved area of sensitivity. The presence of the void space could be either a remnant of access tube installation or an *in-situ* property of the waste, existing before the installation of the access tubes and possibly stemming from inadequate compaction upon deposition.

A calculated moisture increase using ES sensor response laboratory correlation between volumetric moisture content matched closely with a significant rainfall event as recorded by a nearby weather station. This suggests the potential exists for quantitative moisture influx tracking

5.2.3 MSW Characteristics

MSW sampling during Deep Diviner access tube installation showed that the average *in-situ* gravimetric moisture content of the waste was approximately 24%. The MSW

moisture content with depth was highly variable, ranging considerably over relatively short distances. It was also observed that the moisture content was slightly greater below 6.1m depths than above, with average moisture contents of 24% and 19%, respectively. The cause of this relationship is not clear, though it could be a combination of original placement moisture content, historic environmental conditions (i.e. rainfall) or different water retention behaviour of waste at that depth.

Average bulk density of MSW samples was 890 kg/m^3 and ranged from 2166 kg/m^3 to 403 kg/m^3, not including the density of the clay cap. Loss-on-ignition testing yielded volatile solids content of 53.5% by mass.

By analyzing ES sensor data for moisture front velocity during precipitation, the hydraulic conductivity was determined to be 3.2×10^{-5} m/s. Using instantaneous profiling during winter months, rough estimates of MSW hydraulic conductivity were calculated. During vertical winter drainage, the hydraulic conductivity was calculated to be in the range of 8.91×10^{-9} m/s to 1.16×10^{-8} m/s.

5.2.4 Deep Diviner Probe and Moisture Correlation

The Deep Diviner survey data could not be correlated to the moisture content derived from the downhole MSW sampling. There are three likely reasons for this:

1) The presence of void spaces within the sensors' resolution significantly reduced the ability to detect moisture;
2) The MSW sample recovery was 57%, therefore the location of the sample over the sample interval could only be speculated likely resulting in poor depth-correlation (coupled with extreme spatial variation of moisture content); and,

3) The sampling procedure likely disturbed the MSW samples, resulting in inaccurate estimates of volumetric moisture content.

Similarly to the data of the ES probes, Deep Diviner data showed zones of very low SF response, likely indicating the presence of void space.

Despite the lack of a clear quantitative field correlation between field response of the Diviner and laboratory testing of recovered samples, some conclusions may be drawn from the Deep Diviner data. The Deep Diviner surveys generally showed an increase in SF with depth in 11 of 12 holes. This observation likely indicates that there is a combination of less void space and greater volumetric moisture content with greater depth along the access tubes. Based upon the results of the ES probes, these deeper zones will likely respond well to moisture addition events.

5.3 Recommendations and Future Research

The primary objective of this research was to determine if moisture sensing in MSW using capacitance technology was possible. Though accurate field correlations could not be produced using capacitance technology in this study, improved techniques may provide future attempts with more success.

In the laboratory a greater effort needs to be made to ensure that the moisture content throughout the waste column is uniform or that moisture content with depth is known to ensure an accurate laboratory correlation between volumetric moisture content and capacitance sensor readings.

Further investigation is needed to improve the sample recovery of MSW during access tube installation. Larger diameter sampling would likely increase sample recovery

and could decrease sample disturbance, however the constraints of access tube diameter in the probes' current configuration will likely prevent this.

Greater effort should be made to reduce the annular void space surrounding the access tube resulting from installation techniques. Backfilling the void space around the access with a medium of equal water retention behaviour as MSW may allow the moisture to reach the access tube and be within the sensing volume of the capacitance probes.

For future installations of ES probes, it is suggested that a Deep Diviner survey be conducted to find the zones of good access-tube-to-waste contact to ensure strong responses from moisture fluctuations. It should be recognized, however, that these zones might not be entirely representative of the void space/moisture content system on a whole.

REFERENCES

Akaho, E. H. K., Jonah, S. A., Dagadu, C. P. K., Maaku, B. T., Anim-Sampong, S. Kyere, A. W. K. 2001. Thermal Neutron Reflection Method for measurement of total hydrogen contents in Ghanian petroleum products. Applied Radiation and Isotopes. Vol. 55, pp. 617-622

Andrade-Sanchez, P., Upadhyaya, S. K., Aguera-Vega, J. Jenkins, B. M. 2004. Evaluation of a Capacitance-Based Soil Moisture Sensor for Real-Time Applications. American Society of Agricultural Engineers. Vol. 47, No. 4, pp. 1281-1287

Bachrach, R. and Nur, A. 1998. High-resolution shallow seismic experiments in sand, Part I: Water table, fluid flow and saturation. Geophysics. Vol. 63, No. 4, pp. 1225-1233

Beamish, D. and Mattsson, A. 2003. Time-Lapse Airborne EM Surveys Across a Municipal Landfill. Journal of Environmental and Engineering Geophysics. Vol. 8, No. 3, pp. 157-165

Bell, J. P., Dean, T. J. Hodnett, M. G. 1987. Soil Moisture Measurement by an Improved Capacitance Technique, Part II. Field Techniques, Evaulation and Calibration. Journal of Hydrology. Vol. 93, pp. 79-90

Campbell Scientific Online Resource: www.campbellsci.com/cr200. Accessed June 11, 2008

Catley, A. J., Samson, C., Van Geel, P. J. 2007. Use of Seismic Waves to Estimate Moisture Distribution in Solid Waste. 60th Canadian Geotechnical Conference. 21 - 24 October

Catley, A. J., Samson, C., Van Geel, P. J. 2006. Overview of Geophysical Techniques to Measure Moisture Content in Landfills. 59th Canadian Geotechnical Conference, 1 - 4 October

Consenza, P., Marmet, E., Rejiba, F., Cui, Y. J., Tabbagh, A. Charlery, Y. 2006. Correlations between geotechnical and electrical data: A case study at Garchy in France. Journal of Applied Geophysics. Vol. 60, pp. 165-178

de Velasquez, Ma. T.O., Cruz-Rivera, R., Rojas-Valencia, N., Monje-Ramirez, I. Sanchez-Gomez, J. 2003. Determination of field capacity of municipal solid waste with surcharge simulation. Waste Management and Research. Vol. 21, pp. 137-144

Dean, T. J. 1994. The IH capacitance probe for measurement of soil water content. Report No. 125, Institute of Hydrology, UK.

Dean, T. J., Bell, J. P. Baty, A. J. B. 1987. Soil Moisture Measurement by an Improved Capacitance Technique, Part I. Sensor Design and Performance. Journal of Hydrology. Vol. 93, pp. 67-78

Deeds, N. E., McKinney, D. C., ASCE, Associate Member, Pope, G. A. Whitley Jr., G. A. 1999. Difluoromethane as Partitioning Tracer to Estimate Vadose Water Saturations. Journal of Environmental Engineering. Vol. 125, No. 7, pp. 630-633

DoITPoMS (Dissemination of IT for the Promotion of Materials Science) University of Cambridge, Cambrige, UK http://www.msm.cam.ac.uk/doitpoms/tlplib/dielectrics/printall.php Accessed January 9, 2010.

Ebrahimi-Birang, N. E., Maule, C. P. Morley, W. A. 2006. Calibration of a TDR Instrument for Simultaneous Measurements of Soil Water and Soil Electrical Conductivity. American Society of Agricultural and Biological Engineers. Vol. 49, No. 1, pp. 75-82

Evett, S. R. and Parkin, G. W. 2005. Advances in Soil Water Content Sensing: The Continuing Maturation of Technology and Theory. Vadose Zone Journal. Vol. 4, pp. 986-991

Gardner, C. M. K., Dean, T. J. Cooper, J. D. 1998. Soil Water Content Measurement with a High-Frequency Capacitance Sensor. Journal of Agricultural Engineering Resources. Vol. 71, pp. 395-403

Gawande, N. A., Reinhart, D. R., Thomas, P. A., McCreanor, P. T. Townsend, T. G. 2003. Municipal solid waste in situ moisture content measurement using an electrical resistance sensor. Waste Management. Vol. 23, pp. 667-674

Gotz, J., Lankes, H., Weisser, H. and Sommer, K. 2002. Characterization of Products Consisting of Synthetic, Amorphous Silica and Water with Different Moistures by Means of NMR. Chemical Engineering Technology. Vol 25, no. 10, pp. 989-996

Grellier, A., Duquennoi, C., Guerin, R., Munoz, M. L., Ramon, M. C. 2003. Leachate recirculation study of two techniques by geophysical surveys. Proceedings Sardinia 2003, Ninth International Waste Management and Landfill Symposium.

Grellier, S., Bouye, J. M., Guerin, R., Moreau, S., Robain, H., Skhiri, N. 2005. Influence of temperature and moisture on the electrical resistivity of leachate and waste samples. Proceedings Sardinia 2005, Tenth International Waste Management and Landfill Symposium.

Grellier, S., Robain, H., Bellier, G. Skhiri, N. 2006. Influence of temperature on the electrical conductivity of leachate from municipal solid waste. Journal of Hazardous Materials. Vol. B137, pp. 612-617

Grellier, S., Reddy, K. R., Gangathulasi, J., Adib, R., Peters, C. C. 2007. Correlation between Electrical Resistivity and Moisture Content of Municipal Solid Waste in Bioreactor Landfill. Geo-Denver 2007: New Peaks in Geotechnics.

Guerin, R., Munoz, M. L., Aran, C., Laperrelle, C., Hidra, M., Drouart, E., et al. 2004. Leachate recirculation: moisture content assessment by means of a geophysical technique. Waste Management. Vol. 24, pp. 785-794

Han, B., Jafarpour, B., Gallagher, V. N., Imhoff, P. T., Chiu, P. C. Fluman, D. A. 2006. Measuring seasonal variation of moisture in a landfill with the partitioning gas tracer test. Waste Management. Vol. 26, pp. 344-355

Huang, Q., Akinremi, O. O., Rajan, R. S. Bullock, P. 2004. Laboratory and field evaluation of five soil water sensors. Canadian Journal of Soil Science. Vol. 84, No. 4, pp. 431-438

Imhoff, P. T., Jakubowitch, A. Briening, M.L., Chiu, P.C. 2003. Partitioning Gas Tracer Tests for Measurement of Water in Municipal Solid Waste. Journal of the Air & Waste Management Association. Vol. 53, No. 11, pp. 1391-1400

Imhoff, P. T., Reinhart, D. R., Englund, M., Guerin, R., Gawande, N., Han, B., et al. 2007. Review of state of the art methods for measuring water in landfills. Waste Management. Vol. 27, pp. 729-745

Irmak, S. and Irmak, A. 2005. Performance of Frequency-Domain Reflectometer, Capacitance, and Pseudo-Transit Time-Based Soil Water Content Probes in Four Coarse-Textured Soils. Applied Engineering in Agriculture. Vol. 21, No. 6, pp. 999-1008

Jackson, P. D., Northmore, K. J., Meldrum, P. I., Gunn, D. A., Hallam, J. R., Wambura, J., et al. 2002. Non-invasive moisture monitoring within an earth embankment - a precursor to failure. NDT&E International. Vol. 35, pp. 107-115

Jacobsen, O.H. and Schjønning, P. 1993 A laboratory calibration of time domain reflectometry for soil water measurement including the effects of bulk density and texture. Journal of Hydrology. Vol 151, pp. 147-157

Jolly, J., Barker, R. D., Beaven, R. P., Herbert, A. W. 2007. Time Lapse Electrical Imaging to Study Fluid Movement within a Landfill. Proceedings Sardinia 2007, Eleventh International Waste Management and Landfill Symposium. 1 - 5 October,

Kazimoglu, Y. K., McDougall, J. R. Pyrah, I. C. 2006. Unsaturated hydraulic conductivity of landfilled waste. Proceedings of the Fourth International Conference on Unsaturated Soils. No. 147, pp. 1525-1534

Kelleners, T. J., Robinson, D. A., Shouse, P. J., Ayars, J. E. Skaggs, T. H. 2005. Frequency Dependence of the Complex Permittivity and Its Impact on Dielectric Sensor Calibration in Soils. Soil Science Society of America Journal. Vol. 69, pp. 67-76

Kelleners, T. J., Soppe, R. W. O., Robinson, D A., Schapp, M. G., Ayars, J. E. and Skaggs, T. H. 2004a. Calibration of capacitance probe sensors using electric circuit theory. Soil Science Society of America Journal. Vol 68, pp 430-439

Kelleners, T. J., Soppe, R. W. O., Ayars, J. E. Skaggs, T. H. 2004b. Calibration of Capacitance Probe Sensors in a Saline Silty Clay Soil. Soil Science Society of America. Vol. 68, pp. 770-778

Keller, J. M. and Brusseau, M. L. 2003. In-Situ Charaterization of Soil - Water Content Using Gas-Phase Partitioning Tracer Tests: Field Scale Evaluation. Environmental Science & Technology. Vol. 37, pp. 3141-3144

Khire, M. V. and Haydar, M. M. 2007. Leachate Recirculation in bioreactor landfills using geocomposite drainage material. Journal of Geotechnical and Geoenvironmental Engineering. Vol. 133, No. 2, pp. 166-174

Korfiatis, G. P., Demetracopoulos, A. C., Bourodimos, E. L. Nawy, E. G. 1984. Moisture Transport in a Solid Waste Column. Journal of Environmental Engineering. Vol. 110, No. 4, pp. 780-796

Li, R. S. and Zeiss, C. 1999. Automated Moisture Measurement System for In-Situ Moisture Measurement in Landfills. Proceedings of the International Conference of Solid Waste Technology, 15th.

Lunt, I. A., Hubbard, S. S. Rubin, Y. 2005. Soil moisture content estimation using ground-penetrating radar relection data. Journal of Hydrology. Vol. 307, pp. 254-269

Luthi, S. M., Geological Well Logs: Their Use In Reservoir Modeling. © 2001. Springer, Berlin, New York

Masbruch, K. and Ferre, T. P. A. 2003. A time domain transmission method for determining the dependence of the dielectric permittivity on volumetric water content: an application to municipal landfills. Vadose Zone Journal. Vol. 2, pp. 186-192

McBean, E. A., Rovers, F. A. and Farquhar, G. J., Solid waste landfill engineering and design. © 1995. Prentice Hall, Englewood Cliffs, N.J.

Nadler, A. and Lapid, Y. 1996. An improved capacitance sensor for in situ monitoring of soil moisture. Australian Journal of Soil Research. Vol. 34, pp. 361-368

Paetzold, R.F., Matzkanin,G.A., and De Los Santos, A. 1985 Surface soil water content measurement using pulsed nuclear magnetic resonance techniques. Soil Science Society of America. Vol 49, no. 3, pp 537-540

Paltineanu, I. C. and Starr, J. L. 1997. Real-time Soil Water Dynamics Using Multisensor Capacitance Probes: Laboratory Calibration. Soil Science Society of America Journal. Vol. 61, pp. 1576-1585

Polyakov, V., Fares, A. Ryder, M. H. 2005. Calibration of a Capacitance System for Measuring Water Content of Tropical Soil. Vadose Zone Journal. Vol. 4, pp. 1004-1010

Schmugge, T. J., Jackson, T. J. McKim, H. L. 1980. Survey of Methods for Soil Moisture Determination. Water Resources Research. Vol. 16, No. 6, pp. 961-979

Sentek Diviner2000 Manual. © 2007 Sentek Pty Ltd. Online Resource: www.sentek.com.au

Singh, M. A. and Fleming, I. R. 2004. Evaluation of Existing and Potential Methane Generation at the City of Saskatoon Landfill. Department of Civil and Geological Engineering, University of Saskatchewan.

Stacheder, M. 2005. TDR and low-frequency measurements for continuous monitoring of moisture and density in snow pack. International Agrophysics. Vol. 19, pp. 75-78

SWANA Applied Research Foundation. 2004. Moisture Measurement in Municipal Landfills. Solid Waste Association of America.

Tatarniuk, C. 2007. The Feasability of Waste-to-Energy in Saskatchewan Based on Waste Composition and Quantity. M.Sc Thesis, Department of Civil and Geological Engineering, University of Saskatchewan

Thomas, A. M. 1966. In Situ measurement of moisture in soil and similar substances by 'fringe' capacitance. Journal of Scientific Instruments. Vol. 43, pp. 21-27

Topp, G. C. and Davis, J. L. 1985. Measurement of Soil Water Content Using Time-Domain Reflectrometry (TDR): A Field Evaluation Soil Science Society of American Journal. Vol. 41, No. 1, pp. 19-24

Topp, G. C., Davis, J. L. Annan, A. P. 1980. Electromagnetic Determination of Soil Water Content: Measurements in Coaxial Transmission Lines. Water Resources Research. Vol. 16, No. 3, pp. 574-582

Uguccioni, M., and Zeiss, C. 1997 Improvement of leachate prediction though municipal solid waste layers. Journal of the American Water Resources Assoc. Vol 33, no.6, pp 1265-1278.

Wang, J.R., 1980 The dielectric properties of soil-water mixtures at microwave frequencies. Radio Science. Vol. 15, pp. 977-985

Wang J.R., and Schmugge. 1980. An empirical model for the complex permissivity of soils as a function of water content. IEEE Trans. Geosci. Remote Sens. Vol 18, no. 4, pp. 288-295

Wraith, J. M. and Or, D. 1999. Temperature effects on soil bulk dielectric permittivity measured by time domain reflectometry: Experimental evidence and hypothesis development. Water Resources Research. Vol. 35, No. 2, pp. 361-369

Yu, C., Warrick, A. W. Conklin, M. H. 1999. Derived functions of time domain reflectometry for soil moisture measurement. Water Resources Research. Vol. 35, No. 6, pp. 1789-1796

Yuen, S. T. S., McMahon, T. A. Styles, J. R. 2000. Monitoring In Situ Moisture Content of Municipal Solid Waste Landfills. Journal of Environmental Engineering. Vol. 126, No. 12, pp. 1088-1095

Zekkos, D., Bray, D., Kavazanjian Jr, E., Matasovic, M., Rathje, E. M., Riemer, M. F., and Stokoe, K. H. 2006. Unit weight of solid waste. Journal of Geotechnical and Geoenvironmental Engineering. Vol 132, no. 10, pp 1250-1261

APPENDIX A: MSW SAMPLING LOG

Hole ID	Interval [ft], ([m])	Sample Length [m]	Sampled Interval [m]	Description
DH-01				
	0 - 5 (0 - 1.46)	1.48	0 - 1.48	Clay Cap
	5 - 10 (1.52 - 3.05)	0.84	1.52 - 2.36	0 - 20cm - cover soil, mostly fine granular media. Black @ 50-60cm, wood @ ~73cm
	10 - 15 (3.05 - 4.57)	0.55	3.05 - 3.60	0 - 27cm: wood. Powdery material to 40cm. Looks like fine organics to 55cm. Sample looks very dry overall.
	15 - 20 (4.57 - 6.10)	1.17	4.57 - 5.74	Mostly paper waste to 20cm, soil + small amount of wood to 30cm. Remainder of sample looks to be mostly cover soil, black and granular.
	20 - 25 (6.10 - 7.62)	0.94	6.10 - 7.04	finer-grained cover to 20cm, 20-40cm small wood chips and fine while powder, 40-80cm, looks like moist organics; black to end
	25 - 30 (7.62 - 9.14)	0.75	7.62 - 8.37	10-20cm, granular, loose and dry, 20-40cm, black cover soil plus some textiles; 40-75cm med-brown soil. Black and wet
	30 - 35 (9.14 - 10.67)	0.94	9.14 - 10.1	little soil thorughout interval, much plastics, wire, textiles and small amount of wood + much paper
DH-02				
	0 - 5 (0 - 1.46)	1.35	0 - 1.35	Cover soil. -looking black near the bottom of the sample + wetter. Bits of wood at very end of sample
	5 - 10 (1.52 - 3.05)	1.1	1.52 - 2.12	0-20cm cover soil; starting @ 40cm, cover soil mixed with plastic waste. @60cm wood through to 100cm, mixed with plastics and less soil
	10 - 15 (3.05 - 4.57)	1.12	3.05 - 4.17	0-15cm - moist-looking soil. 15-30cm, dry, wood, powder, construction waste. Majority of sample looks to be organics, black, moist, + good amount of wood @ 60cm.
	15 - 20 (4.57 - 6.10)	1.22	4.57 - 5.79	0-20cm, moist cover soil; 20-40cm dry soil + wood. 40-60cm, moist loose soil + wood, black; 60-110cm mostly cover soil, dark moist. 110-122cm loose wood + soil. From 40-122, the sample is mostly cover soil.
	20 - 25 (6.10 - 7.62)	0.41	6.10 - 6.51	0-25cm, loose cover soil, moist. 25-40cm, plastics + paper
	25 - 30 (7.62 - 9.14)	0.72	7.62 - 8.34	0-40cm, loose moist soil + small-sized wood debris; 40-60cm, denser soil, more moist + some wood; 60-72 looks moist + black. The bottom of the sample had very

dense clay.

DH-03			
0 - 5 (0 - 1.46)	1.46	0 - 1.46	Cover soil. Last 60cm more sandy, first intercal more clayey
5 - 10 (1.52 - 3.05)	1.04	1.52 - 2.56	0 - 20cm, loose cover soil; 20-40cm plastics waste mixed with soil - very dark. 40-80cm cover soil, black and dense. 80cm -> wood @ 80cm, remainder loose soil, not too moist + small wood bits.
10 - 15 (3.05 - 4.57)	1.19	3.05 - 4.24	0-13cm, loose soil, dark, moist. 13-18cm wood. 18-30cm plastics, coarse waste. 30-53cm, leaves, dry. 53-119cm, mixed soil, paper, shingles (esp @ 100-110cm)
15 - 20 (4.57 - 6.10)	0.57	4.57 - 5.14	0-20cm, loose soil + small white bits, dry. Mostly soil, moist. 20-45cm, loose wood chips, dry.
20 - 25 (6.10 - 7.62)	0.3	6.10 - 6.40	Very poor sample; loose. Much wood, probably blocking sample tube. Cover soil, large piece of metal in end of tube; overall, fairly moist
25 - 30 (7.62 - 9.14)	0.79	7.62 - 8.41	completely saturated w/ free water. Upon extrusion, mostly fine-grained cover/clay.
30 - 32.5 (9.14 - 9.91)	0.56	9.14 - 9.70	black, wet, cannot see sample through tube. Mostly fine cover.
DH-04			
0 - 5 (0 - 1.46)	1.46	0 - 1.46	Cover soil with v. small portion @ end of sample of waste. ~10cm
5 - 10 (1.52 - 3.05)	1.11	1.52 - 2.63	0 - 20cm, v. dry, wood mostly. 20-40cm - dry sand. 40-60cm, moist fine cover. 60-111cm, dark, moist, sandy cover soil.
10 - 15 (3.05 - 4.57)	1.14	3.05 - 4.19	0-15cm - dark, moist, some cover content. 15-40cm, wood + plastics + paper., 40-68cm, dark moist organics + cover. 68-90cm, dry paper. 90-114cm dark + some wood, moist
15 - 20 (4.57 - 6.10)	1.08	4.57 - 5.07	0-20cm, dark moist cover soil; 20-60cm fine wood chips, becoming dryer; 60-80cm, shingles; 80-108cm more shingles + layered plastics, paper, wood + grass.
20 - 25 (6.10 - 7.62)	0.93	6.10 - 7.03	0-30cm fairly moist + fine, some granular soil + yard waste; 30-80cm mostly cover soil; 80-93cm cover + mixed waste
25 - 27 (7.72 - 8.23)	0.53	7.62 - 8.15	0-20cm, black moist cover; 20-53cm layered plastics + paper + fine organics + small amount of cover; fairly moist

DH-05			
0 - 5 (0 - 1.46)	1.46	0 - 1.46	Cover soil. Coarser @ top becoming finer + darker, deeper
5 - 10 (1.52 - 3.05)	0.46	1.52 - 1.98	cover mixed with fine wood chips + small amount of plastics
10 - 15 (3.05 - 4.57)	0.44	3.05 - 3.49	whole sample is loose wood + cover soil, fine organics
15 - 20 (4.57 - 6.10)	1.35	4.57 - 5.92	0-40cm, moslty fine organics; 40-70cm, moist + dark soil; 70-120cm mostly coarse, dry cover; 120-135cm dark + moist mixed soil + organics
20 - 25 (6.10 - 7.62)	0.98	6.10 - 7.08	0-28cm, loose cover soil, black + dry; 28-60cm mostly coarse wood + dry organics; 60-98cm, fine wood mixed with cover + plastics, dry.
25 - 30 (7.62 - 9.14)	0.93	7.62 - 8.55	0-30cm loose paper, wood, dry; 30-70cm layered paper, wood, plastics, paper, textiles, medium dry; 70-93 more loose organics
30 - 35 (9.14 - 10.67)	0.98	9.14 - 10.12	0-20cm loose cover + dry organics; 20-55cm plastics + coarse wood, small amout of cover + organics
DH-06			
0 - 5 (0 - 1.46)	1.06	0 - 1.06	0-30cm, cover soil; 30-45cm plastics waste; 45-90cm cover soil; 90-106cm, mixed wood + cover soil
5 - 10 (1.52 - 3.05)	0.92	1.52 - 2.50	0-40cm cover; 40-92cm mixed wood, plastics, organics - moist
10 - 15 (3.05 - 4.57)	0.38	3.05 - 3.43	0-20cm, cover soil; 20-38cm soil + wood + fine organics
15 - 20 (4.57 - 6.10)	0.73	4.57 - 5.30	0-18cm, soil; wood @ 20cm + textiles; 30 onward loose coarse soil fill
DH-07			
0 - 5 (0 - 1.46)	1.16	0 - 1.16	cover soil 0-100cm; 100-116cm black organics
5 - 10 (1.52 - 3.05)	0.60	1.52 - 2.12	20-40cm moslty wood; 40-60cm loose dry cover
10 - 15 (3.05 - 4.57)	0.96	3.05 - 3.95	0-50cm mostly wood, only v. small aount of cover; dry; 50-96cm cover soil mostly, dark becoming light.

15 - 20 (4.57 - 6.10)	1.18	4.57 - 5.75	0-16cm, soil cover + wood, fairly dry; 16-55cm shingles, black; 55-118cm fairly well mixed wood, plastics, cover, becoming drier. Much paper
20 - 25 (6.10 - 7.62)	1.04	6.10 - 7.14	0-40cm mixed cover + wood w/ small amt of plastics; 40-104cm no discernable "lithological" changes; well-mixed wood plastic, paper. Not much cover, medium dry.
25 - 30 (7.62 - 9.14)	0.78	7.62 - 8.40	0-25cm cover, loose and dry; 25-40cm dark organics, maybe shingles, plastics; 40-60cm wood + textiles; 60-78cm cover soil
30 - 32.5 (9.14 - 9.91)	0.48	9.14 - 9.62	0-20cm black cover, organics + wood; 20-48cm - mostly cover soil
DH-08			
0 - 5 (0 - 1.46)	0.76	0 - 0.76	soil cover to 54cm. 54-76cm mostly wood waste + organics + styrofoam
5 - 10 (1.52 - 3.05)	0.3	1.52 - 1.82	loose cover + coarse wood waste; moist
10 - 15 (3.05 - 4.57)	0.59	3.05 - 3.64	wood + loose soil to 20cm. 20-30cm mosre coarse wood than soil; 30-60cm black finer wood, soil
15 - 20 (4.57 - 6.10)	1.07	4.57 - 5.65	0-30cm light organics (wood) + cover, very moist. 30-48, more dense w/ cover + finer organics. Remaining 78cm all cover soil
20 - 23 (6.10 - 7.01)	0.51	6.10 - 6.61	0-30cm black wet, difficult to see contents, but very dense; likely high clay content. 30-51cm sandy red cover, drier.
23 - 25 (7.01 - 7.62)	0.46	7.01 - 7.47	0-10cm sandy cover; 10-30cm loose cover mixed with organics; 30-46cm mixed waste, plastics + soil. Overall interval is dense and moist
25 - 30 (7.62 - 9.14)	0.92	7.62 - 8.54	very muddy interval; plastic is smeared and obscures the the details. Wood + fine organics visible. After 46cm, becoming drier soil zone from 60cm - 75cm. Mixed waste otherwise drier soil + plastics. Coarse wood at 46cm.
30 - 35 (9.14 - 10.67)	1.04	9.14 - 10.18	0-25cm moist cover soil + wet organics; 25-45cm drier soil + plastics; 45-60 coarse wood; (poor recovery and large voids in sample tube) 60-75cm loose large voids, coarse wood; 75-104cm mostly dry cover mixed with plastics + some sparse wood debris.
DH-09			
0 - 5 (0 - 1.46)	1.41	0 - 1.41	0-122cm cover soil; 122-141cm coarse wood + plastics, moist + fine organics (grass + leaves)
5 - 10 (1.52 - 3.05)	0.61	1.52 - 2.13	loose soil + coarse wood 0-20cm. 20-40cm very similar to previous 20cm, moderatly moist; 40-61cm soil.

10 - 15 (3.05 - 4.57)	1.04	3.05 - 4.09	0-20cm, mostly soil w/ small bits of wood. 20-60cm soil cover though diameter only half-filled from 30-50cm. 60-104cm dense moderately moist soil + fine organics + plastics
15 - 20 (4.57 - 6.10)	1.07	4.57 - 5.63	0-20cm mostly cover soil; 20-35cm more loose organics + plastics + textiles. 35-70cm cover soil + plastics; remainder cover soil + shingles
20 - 25 (6.10 - 7.62)	NO SAMPLE		
25 - 27 (7.62 - 8.23)	0.53	7.62 - 8.15	Wet cover soil + grass + wood. Saturated. 17-35cm seems to be organics but very dense.
28 - 33 (8.53 - 10.1)	1.34	8.53 - 9.87	0-30cm mostly wet cover soil. 30-55cm mostly cover soil w/ plastics. 55-100cm mostly shingles. 100-120cm moist mixed waste - low density, black, seems to be plastics. 120-134cm - mostly cover
DH-10			
0 - 5 (0 - 1.46)	1.09	0 - 1.09	0-80cm, cover soil. 80-109cm dry + loose, fine organics + cover
5 - 10 (1.52 - 3.05)	1.04	1.52 - 2.56	0-15cm fine organics, moderately moist w/ cover. 15-35cm, coarse wood, much void space, probably not representative of true density; 35-64cm soil, dense, clayey; 64-104cm dense mixed waste; plastics, textiles wood, moist
10 - 15 (3.05 - 4.57)	0.34	3.05 - 3.39	0-15cm, mixed dry cover soil + fine wood and organics. 15-34cm, fine-dry coarse soil, sandy
15 - 20 (4.57 - 6.10)	0.83	4.57 - 5.40	0-25cm cover soil + fine wood debris, dense and moist. 25-35cm coarse wood. 35-55cm more dense, black cover soil + fine organics; becoming less dense 55-83cm, less soil, more coarse wood and plastics
20 - 25 (6.10 - 7.62)	NO SAMPLE		
25 - 30 (7.62 - 9.14)	0.81	7.62 - 8.43	0-36cm - mostly cover soil, dense, with fine organics; 36-54cm dry, low density, fine organics + textiles, 54-74cm, moist interval, very black; 74-81cm, same as 36-54cm.
DH-11			
0 - 5 (0 - 1.46)	1.46	0 - 1.46	cover soil
5 - 10 (1.52 - 3.05)	0.88	1.52 - 2.40	0-25cm, end of cover soil; 25-65cm coarse organics (wood) + mixed plastics and soil (becoming wetter), 65-88cm loose soil + v. fine organics, fairly dry

10 - 15 (3.05 - 4.57)	0.58	3.05 - 3.63	0-20cm loose moist soil + fine organics; coarse wood from 20-40cm; 40-58cm more soil
15 - 20 (4.57 - 6.10)	0.21	4.57 - 4.78	short interval of soil + coarse wood that may have blocked the bit
20 - 25 (6.10 - 7.62)	0.16	6.10 - 6.26	another short soil interval
25 - 30 (7.62 - 9.14)	0.76	7.62 - 8.38	0-46cm - very black and wet, difficult to see contents; some plastics + soil; upon dissection coarse wood, dense soil and fine plastics. 46-76cm drier than previous interval; upon dissection, also wet + dense; mostly non-soil: wood textiles + plastics
30 - 35 (9.14 - 10.67)	1.18	9.14 - 10.32	0-35cm similar to previous interval, dark dense and moist; 35-69cm drier, soil with fine organics;69-89cm shingles + coarse wood + soil; looks moderately moist; 89-118cm stacks of paper, wood and textiles
DH-12			
0 - 5 (0 - 1.46)	1.46	0 - 1.46	cover soil
5 - 10 (1.52 - 3.05)	1.17	1.52 - 2.69	0-20cm loose soil + yard waste (mostly wood); 20-30cm paper; 30-47cm loose soil, mostly dry; 47-117cm cover soil
10 - 11.5 (3.05 - 3.51)	0.4	3.05 - 3.45	looks like mostly cover soil w/ small bits of wood; moist
11.5 - 15 (3.51 - 4.57)	0.69	3.51 - 4.20	very dry throughout, loose soil, fine wood chips, yard waste. Sample split @ 40cm. 1st interval had wet soil @ top, hence the greater mass
15 - 20 (4.57 - 6.10)	0.59	4.57 - 5.16	samples continues with dry wood + soil to about 20cm, then more paper + plastics. @ 40cm mostly soil for the rest of the sample
20 - 25 (6.10 - 7.62)	1.11	6.10 - 7.21	loose soil + wood to 20cm; 20-80cm mixed paper textiles + plastics; very dry; 80-117cm, cover soil
25 - 30 (7.62 - 9.14)	0.74	7.62 - 8.36	0-20cm - mostly loose dry soil + finer organics; 20-39cm more plastics + large wood pieces; 39-74cm mostly plastics + wood w/ little soil content; much paper
30 - 34 (9.14 - 10.36)	0.57	9.14 - 9.71	0-17cm, mostly cover; rest of sample mixed plastics, loose soil + textiles
DH-13			
0 - 5 (0 - 1.46)	1.46	0 - 1.46	cover soil

5 - 10 (1.52 - 3.05)	.64	1.52 - 2.16	top 8cm, continuing cover soil; mixed soil + textiles to 20cm; 20-40cm textiles + plastics; 40-64cm more soil cover + shingles, loose + dry.
10 - 15 (3.05 - 4.57)	0.45	3.05 - 3.29	0-20cm semi-moist, mostly soil, wood + textiles; 20-45cm becoming drier, still fine wood + organics, loosely packed
15 - 20 (4.57 - 6.10)	1.00	4.57 - 5.57	0-15cm loose organics (fine wood + grass) + soil; 15-77cm soil BUT from 15-60, the sample tube is only half-filled with sample, becoming looser towards 77cm; 77-100cm plastics, soil + fine organics.
20 - 25 (6.10 - 7.62)	0.82	6.10 - 6.92	0-38cm loose soil + fine organics, not decomposed; 38-82cm mixed intervals of paper, coarse soil, fine soil. Looks moist and fairly compacted.
25 - 30 (7.62 - 9.14)	0.85	7.62 - 8.47	0-30cm loose soil, mostly dry w. small amount of OM; 30-60cm mixed wood textiles + soil; 60-85cm, soil, very dark, moist + dense
30 - 35 (9.14 - 10.67)	1.34	9.14 - 10.48	0-20cm mostly soil + fine organics; 20-40cm mixed wood + sawdust + plastics; 40-53cm paper, wood + little soil; 53-87cm cover soil, dense, dark + clayey; 87-134cm very dark, dense; mostly wet cover but with plastics + wood

APPENDIX B: DETAILED MSW MOISTURE ANALYSIS DATA

Interval Start (ft)	Interval end (ft)	Length of sampling interval (cm)	length of sample (cm)	% recovery	Incremented sampling (if any) from	to	Mass of bowl (g)	Mass of wet waste (g)	Total Wet Mass (g)	Total Dry Mass (g)	Mass of dry waste (g)	Mass of water (g)	% moisture by wt.	Estimated volume of sample (cm^3)	Density of sample (kg/m^3)	% Moisture by volume
DH-01											**DH-01**					
0.0	5.0	146	146	100			167	2794	2961	2621.72	2454.72	339.28	**12.1**	1954	1430	**17.4**
5.0	9.0	122	84	69			164	968.71	1132.71	923.66	759.66	209.05	**21.6**	1124	862	**18.6**
9.0	14.0	146	55	38			17.21	377.28	394.49	340.64	323.43	53.85	**14.3**	736	513	**7.3**
14.0	19.0	146	117	80			203.1	2030.95	2234.05	1935.03	1731.93	299.02	**14.7**	1565	1297	**19.1**
19.0	24.0	146	94	64			205.9	1358.59	1564.49	1132.71	926.81	431.78	**31.8**	1258	1080	**34.3**
24.0	30.0	183	75	41			166.1	1490.36	1656.46	1313.56	1147.46	342.9	**23.0**	1004	1485	**34.2**
30.0	35.0	146	94	64			237.92	1033.86	1271.78	809.76	571.84	462.02	**44.7**	1258	822	**36.7**
DH-02											**DH-02**					
0.0	5.0	146			n/a		11.81	1295.75	1307.56	1106.49	1094.68	201.07	**15.5**	1806	1811	**24.6**
			135	92	n/a		11.81	1974.94	1986.75	1743.65	1731.84	243.1	**12.3**			
5.0	10.0	146			0	60	11.81	1019.7	1031.51	885.61	873.8	145.9	**14.3**	803	1270	**18.2**
			110	75	60	110	11.81	432.57	444.38	351.11	339.3	93.27	**21.6**	669	647	**13.9**
10.0	15.0	146			0	40	11.84	416.52	428.36	379.79	367.95	48.57	**11.7**	535	778	**9.1**
			112	77	40	112	11.86	697.54	709.4	527.18	515.32	182.22	**26.1**	963	724	**18.9**
15.0	20.0	146			0	40	11.84	547.64	559.48	498.77	486.93	60.71	**11.1**	535	1023	**11.3**
			122	84	40	122	11.84	1377.51	1389.35	1250.71	1238.87	138.64	**10.1**	1097	1256	**12.6**
20.0	25.0	146	41	28			11.84	362.48	374.32	314.34	302.5	59.98	**16.5**	549	661	**10.9**
25.0	30.0	146			0	33	11.84	333.12	344.96	288.24	276.4	56.72	**17.0**	442	754	**12.8**
			72	49	33	72	11.84	717.83	729.67	617.4	605.56	112.27	**15.6**	522	1376	**21.5**
DH-03											**DH-03**					
0.0	5.0	146			0	85	11.84	1951.62	1963.46	1688.88	1677.04	274.58	**14.1**	1137	1716	**24.1**
			146	100	85	146	11.84	1553.94	1565.78	1416.81	1404.97	148.97	**9.6**	816	1904	**18.3**
5.0	10.0	146			0	37	11.81	544.03	555.84	454.45	442.64	101.39	**18.6**	495	1099	**20.5**
			104	71	37	104	11.82	1286.64	1298.46	1112	1100.18	186.46	**14.5**	896	1435	**20.8**
10.0	15.0	146			0	53	11.82	460.08	471.9	364.15	352.33	107.75	**23.4**	709	649	**15.2**
			119	82	53	119	11.81	624.39	636.2	512.52	500.71	123.68	**19.8**	883	707	**14.0**
15.0	20.0	146	57	39			11.81	551.74	563.55	469.1	457.29	94.45	**17.1**	763	723	**12.4**
20.0	25.0	146	30	21			11.81	234.97	246.78	212.64	200.83	34.14	**14.5**	401	585	**8.5**
25.0	30.0	146	79	54			226.88	881.26	1108.14	846.41	619.53	261.73	**29.7**	1057	834	**24.8**
30	32.5	76	56	73			238.33	993.67	1232	977.46	739.13	254.54	**25.6**	749	1326	**34.0**
DH-04											**DH-04**					
0.0	5.0	146	146	100			206	3221	3427	3057	2851	370	**11.5**	1954	1649	**18.9**
5.0	10.0	146			0	35	11.88	394.37	406.25	333.6	321.72	72.65	**18.4**	468	842	**15.5**
			111	76	35	111	11.88	1464.78	1476.66	1245.06	1233.18	231.6	**15.8**	1017	1440	**22.8**
10.0	15.0	146			0	40	11.88	421.19	433.07	304.7	292.82	128.37	**30.5**	535	787	**24.0**
					40	68	11.84	330.2	342.04	254.3	242.46	87.74	**26.6**	375	881	**23.4**
			114	78	68	114	11.88	457.98	469.86	321.7	309.82	148.16	**32.4**	615	744	**24.1**
15.0	20.0	146			0	50	11.95	459.76	471.71	335.6	323.65	136.11	**29.6**	669	687	**20.3**
			108	74	50	108	11.92	538.13	550.05	438.45	426.53	111.6	**20.7**	776	693	**14.4**
20.0	25.0	146			0	50	11.9	704.33	716.23	599.8	587.9	116.43	**16.5**	669	1053	**17.4**
			93	64	50	93	11.9	928.27	940.17	833.95	822.05	106.22	**11.4**	575	1613	**18.5**

25.0	27.0	61	53	87		11.9	522.85	534.75	406.31	394.41	128.44	**24.6**	709	737	**18.1**
DH-05										**DH-05**					
0.0	5.0	146	146	100		230.57	3297.43	3528	3056	2825.43	472	**14.3**	1954	1688	**24.2**
5.0	10.0	146	46	32		11.89	338.31	350.2	232.87	220.98	117.33	**34.7**	615	550	**19.1**
10.0	15.0	146	44	30		12	277.59	289.59	215.5	203.5	74.09	**26.7**	589	472	**12.6**
15.0	20.0	146			0	40	12.01	345.64	357.65	288.65	276.64	69	**20.0**	535	646	**12.9**
			135	92	40	135	11.95	1858.28	1870.23	1673.99	1662.04	196.24	**10.6**	1271	1462	**15.4**
20.0	25.0	146			0	51	12	552.94	564.94	456.6	444.6	108.34	**19.6**	682	810	**15.9**
			98	67	51	98	12.01	325.55	337.56	247.05	235.04	90.51	**27.8**	629	518	**14.4**
25.0	30.0	146	93	64			11.91	779.29	791.2	589.75	577.84	201.45	**25.9**	1244	626	**16.2**
30.0	35.0	146			0	40	11.98	343.17	355.15	271.2	259.22	83.95	**24.5**	535	641	**15.7**
			98	67	40	98	11.91	465.94	477.85	358.54	346.63	119.31	**25.6**	776	600	**15.4**
DH-06										**DH-06**					
0.0	5.0	146	106	73			203.22	2469.74	2672.96	2400.77	2197.55	272.19	**11.0**	1418	1741	**19.2**
5.0	10.0	146			0	40	17.31	712.18	729.49	656.94	639.63	72.55	**10.2**	535	1331	**13.6**
			98	67	40	98	11.77	456.21	467.98	242.35	230.58	225.63	**49.5**	776	588	**29.1**
10.0	15.0	146	38	26			11.86	322.2	334.06	279	267.14	55.06	**17.1**	508	634	**10.8**
15.0	20.0	146	73	50			11.87	793.29	805.16	654.5	642.63	150.66	**19.0**	977	812	**15.4**
DH(ES)-07										**DH(ES)-07**					
0.0	5.0	146	116	79			164.84	2689.88	2854.72	2522.72	2357.88	332	**12.3**	1552	1733	**21.4**
5.0	10.0	146	60	41			11.85	488.96	500.81	414.61	402.76	86.2	**17.6**	803	609	**10.7**
10.0	15.0	146			0	50	11.84	281.85	293.69	202.05	190.21	91.64	**32.5**	669	421	**13.7**
			96	66	50	90	11.88	867.21	879.09	782.45	770.57	96.64	**11.1**	535	1620	**18.1**
15.0	20.0	146			0	50	11.88	461.02	472.9	406.61	394.73	66.29	**14.4**	669	689	**9.9**
			118	81	50	118	11.84	661.88	673.72	446.69	434.85	227.03	**34.3**	910	727	**25.0**
20.0	25.0	146			0	50	11.87	334.85	346.72	238.6	226.73	108.12	**32.3**	669	501	**16.2**
			104	71	50	104	11.85	378.61	390.46	296.57	284.72	93.89	**24.8**	723	524	**13.0**
25.0	30.0	146	78	53			11.87	813.08	824.95	649.7	637.83	175.25	**21.6**	1044	779	**16.8**
30.0	32.5	76	48	63			333.51	441.15	774.66	691.15	357.64	83.51	**18.9**	642	687	**13.0**
DH-08										**DH-08**					
0.0	5.0	146	76												
					54	76	17.09	156.75	173.84	89.18	72.09	84.66	**54.0**	294	533	**28.8**
5.0	10.0	146	30	21			16.19	257.38	273.57	191.9	175.71	81.67	**31.7**	401	641	**20.3**
10.0	15.0	146	59	40	0	32	17.21	321.45	338.66	211.16	193.95	127.5	**39.7**	428	751	**29.8**
					32	59	17.5	267.32	284.82	207.34	189.84	77.48	**29.0**	361	740	**21.4**
15.0	20.0	146	108	74	0	48	11.85	641.05	652.9	488.5	476.65	164.4	**25.6**	642	998	**25.6**
					48	108	17.46	1292.64	1310.1	1157.6	1140.14	152.5	**11.8**	803	1610	**19.0**
20.0	23.0	91	51	56	0	25	17.41	416.69	434.1	305.33	287.92	128.77	**30.9**	335	1246	**38.5**
					25	51	16.64	388.56	405.2	280.63	263.99	124.57	**32.1**	348	1117	**35.8**
23.0	25.0	61	46	75	0	24	17.05	300.75	317.8	260	242.95	57.8	**19.2**	321	937	**18.0**
					24	46	16.97	289.5	306.47	215.31	198.34	91.16	**31.5**	294	983	**31.0**
25.0	30.0	146	92	63	0	25	16.23	338.07	354.3	266.83	250.6	87.47	**25.9**	335	1011	**26.1**
					25	46	17.01	173.36	190.37	125.3	108.29	65.07	**37.5**	281	617	**23.2**
					46	71	16.71	250.42	267.13	206.76	190.05	60.37	**24.1**	335	749	**18.0**
					71	92	17.23	241.73	258.96	209.52	192.29	49.44	**20.5**	281	860	**17.6**
30.0	35.0	146	104	71	0	29	17.07	228.74	245.81	170	152.93	75.81	**33.1**	388	589	**19.5**
					29	60	16.64	294.5	311.14	203.07	186.43	108.07	**36.7**	415	710	**26.1**

					60	104	16.91	326.2	343.11	286.61	269.7	56.5	**17.3**	589	554	**9.6**
DH-09								0			**DH-09**					
0.0	5.0	146	141		122	141	11.84	216.31	228.15	142.13	130.29	86.02	**39.8**	254	851	**33.8**
5.0	10.0	146	120	82	0	40	11.89	361.15	373.04	261.7	249.81	111.34	**30.8**	535	675	**20.8**
					40	61	11.87	327.69	339.56	282.92	271.05	56.64	**17.3**	281	1166	**20.2**
10.0	15.0	146	104	71	0	59	11.83	736.47	748.3	606.5	594.67	141.8	**19.3**	789	933	**18.0**
					59	104	11.82	540.38	552.2	455.3	443.48	96.9	**17.9**	602	897	**16.1**
15.0	20.0	146	106	73	0	20	12.04	293.6	305.64	244.25	232.21	61.39	**20.9**	268	1097	**22.9**
					20	35	11.91	145.4	157.31	96.32	84.41	60.99	**41.9**	201	724	**30.4**
					35	71	11.88	790.72	802.6	707.6	695.72	95	**12.0**	482	1642	**19.7**
					71	86	12.09	194.38	206.47	168.38	156.29	38.09	**19.6**	201	968	**19.0**
					86	106	11.6	340.5	352.1	325.23	313.63	26.87	**7.9**	268	1272	**10.0**
20.0	25.0	no sample	0	0												
25.0	27.0	61	53	87	0	23	17.35	295.52	312.87	228.77	211.42	84.1	**28.5**	308	960	**27.3**
					23	53	15.96	575.04	591	477.4	461.44	113.6	**19.8**	401	1433	**28.3**
28.0	33.0	146	134	92	0	30	17.1	446.3	463.4	339.88	322.78	123.52	**27.7**	401	1112	**30.8**
					30	52	17.4	311.5	328.9	282	264.6	46.9	**15.1**	294	1058	**15.9**
					52	90	17.39	453.91	471.3	417.1	399.71	54.2	**11.9**	508	893	**10.7**
					90	114	17.5	237.2	254.7	173.18	155.68	81.52	**34.4**	321	739	**25.4**
					114	134	17.23	280.21	297.44	218.35	201.12	79.09	**28.2**	268	1047	**29.6**
DH-10								0			**DH-10**					
0.0	5.0	146			80	109	11.91	290.27	302.18	202.11	190.2	100.07	**34.5**	388	748	**25.8**
5.0	10.0	146	104	71	0	34	12.02	198.98	211	157.5	145.48	53.5	**26.9**	455	437	**11.8**
					34	64	11.97	869.53	881.5	792.5	780.53	89	**10.2**	401	2166	**22.2**
					64	104	11.87	441.13	453	311.92	300.05	141.08	**32.0**	535	824	**26.4**
10.0	15.0	146	34	23			11.9	309.1	321	250.23	238.33	70.77	**22.9**	455	679	**15.6**
15.0	20.0	146	83	57	0	35	11.9	402.9	414.8	327.81	315.91	86.99	**21.6**	468	860	**18.6**
					35	58	11.83	260.34	272.17	185.7	173.87	86.47	**33.2**	308	846	**28.1**
					58	83	11.85	218.51	230.36	136.81	124.96	93.55	**42.8**	335	653	**28.0**
20.0	25.0	no sample	0	0												
25.0	30.0	146	81	55	0	18	11.87	196.53	208.4	160.91	149.04	47.49	**24.2**	241	816	**19.7**
					18	36	11.87	354.54	366.41	310.19	298.32	56.22	**15.9**	241	1472	**23.3**
					36	55	11.84	239.4	251.24	153.84	142	97.4	**40.7**	254	942	**38.3**
					55	81	11.85	243.98	255.83	169.77	157.92	86.06	**35.3**	348	701	**24.7**
DH-11								0			**DH-11**					
5.0	10.0	146	113	77	0	25	11.67	387.08	398.75	321.29	309.62	77.46	**20.0**	335	1157	**23.2**
					25	50	11.94	159.76	171.7	120	108.06	51.7	**32.4**	335	478	**15.5**
					50	88	11.81	268.45	280.26	181.76	169.95	98.5	**36.7**	508	528	**19.4**
10.0	15.0	146	58	40	0	30	11.8	253.05	264.85	200.22	188.42	64.63	**25.5**	401	630	**16.1**
					30	58	11.93	181.44	193.37	125.99	114.06	67.38	**37.1**	375	484	**18.0**
15.0	20.0	146	21	14			12.04	285.97	298.01	251.03	238.99	46.98	**16.4**	281	1018	**16.7**
20.0	25.0	146	16	11			11.92	190.24	202.16	157.54	145.62	44.62	**23.5**	214	889	**20.8**
25.0	30.0	146	76	52	0	24	11.95	260.33	272.28	185.18	173.23	87.1	**33.5**	321	811	**27.1**
					24	46	11.97	304.02	315.99	222.05	210.08	93.94	**30.9**	294	1033	**31.9**
					46	76	11.89	269.61	281.5	156.43	144.54	125.07	**46.4**	401	672	**31.2**
30.0	35.0	146	118	81	0	35	11.88	398.62	410.5	310	298.12	100.5	**25.2**	468	851	**21.5**
					35	69	12.13	397.17	409.3	330.48	318.35	78.82	**19.8**	455	873	**17.3**
					69	93	11.11	200.14	211.25	178.65	167.54	32.6	**16.3**	321	623	**10.2**

					93	118	12	262.69	274.69	218.81	206.81	55.88	**21.3**	335	785	**16.7**
DH-12								0			**DH-12**					
5.0	10.0	146	117	80	0	70	11.9	1340	1351.9	1207.2	1195.3	144.7	**10.8**	937	1431	**15.4**
					70	117	11.86	398.14	410	283.9	272.04	126.1	**31.7**	629	633	**20.1**
10.0	11.5	46	40	27			11.8	459.6	471.4	366.8	355	104.6	**22.8**	535	859	**19.5**
11.5	15.0	107	69	47	0	40	11.85	418.15	430	358.6	346.75	71.4	**17.1**	535	781	**13.3**
					40	69	11.84	156.26	168.1	128.6	116.76	39.5	**25.3**	388	403	**10.2**
15.0	20.0	146	59	40	0	40	12	220.4	232.4	175.2	163.2	57.2	**26.0**	535	412	**10.7**
					40	59	11.85	185.77	197.62	169.8	157.95	27.82	**15.0**	254	731	**10.9**
20.0	25.0	146	111	76	0	38	11.9	270.7	282.6	193.4	181.5	89.2	**33.0**	508	532	**17.5**
					38	81	11.9	328.3	340.2	240.6	228.7	99.6	**30.3**	575	571	**17.3**
					81	111	11.9	664.1	676	605.9	594	70.1	**10.6**	401	1654	**17.5**
25.0	30.0	146	74	51	0	39	12.2	362.9	375.1	298.73	286.53	76.37	**21.0**	522	695	**14.6**
					39	74	11.8	282.3	294.1	199.56	187.76	94.54	**33.5**	468	603	**20.2**
30.0	34.0		57	39			12	481.3	493.3	379.84	367.84	113.46	**23.6**	763	631	**14.9**
DH-13								0			**DH-13**					
5.0	10.0	146	64	44	0	35	11.9	339.9	351.8	261.3	249.4	90.5	**26.6**	468	726	**19.3**
					35	64	11.91	325.7	337.61	263.47	251.56	74.14	**22.8**	388	839	**19.1**
10.0	15.0	146	45	31	0	24	11.84	274.17	286.01	237.22	225.38	48.79	**17.8**	321	854	**15.2**
					24	45	12.09	132.37	144.46	104.81	92.72	39.65	**30.0**	281	471	**14.1**
15.0	20.0	146	100	68	0	15	11.88	163.81	175.69	149.18	137.3	26.51	**16.2**	201	816	**13.2**
					15	77	1.89	889.91	891.8	784.4	782.51	107.4	**12.1**	830	1073	**12.9**
					77	100	11.86	197.54	209.4	159.91	148.05	49.49	**25.1**	308	642	**16.1**
20.0	25.0	146	82	56	0	37	11.87	209.82	221.69	174.44	162.57	47.25	**22.5**	495	424	**9.5**
					37	60	11.94	237.6	249.54	193.49	181.55	56.05	**23.6**	308	772	**18.2**
					60	82	11.99	227.91	239.9	158.33	146.34	81.57	**35.8**	294	774	**27.7**
25.0	30.0	146	85	58	0	30	11.91	222.89	234.8	182.73	170.82	52.07	**23.4**	401	555	**13.0**
					30	58	11.85	210.85	222.7	169.4	157.55	53.3	**25.3**	375	563	**14.2**
					58	85	11.91	457.39	469.3	416.2	404.29	53.1	**11.6**	361	1266	**14.7**
30.0	35.0	146	134	92	0	23	11.9	280.7	292.6	257.3	245.4	35.3	**12.6**	308	912	**11.5**
					23	53	12	335.3	347.3	252.77	240.77	94.53	**28.2**	401	835	**23.5**
					53	87	12.1	532.4	544.5	461.8	449.7	82.7	**15.5**	455	1170	**18.2**
					87	110	11.9	234.5	246.4	181.05	169.15	65.35	**27.9**	308	762	**21.2**
					110	134	11.9	444.5	456.4	359.36	347.46	97.04	**21.8**	321	1384	**30.2**

APPENDIX C: ENVIROSCAN GRAPHS AND CLIMATE DATA

Date	Mean Temp (□C)	Total Precip (mm)
5/15/2007	10.2	0
5/16/2007	12	0
5/17/2007	17.7	0
5/18/2007	7.1	0
5/19/2007	6.5	1.5
5/20/2007	10.7	0
5/21/2007	7.8	4
5/22/2007	9.8	0.5
5/23/2007	7.9	0
5/24/2007	8.3	0
5/25/2007	8.7	0
5/26/2007	11.3	0
5/27/2007	16.2	0
5/28/2007	15	4
5/29/2007	8.5	18
5/30/2007	9	0
5/31/2007	13.5	0
6/1/2007	16.9	0
6/2/2007	19.2	0
6/3/2007	17.7	0
6/4/2007	14.8	0
6/5/2007	16.7	0
6/6/2007	9.8	0.6
6/7/2007	9.4	0
6/8/2007	13.9	0
6/9/2007	12	0.4
6/10/2007	14.1	0
6/11/2007	18.4	2.6
6/12/2007	16.4	0
6/13/2007	16.1	0
6/14/2007	15.7	0
6/15/2007	12.9	0
6/16/2007	13.9	0
6/17/2007	13.4	86.4
6/18/2007	13.8	15.6
6/19/2007	14.2	0
6/20/2007	15.7	0.4
6/21/2007	18.3	0
6/22/2007	18.2	0
6/23/2007	17.9	0
6/24/2007	14.6	0
6/25/2007	12.1	8.6
6/26/2007	10.4	7.4
6/27/2007	10.9	0
6/28/2007	14.6	0
6/29/2007	17.5	0
6/30/2007	20.1	9
7/1/2007	19.3	0
7/2/2007		0
7/3/2007		
7/4/2007	20.4	0
7/5/2007	20.7	0
7/6/2007	24.7	0.5
7/7/2007	18.9	1.5
7/8/2007	15.8	0
7/9/2007	15	13
7/10/2007	14.6	0
7/11/2007	15.9	0
7/12/2007	19.3	0
7/13/2007	23.1	0
7/14/2007	22	0
7/15/2007	21.9	0.5
7/16/2007	22.3	0
7/17/2007	22.5	0
7/18/2007	21.5	0
7/19/2007		0
7/20/2007	22.6	1
7/21/2007	23.8	4
7/22/2007	23	0
7/23/2007		0
7/24/2007	26.1	0
7/25/2007	19.7	0
7/26/2007	18.2	0
7/27/2007	23.4	0
7/28/2007	23.3	0
7/29/2007	24.4	0
7/30/2007	27	0
7/31/2007	17.1	1.5
8/1/2007	15.7	0
8/2/2007	17.7	0
8/3/2007	22.9	0
8/4/2007	20.8	0
8/5/2007	18.7	0
8/6/2007	16.8	0.5
8/7/2007	22.2	0
8/8/2007	19.6	0
8/9/2007	15.2	2
8/10/2007	13.7	4.5
8/11/2007	15.1	8
8/12/2007	15.9	1
8/13/2007	16	0
8/14/2007	12.4	0

Date	Mean Temp (□C)	Total Precip (mm)
8/15/2007	13.2	0
8/16/2007	13.6	0
8/17/2007	15.8	
8/18/2007		
8/19/2007		
8/20/2007		
8/21/2007		
8/22/2007	11.7	0.5
8/23/2007	11.3	0
8/24/2007	11.5	0.5
8/25/2007	17.3	0.5
8/26/2007	10.9	0
8/27/2007	12.3	0
8/28/2007	12.4	0
8/29/2007	12.5	0
8/30/2007	16.6	0
8/31/2007	23.9	0
9/1/2007	14.2	0
9/2/2007	14.1	0
9/3/2007	17.2	0
9/4/2007	20.6	0
9/5/2007	15.3	0
9/6/2007	11.1	4
9/7/2007	9.1	1.5
9/8/2007	9.5	0.5
9/9/2007	9.6	0
9/10/2007	10.8	2.5
9/11/2007	13.3	0.5
9/12/2007	8.9	1
9/13/2007	5.1	1
9/14/2007	8.8	0
9/15/2007	12.9	0
9/16/2007	15.9	0
9/17/2007	9	0
9/18/2007	9	0
9/19/2007	4.1	0
9/20/2007	5.6	0.5
9/21/2007	8.5	0
9/22/2007	13	0
9/23/2007	6.2	7
9/24/2007	7.3	1
9/25/2007	8.7	0
9/26/2007	9	0
9/27/2007	8.8	1
9/28/2007	15.3	1.5
9/29/2007	5.8	2
9/30/2007	5.8	0

Date	Mean Temp (□C)	Total Precip (mm)
10/1/2007	10.9	0
10/2/2007	9.1	0
10/3/2007	6.9	0
10/4/2007	3.1	0
10/5/2007	3.3	0
10/6/2007	2.7	0.5
10/7/2007	5.7	0.5
10/8/2007	3.7	0
10/9/2007	4.1	0
10/10/2007	5.7	0
10/11/2007	4.1	9.5
10/12/2007	7	1
10/13/2007	8	1.5
10/14/2007	7	0
10/15/2007	10.3	0
10/16/2007	8.3	0
10/17/2007	7.1	0
10/18/2007	5.4	0
10/19/2007	5.3	0.5
10/20/2007	1.8	0
10/21/2007	3.6	0
10/22/2007	5.3	0
10/23/2007	7.2	0
10/24/2007	13.5	0
10/25/2007	5.2	0
10/26/2007	-3.3	0
10/27/2007	-2.7	0.5
10/28/2007	6.3	0
10/29/2007	6.8	0
10/30/2007	2.5	0
10/31/2007	1.8	0
11/1/2007	2.7	0
11/2/2007	2.6	0
11/3/2007	1.9	0
11/4/2007	2.3	0
11/5/2007	-5	0
11/6/2007		0
11/7/2007		0
11/8/2007	0.8	0
11/9/2007	-1.3	0
11/10/2007	-1.3	0
11/11/2007	2	1
11/12/2007	3.8	0
11/13/2007	4.2	0
11/14/2007	-1.6	0
11/15/2007	-1.5	0
11/16/2007	-4.2	0

Date	Mean Temp (□C)	Total Precip (mm)
11/17/2007	-1.6	0
11/18/2007	-0.8	8.5
11/19/2007	-2.4	0
11/20/2007	-6.2	1
11/21/2007	-11	0.5
11/22/2007	-10.1	0
11/23/2007	-6.5	0
11/24/2007	-4.1	0
11/25/2007	-10.6	1.5
11/26/2007	-22.8	1
11/27/2007	-19.7	3
11/28/2007	-21.5	0.5
11/29/2007	-21.7	0
11/30/2007	-18.5	0
12/1/2007	-18.3	0
12/2/2007	-19.8	0.5
12/3/2007	-15.5	2.5
12/4/2007	-17.8	0
12/5/2007	-16.7	1
12/6/2007	-20.9	0
12/7/2007	-22.8	0
12/8/2007	-24.1	0
12/9/2007	-17.7	0
12/10/2007	-12.8	1
12/11/2007	-13.7	0
12/12/2007	-11.8	3
12/13/2007	-16.3	0.5
12/14/2007	-12	1
12/15/2007	-11.1	0
12/16/2007	-12.4	1
12/17/2007	-15.2	0
12/18/2007		0
12/19/2007		
12/20/2007	-13.1	1
12/21/2007	-13.3	0.5
12/22/2007	-22.1	0
12/23/2007	-18.7	0
12/24/2007	-7.2	1
12/25/2007	-4.9	0.5
12/26/2007	-8.1	0
12/27/2007	-10.2	0
12/28/2007	-10.2	0
12/29/2007	-11.7	0
12/30/2007	-19.6	0
12/31/2007	-22.6	0
1/1/2008	-18.5	0
1/2/2008	-9.8	0

Date	Mean Temp (□C)	Total Precip (mm)
1/3/2008	-5.3	0
1/4/2008	-2.2	0
1/5/2008	-0.2	0
1/6/2008	-5.6	0
1/7/2008	-12.6	0
1/8/2008	-15.7	0
1/9/2008	-16.7	0
1/10/2008	-14.5	0.5
1/11/2008	-13.9	0
1/12/2008	-10.2	0.5
1/13/2008	-10.9	0
1/14/2008	-7.6	0.5
1/15/2008	-7.7	2.5
1/16/2008	-18.4	0
1/17/2008	-17.2	0.5
1/18/2008	-22.5	0
1/19/2008	-20.6	0
1/20/2008	-24	0.5
1/21/2008	-17.7	0
1/22/2008	-17.6	2
1/23/2008	-21.2	0
1/24/2008	-15.2	0.5
1/25/2008	-14.5	0
1/26/2008	-14	0
1/27/2008	-12.7	0.5
1/28/2008	-23.6	2.5
1/29/2008	-35.2	0
1/30/2008	-31.3	0
1/31/2008	-25	1
2/1/2008	-26.5	0
2/2/2008	-22.2	0.5
2/3/2008	-25.1	0
2/4/2008	-24.9	0
2/5/2008	-17.5	0
2/6/2008	-11	1.5
2/7/2008	-19.9	0
2/8/2008	-22.4	0
2/9/2008	-30.5	0
2/10/2008	-30.3	0.5
2/11/2008	-16.8	1
2/12/2008	-13.4	0.5
2/13/2008	-22.6	1.5
2/14/2008	-24.7	0.5
2/15/2008	-10.3	2
2/16/2008	-2.4	0
2/17/2008	-14.9	0
2/18/2008	-19	0

Date	Mean Temp (□C)	Total Precip (mm)
2/19/2008	-19.9	0
2/20/2008	-17.7	0
2/21/2008	-12.9	0
2/22/2008	-10.6	0
2/23/2008	-10.2	0
2/24/2008	-10.6	0
2/25/2008	-9.3	0
2/26/2008	-10.3	0
2/27/2008	-7.7	0
2/28/2008	-5.3	0
2/29/2008	-10.4	0
3/1/2008	-2.5	0
3/2/2008	-13.5	0
3/3/2008	-16.7	0
3/4/2008	-14.5	0
3/5/2008	-17.9	0
3/6/2008	-22.4	0
3/7/2008	-7.2	1
3/8/2008	-7	0
3/9/2008	-3.6	0
3/10/2008	-0.6	0
3/11/2008	0.3	0
3/12/2008	2	0
3/13/2008	-4.3	0
3/14/2008	-5.9	0
3/15/2008	-2.4	0
3/16/2008	-9.5	0
3/17/2008	-7.7	1
3/18/2008	-2	0
3/19/2008	-1.5	0
3/20/2008	-1.2	0
3/21/2008	-3.4	0
3/22/2008	-4.5	0
3/23/2008	0.4	0
3/24/2008	0	1.5
3/25/2008	-2	0.5
3/26/2008	-4.1	0
3/27/2008	-5.4	0
3/28/2008	-3.8	0
3/29/2008	-4	0
3/30/2008	-6.6	0
3/31/2008	-4.8	0
4/1/2008	-5.1	0
4/2/2008	-0.8	0.5
4/3/2008	2.8	0
4/4/2008	-3.9	1
4/5/2008	-6.5	0
4/6/2008	0.8	0.5
4/7/2008	-0.7	0
4/8/2008	1.4	0
4/9/2008	3.5	0.5
4/10/2008	1.8	0
4/11/2008	5.1	1
4/12/2008	4.2	0.5
4/13/2008	13.6	0
4/14/2008	7.8	0
4/15/2008	6	0
4/16/2008	4.6	0
4/17/2008	7.4	0
4/18/2008		0.5
4/19/2008		1
4/20/2008		9
4/21/2008		0.5
4/22/2008	-6	0.5
4/23/2008	-4.6	
4/24/2008	-0.6	0
4/25/2008	2.8	2.5
4/26/2008	0.7	0.5
4/27/2008	1.8	0
4/28/2008	7.7	0
4/29/2008	11.2	0
4/30/2008	9	2
5/1/2008	6	0.5
5/2/2008	4.9	0
5/3/2008	6.8	0
5/4/2008	7.4	0
5/5/2008	9	0
5/6/2008	8.8	0.5
5/7/2008	5.2	0
5/8/2008	5.1	0
5/9/2008	3.9	0
5/10/2008	6.5	0
5/11/2008	11.2	0
5/12/2008	8.3	0.5
5/13/2008	9.4	0
5/14/2008	11.3	0
5/15/2008	13.9	0
5/16/2008	16.3	0
5/17/2008	13.8	0
5/18/2008	16.7	0

APPENDIX D: DEEP DIVINER PLOTS

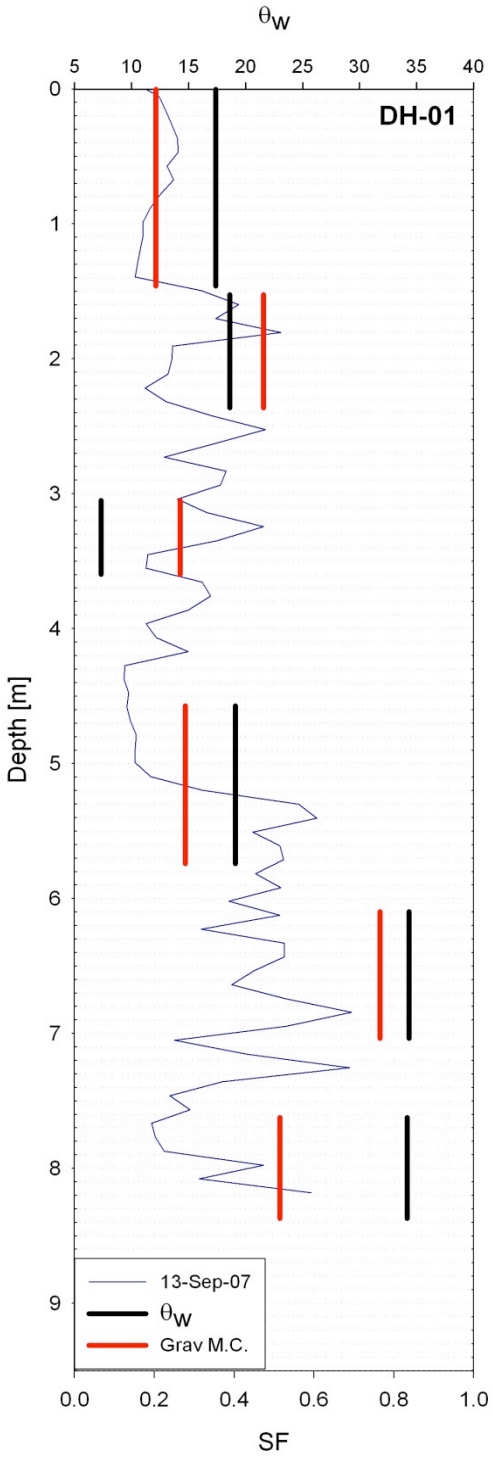

Figure D-1 – Deep Diviner survey for Hole DH-01, with volumetric and gravimetric moisture results from MSW samples.

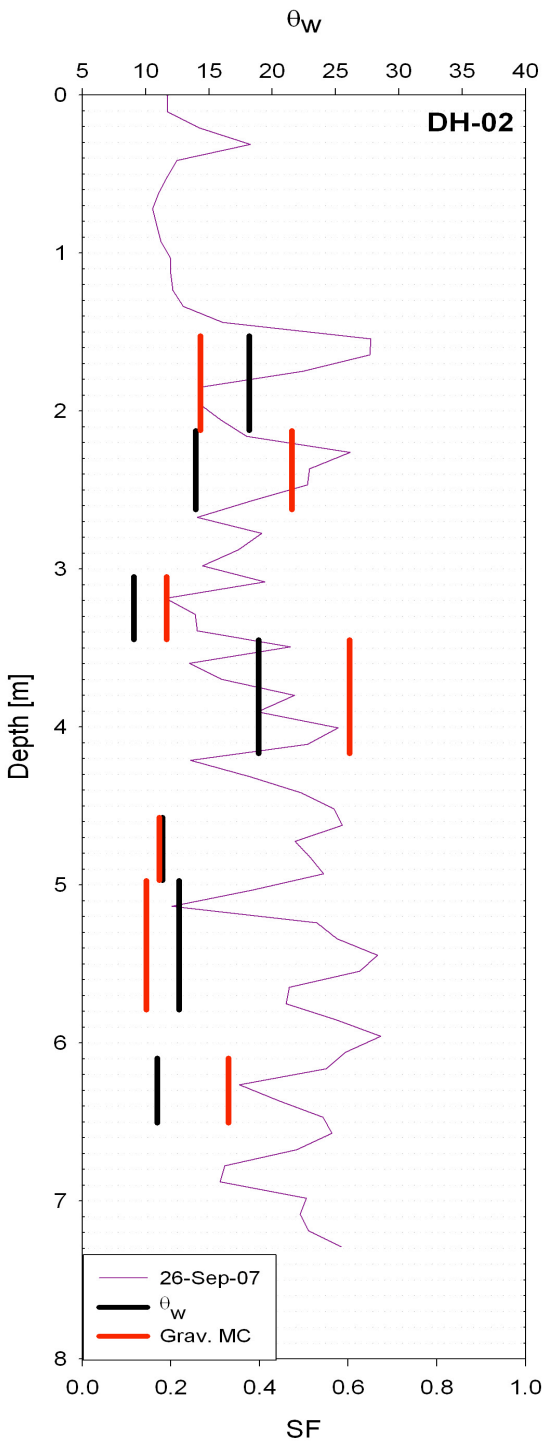

Figure D-2 – Deep Diviner survey for Hole DH-02, with volumetric and gravimetric moisture results from MSW samples.

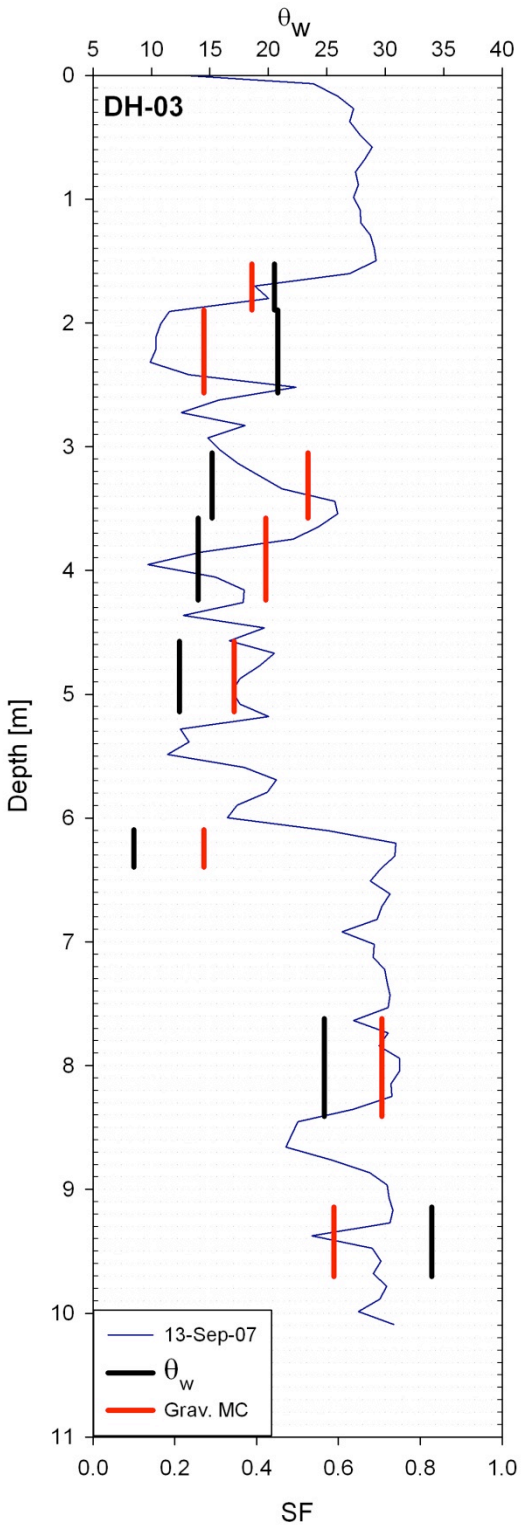

Figure D-3 – Deep Diviner survey for Hole DH-03, with volumetric and gravimetric moisture results from MSW samples.

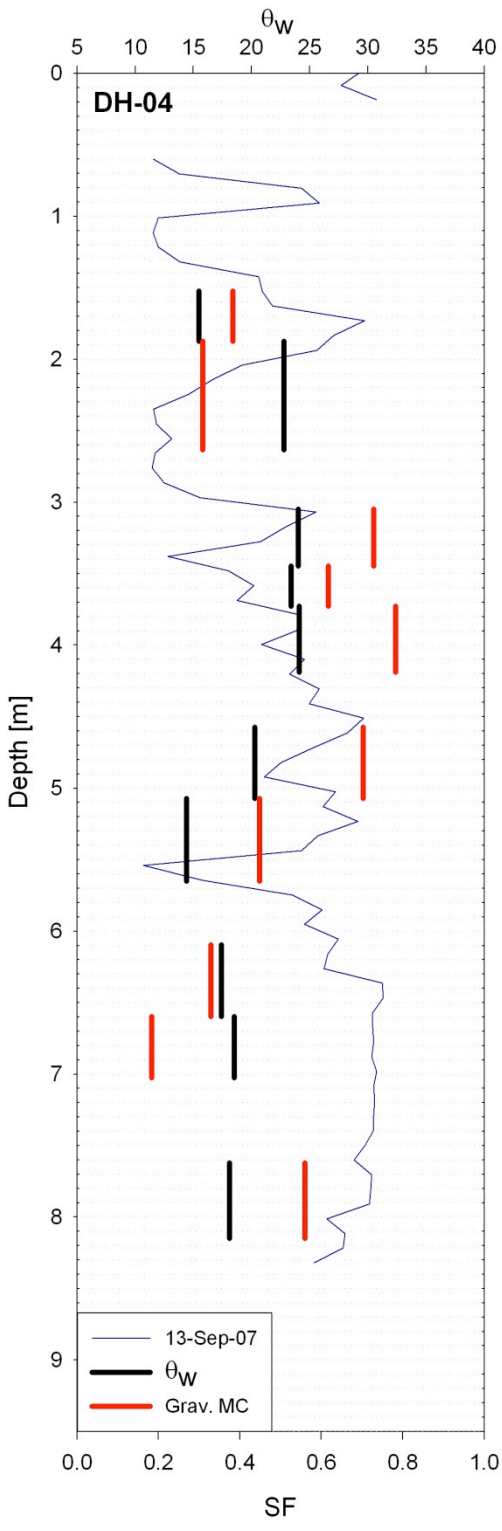

Figure D-4 – Deep Diviner survey for Hole DH-04, with volumetric and gravimetric moisture results from MSW samples.

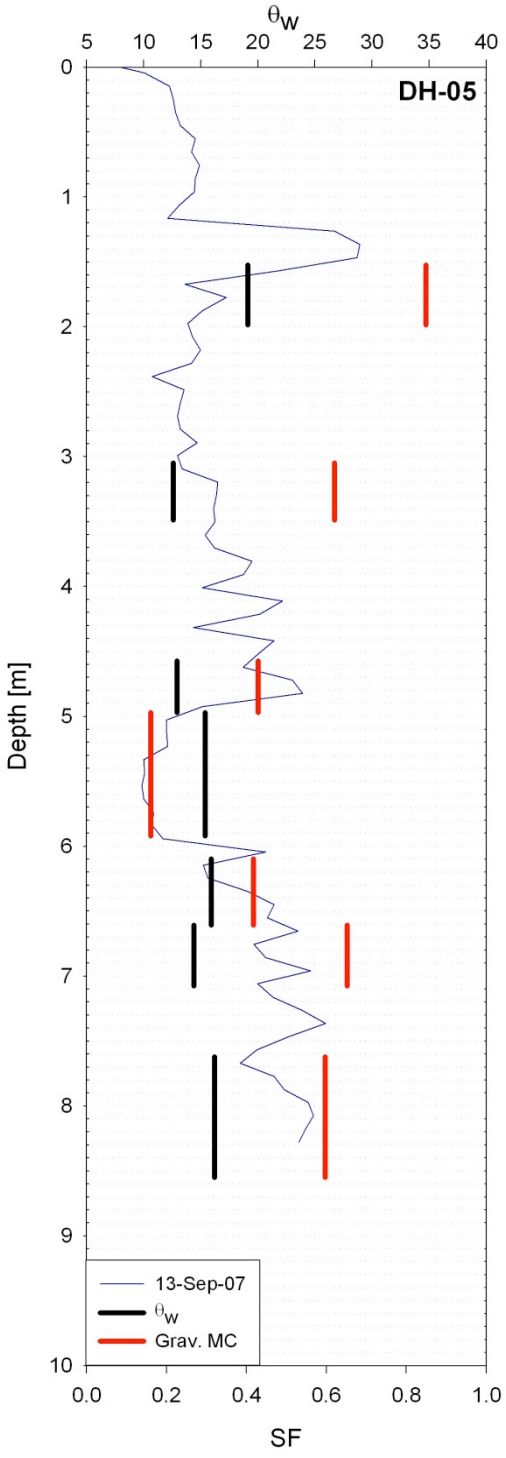

Figure D-5 – Deep Diviner survey for Hole DH-05, with volumetric and gravimetric moisture results from MSW samples.

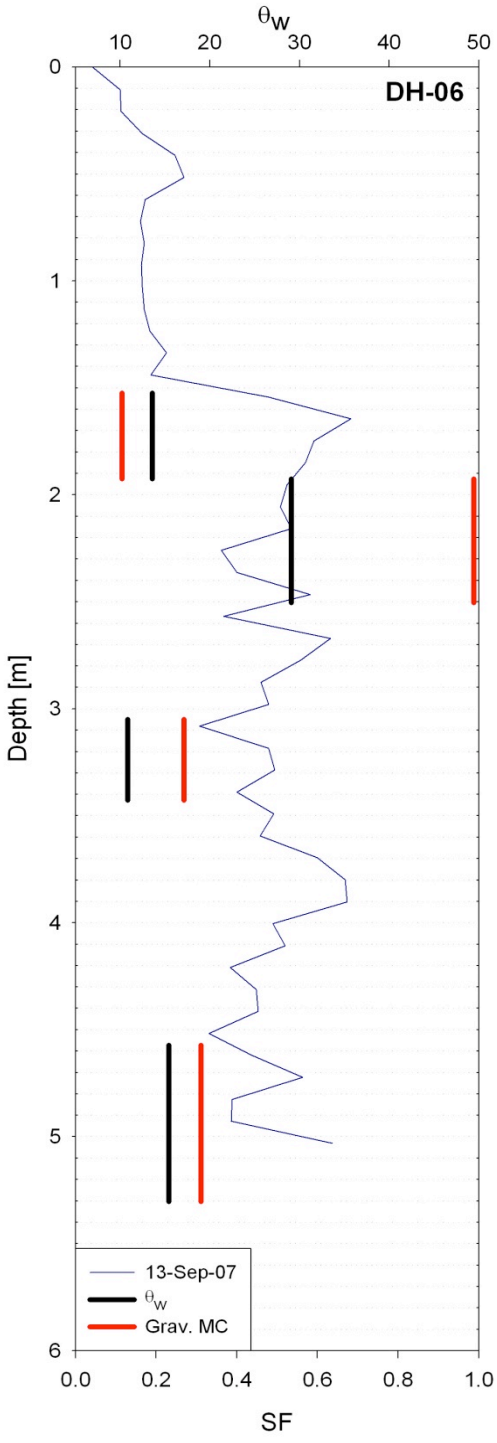

Figure D-6 – Deep Diviner survey for Hole DH-06, with volumetric and gravimetric moisture results from MSW samples.

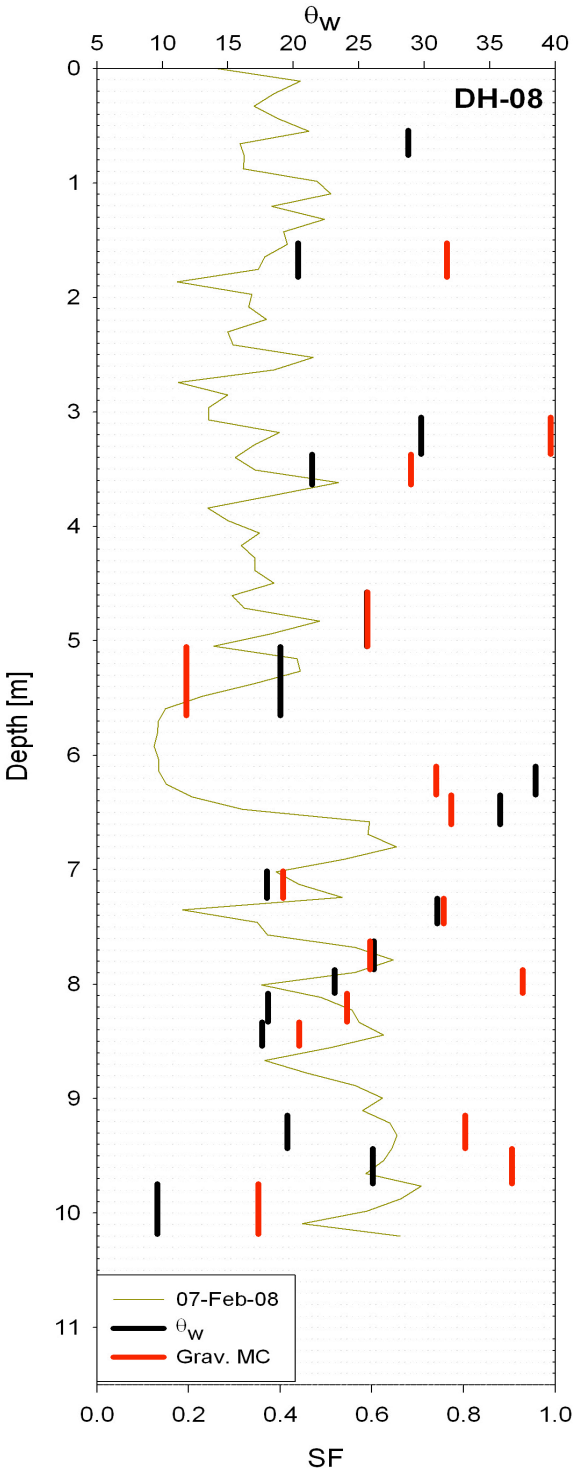

Figure D-7 – Deep Diviner survey for Hole DH-08, with volumetric and gravimetric moisture results from MSW samples.

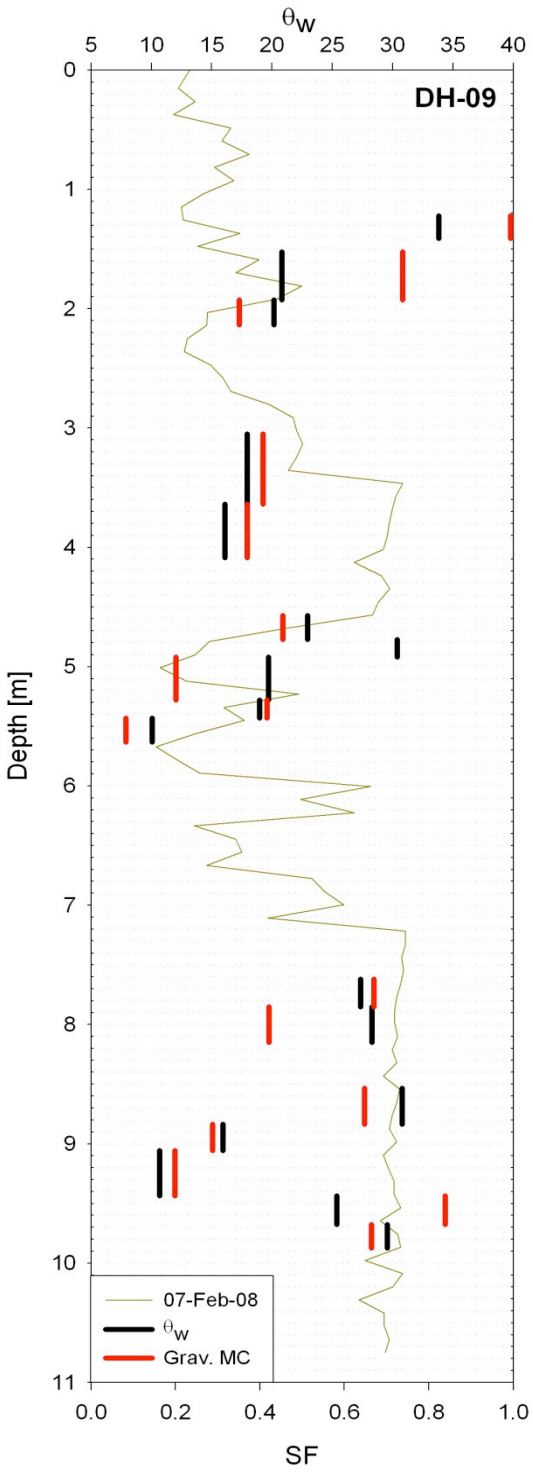

Figure D-8 – Deep Diviner survey for Hole DH-09, with volumetric and gravimetric moisture results from MSW samples.

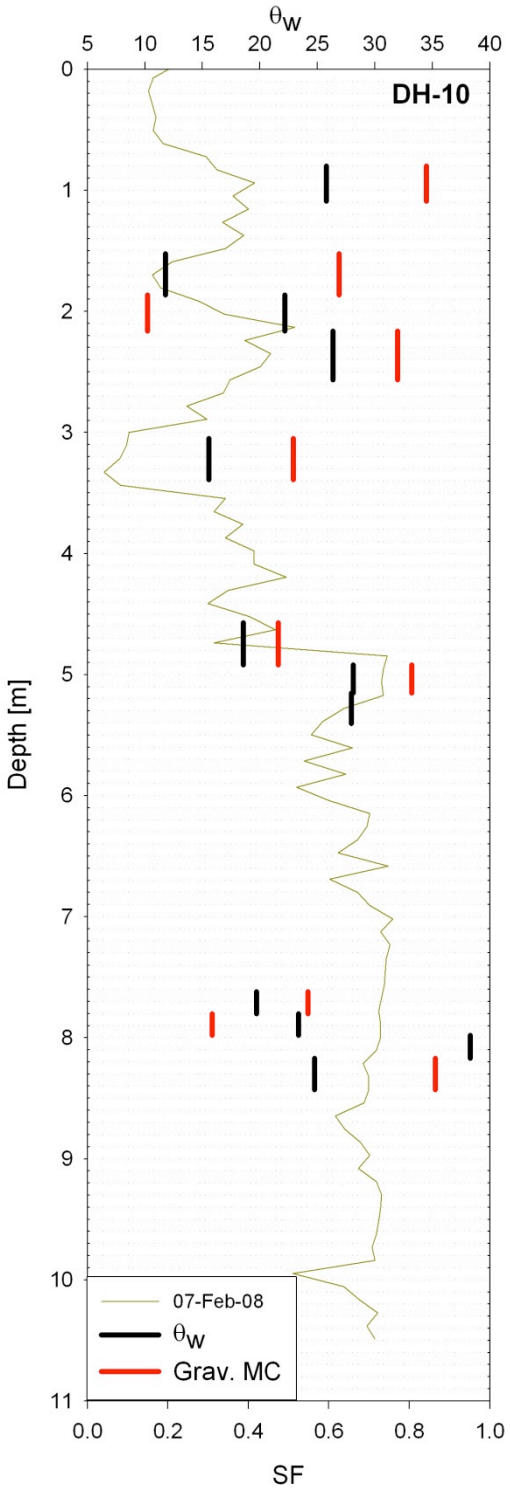

Figure D-9 – Deep Diviner survey for Hole DH-10, with volumetric and gravimetric moisture results from MSW samples.

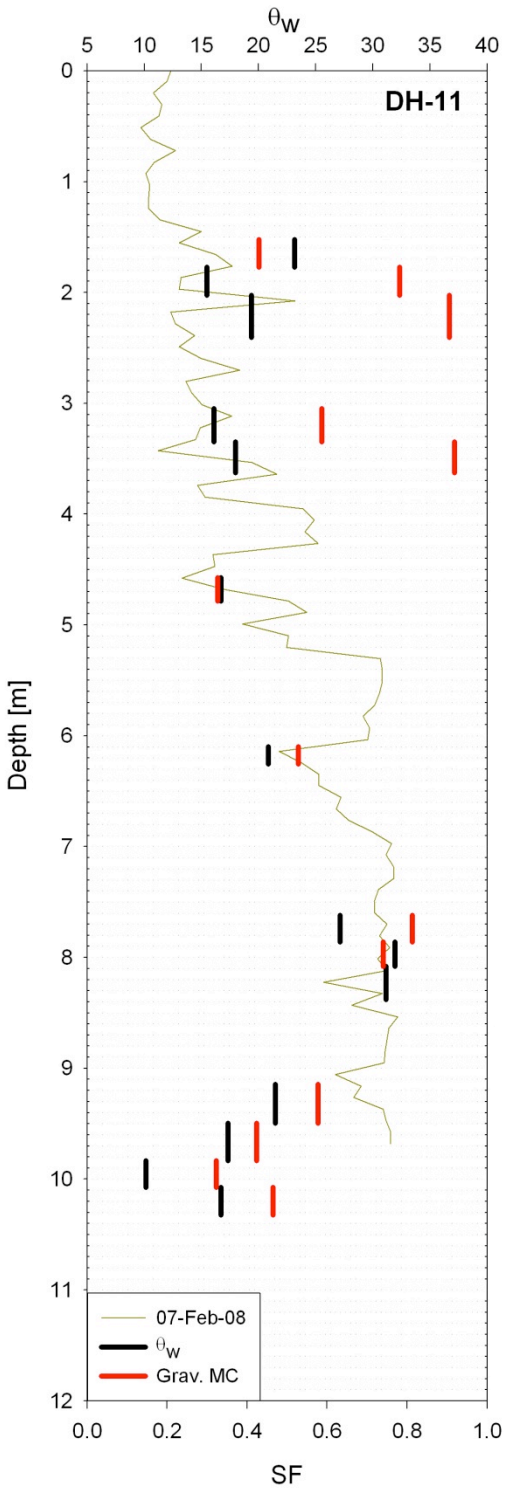

Figure D-10 – Deep Diviner survey for Hole DH-11, with volumetric and gravimetric moisture results from MSW samples.

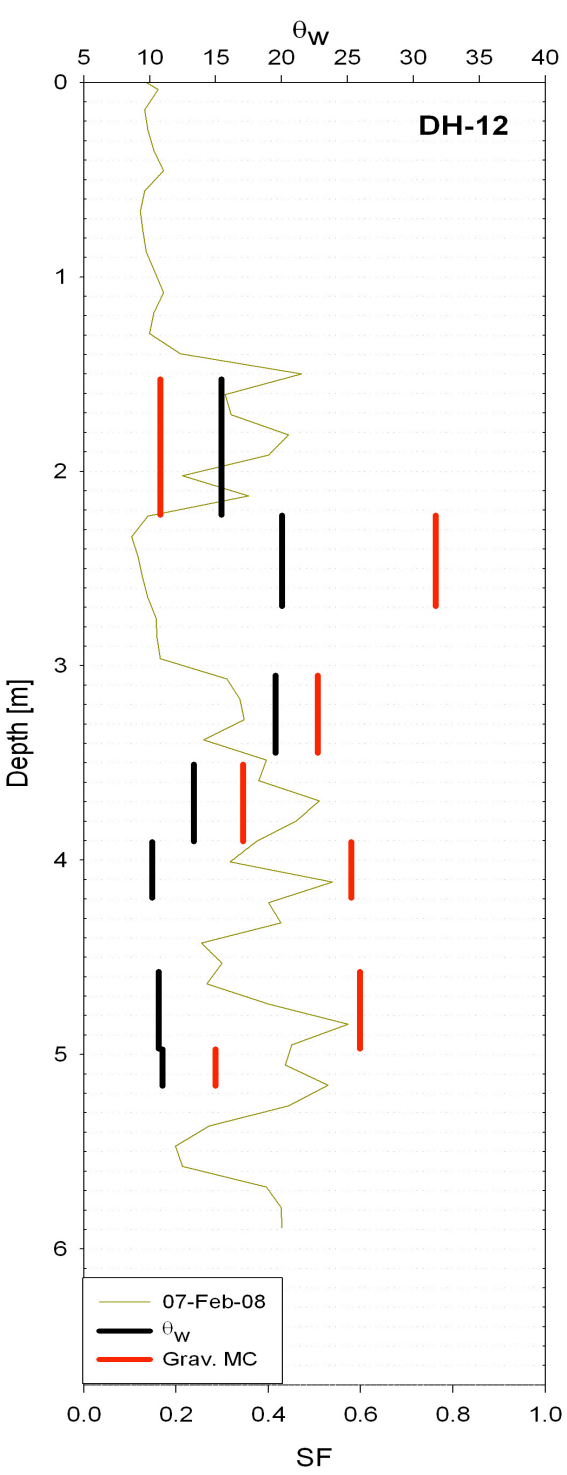

Figure D-11 – Deep Diviner survey for Hole DH-12, with volumetric and gravimetric moisture results from MSW samples.

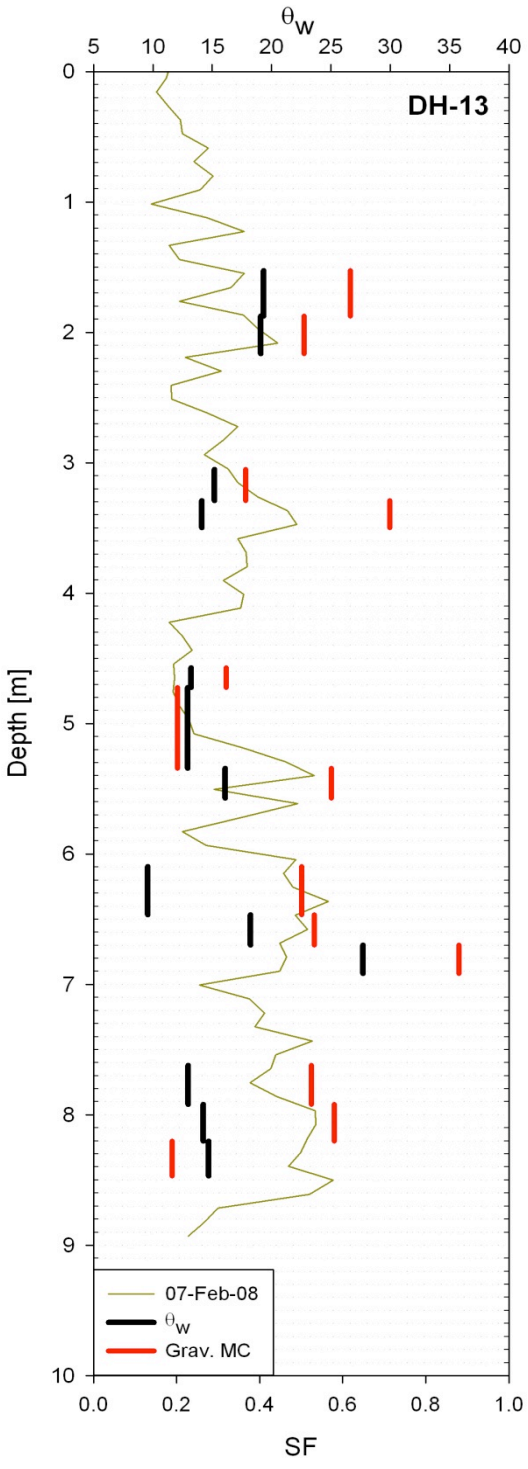

Figure D-12 – Deep Diviner survey for Hole DH-13, with volumetric and gravimetric moisture results from MSW samples.